THE CRYSTAL AND MOLECULAR STRUCTURES OF A DIMER OF A CYCLOBUTADIENE DERIVATIVE

THE CRYSTAL STRUCTURE OF BIS-(2-BROMOPYRIDINE)-DODECAHYDRODECABORANE

Thesis by

Charles Julius Fritchie, Jr.

In Partial Fulfillment of the Requirements

For the Degree of

Doctor of Philosophy

California Institute of Technology

Pasadena, California

1963

ACKNOWLEDGEMENTS

A most valuable silent partner in the writing of this thesis and valuable source of counsel during the course of the research work described herein has been my faculty advisor, Dr. Edward W. Hughes. The success of the work reviewed here is due in large part to his continued inspiration and guidance, and for all his help I must thank him.

My gratitude must also be expressed to many other associates. I am especially grateful to Dr. Richard E. Marsh for writing the triclinic least squares program, for allowing me to use many other programs written by himself and various members of his research group, and for many helpful suggestions concerning the use of these programs. The discussions I have held with many fellow students have been very beneficial to me. I also wish to thank Dr. Gus Palenik for processing some data at the U.S. Naval Ordnance Test Station and for the use of his programs during the work executed there.

For suggesting the research problems and providing crystals of the materials investigated, my thanks go to Dr. J. D. Roberts, Dr. M. C. Caserio, Dr. L. A. Burkardt, and Dr. N. Fetter, as well as Dr. Hughes.

For financial support during the course of this work, the Institute has granted several scholarships and assistantships, and the E. I. duPont de Nemours Company and the Woodrow Wilson Foundation have given me fellowships. A great deal of the work on $B_{10}H_{12}(C_5H_4NBr)$ was carried out at the U.S. Naval Ordnance Test Station at China Lake, California, with the support of the United States Navy. To all these groups I express my appreciation.

Finally, I must express my deepest thanks to my parents and to all of my early teachers, who are in large part responsible for my presence at this Institute.

ABSTRACT

The Crystal and Molecular Structures of a Dimer of a Cyclobutadiene Derivative

The molecular structure of this compound, previously suggested by other chemical work, has been conclusively established. Bond lengths and angles within the tricyclooctadiene skeleton were established with a precision exceeding that of any other study of a substituted cyclobutane and of any save one study of a substituted cyclobutene. Lengthening of the average C-C single and double bond in a C_4 ring is confirmed, and a shortening of the average external bond is also found. All bonds are normal (considering the above effects) except a C-C single bond in the configuration F-C-C-F, which is found to be 1.500 $\pm$ 0.009 Å rather than the expected 1.58 Å. The difference is attributed to change in the carbon hybridization state by the presence of the fluorine atoms.

The cyclobutane ring is accurately planar, but the two cyclobutene rings are slightly folded, with dihedral angles of 177° and 178° between the two halves. This folding is probably due to steric crowding within the molecule. The angles between the mean planes of the three rings, fused in a stairstep arrangement, are 113.3° and 113.7°.

Bis-(2-bromopyridine)-dodecahydrodecaborane

The crystal structure of this compound has been determined, all atoms including hydrogen being located by examination of Patterson syntheses and use of the heavy atom technique. The compound has the same borohydride skeleton within experimental error as diacetonitrile-dodecahydrodecaborane, the first of the $B_{10}H_{12}R_2$ compounds with R an

electron donor to be studied crystallographically. The B-B bond distances in the borohydride radical differ from those in the parent compound, $B_{10}H_{14}$, and the positions of bridge hydrogens attached to borons 5 through 10 in $B_{10}H_{14}$ are changed. There are two hydrogen bridges in the $B_{10}H_{12}R_2$ compounds, compared with four in $B_{10}H_{14}$. Bond distances in the bromopyridine ligands are unchanged by attachment to the borohydride skeleton, but some angles are slightly abnormal. The abnormalities can be explained in terms of intramolecular steric repulsion.

TABLE OF CONTENTS

THE MOLECULAR AND CRYSTAL STRUCTURES OF A DIMER OF A CYCLOBUTADIENE DERIVATIVE

INTRODUCTION

As part of a study of small-ring compounds, Professor Roberts' research group isolated (1) a crystalline material with the empirical formula $C_{44}H_{30}F_2$. This material was the result of an attempt to prepare 1-fluoro-2,3,4-triphenylcyclobutadiene and was on this basis assigned the dimeric formula $[\phi_3FC_4]_2$. Preliminary suggestions for the molecular structure of this dimer were the substituted cubane (I) and the cis- and trans-tricyclooctadienes (II) and (III). In each of these formulas, six of the R's are phenyl groups and two are fluorine atoms. The possi-

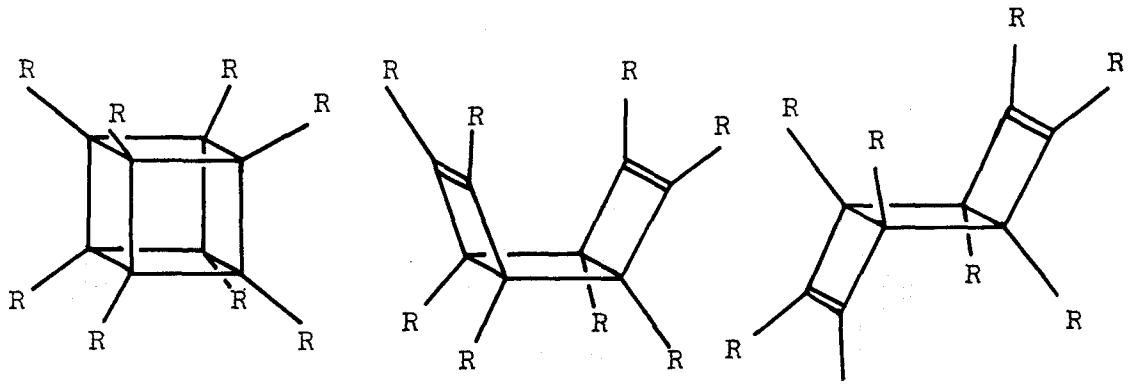

I II III

bility that the compound might have the novel structure (I) and the virtual certainty that it has a central framework or "skeleton" of several joined and highly strained four-membered rings led to the decision that this material should be studied crystallographically. Both the determination of the molecular structure and the accurate measurement of bond lengths and angles in this unusual system were primary points of interest.

EXPERIMENTAL DATA

A sample of the material consisting of colorless, approximately equidimensional crystals ranging in size from about 0.01 to 0.5 mm. was provided by Drs. Roberts and Caserio. Most of the crystals used in this work were selected from this original group, but when additional photographs became necessary near the end of the refinement it was discovered that the crystals had become covered with a thin layer of powder, apparently of identical crystalline form. Some of the material was recrystallized from a mixture of approximately equal parts of chloroform and absolute ethanol. This group of crystals contained some equidimensional blocks, but was primarily composed of needles. All crystals used for diffraction photographs were small blocks about 0.1-0.2 mm. in diameter.

Rotation and equi-inclination Weissenberg photographs taken with CuKα radiation showed the crystals to be triclinic. A primitive unit cell was chosen with approximate parameters a = 9.23 Å, b = 14.49 Å, c = 13.18 Å, α = 96°53', β = 88°22', and γ = 114°38'. These values were later refined with data primarily from photographs of crystals rotated about the [011] and [01$\bar{1}$] axes, taken by copper radiation and using a precision Straumanis-type Weissenberg camera. For these calculations, the copper Kα wavelengths were assumed to be 1.54050 and 1.54434 Å. The parameters d^*_{011}, $d^*_{01\bar{1}}$, a^*, and the angles between $\underline{a}^*$ and the diagonal vectors $\underline{d}^*_{011}$ and $\underline{d}^*_{01\bar{1}}$ were adjusted by least squares to furnish the "best" calculated values of $\sqrt{w}\ \frac{\sin^2\theta}{\lambda^2}$ for 13 reflections measured on the (01$\bar{1}$) photograph and 7 reflections measured on the (011) photograph.

For the $(01\bar{1})$ data, $\sqrt{w}$ was taken to be $1/\sin 2\theta$ for each reflection, and for the (011) data, each $\sqrt{w}$ was set equal to 1. The resulting parameters, together with the fact, determined from an ordinary [100] Weissenberg photograph, that the angle between $\underline{d}^*_{011}$ and $\underline{d}^*_{01\bar{1}}$ is 90°00' ± 01' were used to find the lattice parameters for the previously adopted unit cell. The resulting values are

$a = 9.297 \pm .003$ Å $b = 14.406 \pm .005$ Å $c = 13.120 \pm .004$ Å

$\alpha = 96°47' \pm 02'$ $\beta = 88°23' \pm 02'$ $\gamma = 114°28' \pm 02'$

The estimates of uncertainty are about three times the values of σ obtained from the least squares analysis, and are based on the difference between the values of a^* independently derived from the two precision films.

The density of the crystals was determined by preparing a solution of carbon tetrachloride and acetone in which several small crystals would remain suspended, and then measuring the density of this solution with a small pycnometer. The density of the crystals was thus found to be $1.254 \pm .002$ gm/cm^3. The presence of two of the $C_{44}H_{30}F_2$ molecules (hereafter called HPT, a short mnemonic for the systematic name), in the unit cell demands a density of $1.248 \pm .001$ gm/cm^3. The agreement between these two density values is quite reasonable and indicates that the asymmetric unit in this crystal consists of at least one molecule.

The choice of space group from the two available is not easy, and only the full structure determination has conclusively proved it to be P $\bar{1}$. A Howell-Rogers-Phillips (2) statistical test was performed on the three-dimensional data and the resulting graph is shown in Figure 1.

Figure 1. Howells-Rogers-Phillips Statistical Test.

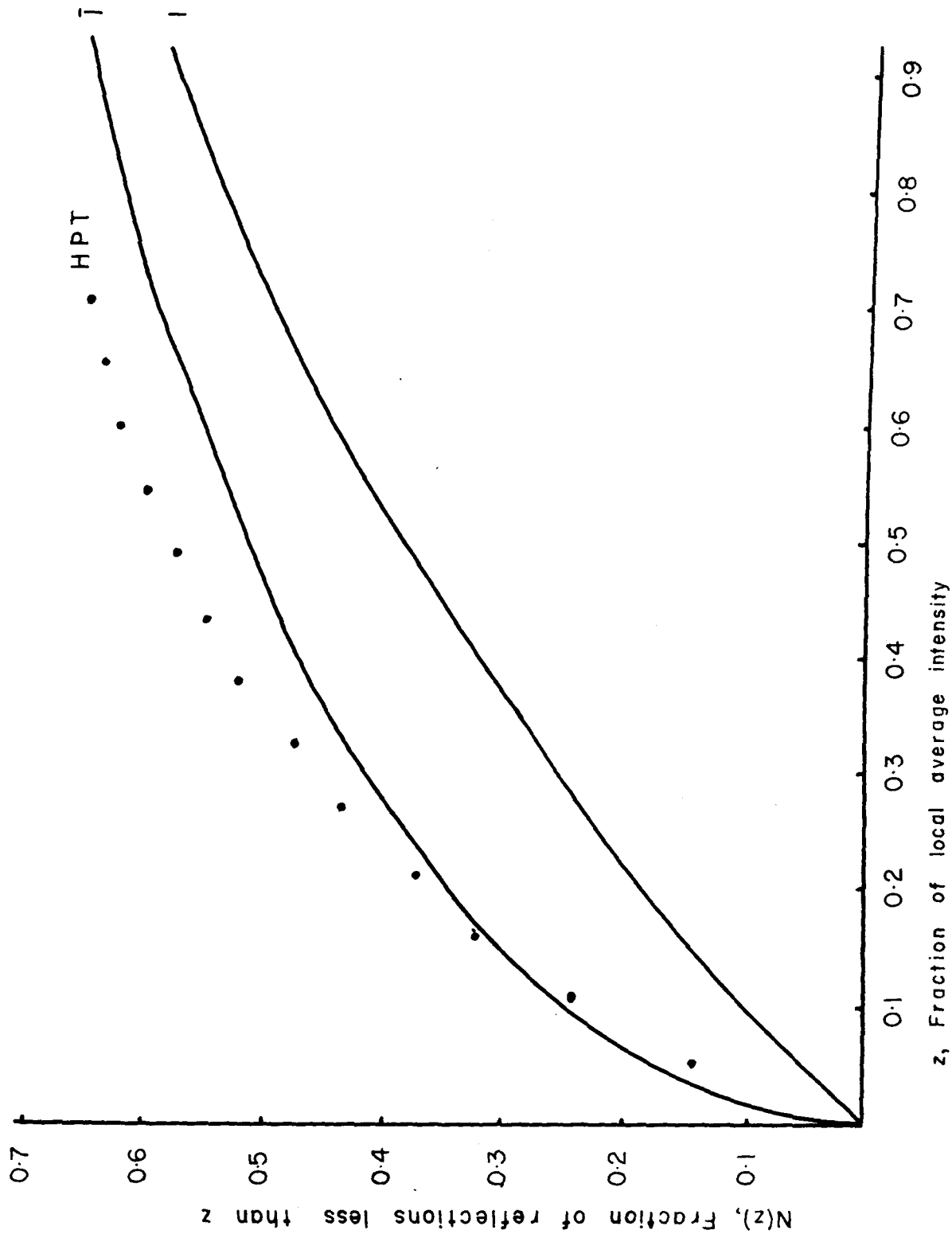

The early indication of the centric nature of the space group given by this test was encouraging. Had P 1 proved to be the space group, the parameters of two complete molecules, or 92 "heavy atoms," would have been required to determine the crystal structure. A further indication of the existence of a center of symmetry in the crystal, and also of a pseudo-center of symmetry in a large part of the molecule, was given by the appearance of the three-dimensional Patterson function. This subject is discussed more fully in a later section.

The multiple-film equi-inclination Weissenberg technique, utilizing copper Kα radiation filtered by 0.005" nickel foil, was used for the collection of all intensity data. The zero through sixth layers about [100], the zero through third layers about [0$1\bar{1}$], and the zero layer about [011] were photographed, using two sets of three films each for each layer except (6kℓ), where a single set of three films was sufficient. One of these sets was exposed about ten times as long as the other, in order to increase the range of estimable intensities. The intensities of diffraction spots on these films were measured visually by comparison with an intensity scale prepared with one of the crystals used for the Weissenberg photographs. It was necessary to use seven crystals in collecting the data because the crystals, although stable in air, turned yellow after prolonged exposure to X-radiation. These crystals were all similar in size and shape; they were approximately equidimensional blocks ranging from 0.14 to 0.20 mm. on edge.

All of the crystals used were twins. In every case, one of the twins was about ten times larger than the other, and on all layers except the zero layer the spots from the twins could be distinguished. Only the

intensity maxima produced by the larger twin were estimated. The nature of the twinning--$\underline{b}^*$ and $\underline{c}^*$ of one twin conciding with $\underline{c}^*$ and $\underline{b}^*$ respectively of the other twin--together with the fact that $\underline{b}^*$ and $\underline{c}^*$ are within experimental error equal in length, resulted in the (0kℓ) spots of one twin falling exactly on the (0ℓk) spots of the other. No attempt was made to separate these intensities. The diffraction peaks were indexed and estimated as if belonging entirely to the larger twin. The resulting intensities were used to obtain $|F_o|^2$ and $|F_o|$ values which were used in calculating the Patterson and early Fourier functions; for the least-squares calculations no (0kℓ) data except unobserved ones were used.

Absorption of X-rays by these small crystals is considered to be negligible ($\mu R = 0.074$ for $R = 0.1$ mm.), and no such correction has been made. The intensities within each six-film set were brought to a single scale using the reflections which could be estimated on more than one film. The resulting sets of intensities were converted to the squares of the corresponding structure factors by a Burroughs 220 computer using a program (LP) described in the Appendix. These $|F_o|^2$ values were brought to a single scale by comparison of those values measured on two or more sets of films. Finally, the whole set of intensities was put on an approximately absolute scale, and an average temperature factor of 2.6 was found, using Wilson's method (3).

A total of 2937 observed reflections and 1132 unobserved reflections were used in the final calculations. There were also 303 observed (0kℓ) reflections. The approximate $|F_o|$ values for these were compared with the calculated values to verify that no gross irregularities exist.

DETERMINATION OF TRIAL STRUCTURE

Interpretation of the Patterson Function

At the outset it was apparent that some unusual method of attack would be needed to solve a structure as large as this one, containing no exceptionally dense atoms. It was impossible to propose a trial structure on the basis of molecular packing because the chemical structure was largely unknown.

Patterson has demonstrated (4) that the location of molecular pseudo-centers of symmetry in centrosymmetric space groups can often be found by the following consideration. If the $2n$ atoms in the unit cell are divided into groups A and A' of n atoms each, with each atom in A related to one in A' by a crystallographic center of symmetry I, and if $2p$ of the n atoms in A are arranged in subgroups B_1 and B_2 with each atom in B_1 related to one in B_2 by the molecular pseudo-center of symmetry M, then the coordinates of the $2p$ atoms in B_1 and B_2 can be approximately expressed as $(\underline{C} + \underline{c}_i)$ and $(\underline{C} - \underline{c}_i)$, where $\underline{C}$ is the vector from I to M and each $\underline{c}_i$ $(i = 1,2,\cdots,p)$ is a vector from M to one of the atoms in B_1. There are also $2p$ atoms in corresponding subgroups B_1' and B_2' of A', whose coordinates are approximately $(-\underline{C} - \underline{c}_i)$ and $(-\underline{C} + \underline{c}_i)$. Patterson pointed out that there are vectors of weight $2p$ at the points $\pm 2\underline{C}$ in the vector set generated by the atoms in B_1, B_2, B_1', and B_2', as a result of superposition of the vectors $[\pm(\underline{C} + \underline{c}_i) \mp (-\underline{C} + \underline{c}_i)]$ and $[\pm(\underline{C} - \underline{c}_i) \mp (-\underline{C} - \underline{c}_i)]$. These peaks should be easily identifiable if $2p$ is an appreciable fraction of $2n$, and thus the molecular pseudo-center of symmetry, M, should be easily located.

Further consideration of the above expressions for the atomic coordinates disclosed the fact that even more information is available. The total vector set generated by the groups of atoms B_1, B_2, B_1', and B_2' is:

4p peaks at	$[\pm(\underline{C} \pm \underline{c}_1) \mp (\underline{C} \pm \underline{c}_1)] = \underline{0}$
2p peaks at	$[(\underline{C} \pm \underline{c}_1) - (-\underline{C} \pm \underline{c}_1)] = \underline{2C}$
2p peaks at	$[-(\underline{C} \pm \underline{c}_1) + (-\underline{C} \pm \underline{c}_1)] = -\underline{2C}$
2 peaks at each of	$[(+\underline{C} + \underline{c}_1) - (+\underline{C} - \underline{c}_1)] = \underline{2c}_1$
2 peaks at each of	$[(+\underline{C} - \underline{c}_1) - (+\underline{C} + \underline{c}_1)] = -\underline{2c}_1$
1 peak at each of	$[(+\underline{C} - \underline{c}_1) - (\mp\underline{C} - \underline{c}_1)] = \pm\underline{2C} + \underline{2c}_1$
1 peak at each of	$[(+\underline{C} - \underline{c}_1) - (\mp\underline{C} + \underline{c}_1)] = \pm\underline{2C} - \underline{2c}_1$

If these vectors are grouped into the sets $S = (\underline{0}, \underline{2c}_1, -\underline{2c}_1)$, $T = (\underline{2C}, \underline{2C} + \underline{2c}_1, \underline{2C} - \underline{2c}_1)$, and $T' = (-\underline{2C}, -\underline{2C} + \underline{2c}_1, -\underline{2C} - \underline{2c}_1)$, it is obvious that the three sets S, T, and T' can be superimposed by simple translation. Furthermore, each set is centrosymmetric. If $\underset{\sim}{4p}$ is less than $\underset{\sim}{2n}$, the $(\underset{\sim}{2n} - \underset{\sim}{4p})$ remaining atoms in A and A' generate vectors which cannot be grouped into sets superimposable by translations of $\pm\ \underline{2C}$, and superposition methods such as use of the minimum function (5) can be used to extract the set T (for example) from the total vector set. Use of these ideas requires that two conditions be met: $\underset{\sim}{2p}$ should be an appreciable fraction (probably at least 1/5) of $\underset{\sim}{2n}$ so that the vectors $\pm\ \underline{2C}$ can be identified, and $\underset{\sim}{4p}$ should be substantially less than $\underset{\sim}{2n}$ so that worthwhile simplification of the vector set will result.

At the time the three dimensional data became available, chemical work by Nagarajan and Caserio (6) had ruled out proposed structure (I)

by proving the existence of two carbon-carbon double bonds in the molecule. It will be noticed that of the two most plausible structures remaining, (III) possesses a molecular pseudo-center of symmetry with $\underset{\sim}{2p} = 16$ (assuming the α-atoms of the eight R-groups to be the same), six phenyl ring pseudo-centers each with $\underset{\sim}{2p} = 6$, and two cyclobutene pseudo-centers each with $\underset{\sim}{2p} = 4$. Structure (II) shows simply the 6-fold and 4-fold pseudo-centers (plus an additional 4-fold pseudo-center which in structure (III) is part of the larger 16-fold one).

The three-dimensional Patterson function, sharpened by the weighting function $(6/f_C) \exp[-2.368 \sin^2 \theta/\lambda^2]$, where f_C is the value of the carbon form-factor for the given reflection, was calculated and plotted on 2' x 2' x 3/16" sheets of clear plastic. These sheets were stacked in the proper fashion to give a three-dimensional representation of the sharpened Patterson function.

Examination of this Patterson "map" showed a single large peak at (u, v, w) = (0.1407, 0.5310, 0.4890) whose maximum is about one-sixth the value of the origin maximum. Only one other peak in the Patterson function exceeds one-twelfth the value of the origin peak, and the special position of this maximum at (1/2, 0, 0) shows it to be double the usual weight. The large general peak is very sharp, a fact strongly suggesting that it is indeed a peak of the $\underline{2C}$ type discussed above. Thus $P\bar{1}$ gained credence as the true space group and proposed structure (III) seemed likely to be the true molecular formula.

Following the assumption that the structure could be divided into a group of sixteen atoms (about one-third of 46) arrayed about a molecular pseudo-center of symmetry and a group of about thirty atoms more randomly

oriented, it was decided to use the second fact pointed out in the discussion above--that the environments of the point 2C and of the origin are similar and centrosymmetric with respect to the vectors generated by the group of sixteen atoms and different with respect to all other vectors. A minimum function, M_1, was prepared by inverting the Patterson function through a center of symmetry at the point 2C = (0.1407, 0.5310, 0.4890), superimposing this on the original Patterson function with points 2C in the two maps coinciding, and taking M_1 as the point-by-point minimum of the two superimposed maps. The origin of M_1 was taken to coincide with 2C in the original maps. The origin of the sharpened Patterson map was then superimposed on the origin of M_1 and a second minimum map, M_2, was constructed in a similar fashion. This use of the minimum function differs from the general use in that its purpose is to reduce the size of a vector set rather than to obtain from the vector set the atoms generating it.

Examination of M_2 showed that the peaks about the origin are grouped to give approximately 2/m symmetry, but none higher. This fact clearly confirms the rejection of structures (I) and (II). The outstanding feature of M_2 and of the area around the origin in the Patterson map is a plane of peaks passing near the origin. A separate drawing of the Patterson function in this plane was made, and is shown in Figure 2. This group of peaks is precisely what is demanded by structure (III) and could not be interpreted in any other chemically reasonable way. A centrosymmetric group of 16 atoms (8 independent) was fit by a simple least-squares procedure to 21 of the most nearly resolved of the peaks, to give a trial model for the C_{16} rigid framework of the molecule. One

Figure 2. Section of HPT Sharpened Patterson.

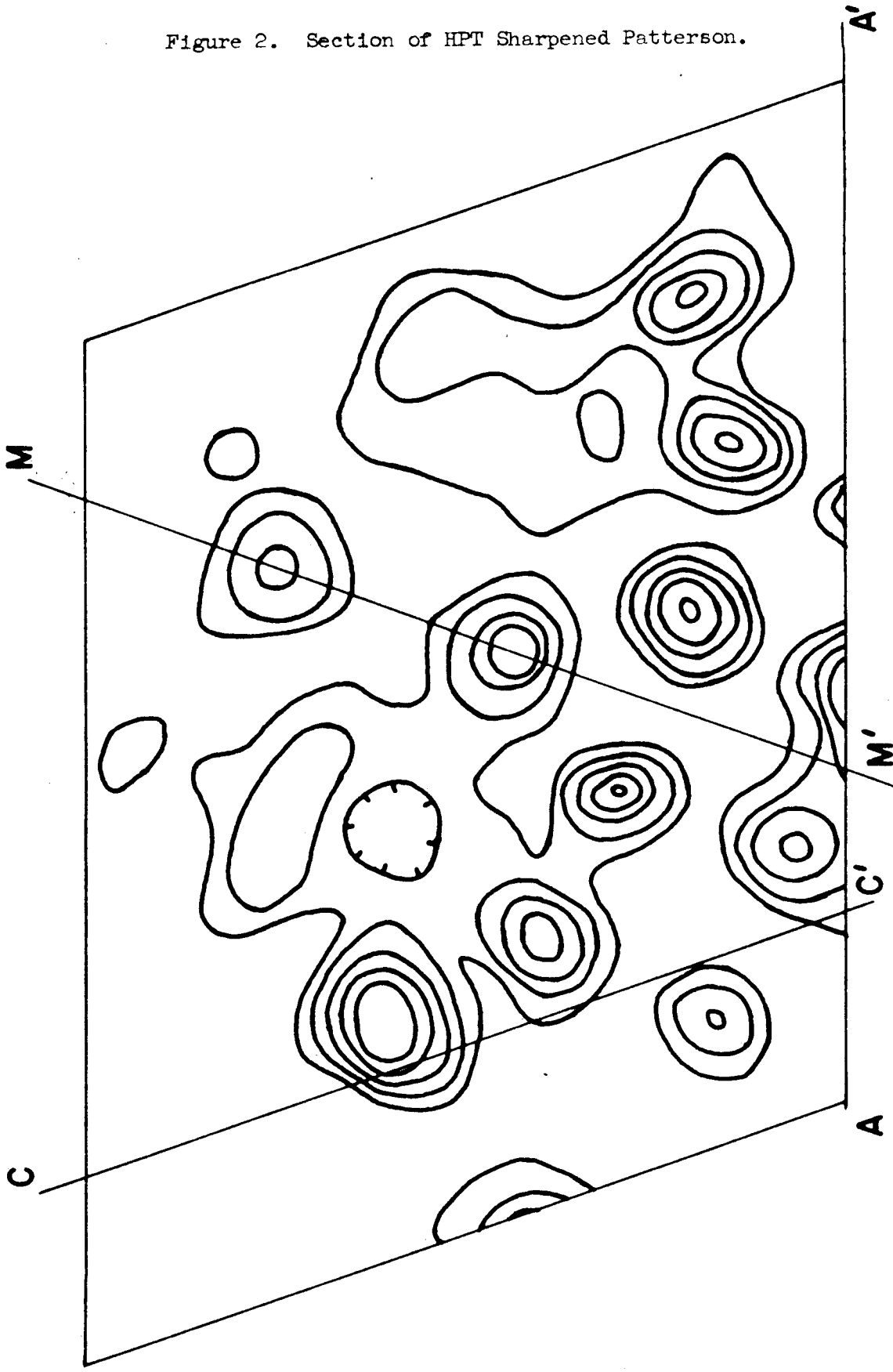

AA' and CC' are the traces of planes (100) and (001). MM' is the trace of the pseudo-mirror.

further piece of information could be drawn from M_2 at this time. Although two of the eight α-substituent atoms are known to be heavier than the remaining six, M_2 showed nearly exact 2/m symmetry with regard to peak heights as well as locations. The precision of the approximate mirror symmetry is evident from an examination of Figure 2. This precision indicates that the fluorine and carbon atoms must be separately arranged so as each to display average 2/m symmetry. In space group P $\bar{1}$, molecules of 2 or m symmetry would have average symmetry 2/m (the average molecule being obtained by superimposing one molecule on its image produced by a center of symmetry), but a molecule of $\bar{1}$ symmetry would give an average molecule of $\bar{1}$ symmetry. M symmetry could be ruled out because it would require one of the fluorine atoms to move from one of the C_4 rings of the dimeric pair to the other. Structures (IV) and (V)

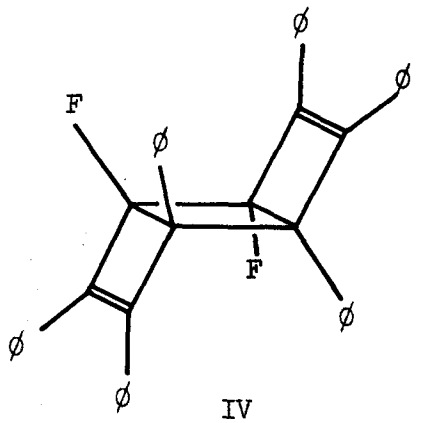

IV

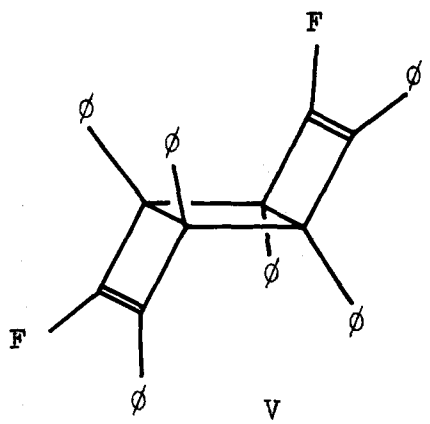

V

have symmetry 2. Chemical evidence, suggesting the presence of a $\phi\text{-}\dot{C}\text{=}\dot{C}\text{-}\phi$ group, ruled out (V). Structure (IV) was thus considered almost certainly the true one.

The encouraging success in interpreting the Patterson function up to this point led to an effort to confirm (IV) as the molecular structure and to determine the rotational configuration of the six phenyl groups by

a method similar to that used thus far. The six-fold phenyl peaks of type 2C should be the next strongest peaks in the Patterson map, after the origin and the 16-fold peak previously identified. Unfortunately there were more than six peaks of the expected height. Furthermore, the parameters determined for the C_{16} central skeleton were imprecise enough to preclude identification of the peaks by calculation of ideal locations. Such locations were predicted and some did coincide with peaks, but enough were found to be between peaks to cast doubt upon the validity of this procedure.

Completion of the Trial Structure with Fourier Techniques

When about one-third (16) of the atoms other than hydrogen had been approximately located by direct interpretation of the Patterson function as described above, and with confirmation from the same source of $P\bar{1}$ as the space group, it was considered feasible to test the power of this sixteen-atom nucleus as a phase-determining group for the electron density function. The first electron density Fourier series was calculated using 928 reflections chosen from the data list without regard to scattering angle, the only criterion being that the calculated value of $|F|$ should exceed or, in the case of very strong reflections, exceed one-half of the experimental structure factor amplitude. The resulting crude electron density map showed sixteen well-resolved peaks at the sites chosen for the initial group of atoms, but a randomly varying density in the remainder of the unit cell.

An attempt was made at this time to locate the fluorine atoms by packing considerations. Positions for para atoms of hypothetical phenyl rings were calculated, on the assumption that all eight of the

substituents were phenyl rings. Contrary to hopes, all eight of these para atoms fit into the unit cell without unduly close contacts, and this line of reasoning was discarded.

Reexamination of the electron density function revealed that a peak representing one of the α-substituent atoms was V-shaped, suggesting the location of the two ortho atoms of a phenyl ring. For comparison with the F_o Fourier series, a difference series was calculated. In addition to the class of reflections used in the F_o series, where both $|F_o|$ and $|F_c|$ are large, the difference map includes all terms with $|F_o| > |F_c|$. The former class of reflections reproduces largely the similarities between the true structure and the model; the latter group, which with incomplete structures supplies many of the dominant terms in the ΔF series, emphasizes points in which the model fails to emulate the true structure and is thus more valuable in locating a few missing or grossly misplaced atoms. Because of the failure of the F_o series to reveal many of the missing atoms, only low-order diffraction maxima were used to calculate the difference series. It was felt that a search for the groups of atoms making up the phenyl rings might be more successful than a search for individual atoms. The difference Fourier map was in fact little more helpful than the original Fourier, but did have a region of positive density in the region assigned to the first phenyl ring on the basis of the F_o map. A regular hexagon of carbon atoms was added to the trial model to represent this ring and a second set of structure factors was calculated. A second F_o Fourier series, F_2, was summed, using phases based on the second set of structure factors. Like the ΔF map, F_2 was limited to reflections for which $\sin\theta/\lambda$ is less than 0.3 $Å^{-1}$.

In the resulting map, the first phenyl ring (which later proved to be twisted from its correct orientation) was present, but the peaks representing the ortho and meta atoms were weaker than the peaks representing other atoms included in the phasing calculations. Two additional rings seemed to be present. When the corresponding areas in the difference map were found to be positive, these rings were also added to the model. A third set of structure factors and a third Fourier map, F_3, were calculated. For this calculation, the R-factor ($R = \Sigma||F_o| - |F_c||/\Sigma|F_o|$) was similar to that of the two previous calculations, about 60%. This new map, F_3, verified the correctness of the second and third phenyl rings added to the model, but again the first ring seemed weak. No new rings could be conclusively identified. Positions for para atoms of hypothetical phenyl rings in all the remaining substituent positions were calculated, and three of these were found to be positive in both F_3 and the difference function. These atoms were added to the model, but the ortho and meta atoms of the first phenyl ring were omitted. A fourth set of structure factors was then calculated and used as the basis for a second difference Fourier function, ΔF_2. This function contained peaks representing the phenyl ring which had been omitted from the model, but again at rather low heights. In addition, all atoms used in the phasing calculations were shown to be correct by being in approximately flat regions of approximately zero electron density, and two additional phenyl rings were discovered. At this point, only four atoms (the ortho and meta atoms of one phenyl ring) were missing.

The 42 atoms in the model at this time (all treated as carbon atoms) were subjected to several cycles of least squares calculations.

After each cycle the calculated parameter shifts were modified so as to keep all bond lengths and angles within reasonable ranges. After four such cycles, another electron density map was computed. In calculating the set of structure factors in which this map was based, the phenyl ring which had consistently appeared weak in the early Fourier functions, and which was badly distorted by each least squares cycle, was treated as consisting of two (α and para) carbon atoms and four hydrogen atoms. The resulting electron density map revealed all the atoms of the missing ring, showed the one which had been doubtful to be twisted slightly from its previous position, and confirmed the identity of the fluorine atoms by showing them to be much denser than any carbon atom. This map contained only two, very small "spurious" peaks and thus strongly indicated the correctness of the trial structure. The R-value calculated with all (carbon and fluorine) atoms and including the 1,501 reflections with $\sin\theta/\lambda$ less than 0.4 Å^{-1}, was about 51%.

Refinement of the Trial Structure

The initial model was refined exclusively by the least squares method (7), combined in the early stages with occasional alteration of the positions to maintain bond distances near expected values. The progress of the refinement is summarized in Table 1.

The slowness of the refinement, apparent from an examination of Table 1, was caused by the difficulty in finding a proper weighting function. Cycles I through I-H were carried out on a Burroughs 220 computer using a triclinic refinement program written by Dr. R. E. Marsh. This program minimizes $\Sigma w(|F_o|^2 - |F_c|^2)^2$; thus if one makes the usual

TABLE 1

Summary of Least Squares Refinement

Cycle	$\left(\frac{\sin^2\theta}{\lambda^2}\right)_{max}$	R	$\sqrt{w}$ *
I	.05	.28	$1/f_c$
II	.05	23	
III	.09	28	
IV	.09	25	
V	.09	24	
VI	.09	22	
VII	.14	28	
VIII	.14	25	
IX	.14	25	
X	.14	25	$1/(8 + 0.036\ \|F_o\|^2)$
	.05	15	$1/(4 + 0.1\ \|F_o\|)$
I'	.08	18	$1/\|F_o\|$ if observed; $1/2(\|F_o\| x \|F_{min}\|)^{1/2}$ if unobserved
II'	.08	17	
III'	.11	19	
IV'	.11	17	
V'	.165	21	
VI'	.19	18	
VII'	.50	20	
VIII'	.50	18	
I"	.50	17	$1/\|F\|^2$ or $1/4\|F_o\| x \|F_{min}\|$ if observed or unobserved
II"	.50	17	
III"	.50	> 17	
II"-2	.50	18	
III"-3	.50	18	

TABLE 1 (continued)

Cycle	$\left(\frac{\sin^2\theta}{\lambda^2}\right)_{max}$	R	$\sqrt{w}$*
IV"	.50	18	$1/(1 - 0.039\|F_o\| + 0.000429\|F_o\|^2)$
V"	.50	19	
VI"	.50	17.6	$1/\|F_o\|$ or $1/2(\|F_o\| x \|F_{min}\|)^{1/2}$
VII"	.50	17.2	
VIII"	.50	16.6	
I'"			
II'"	.50	12.7	
IV'"	.50	11.9	
V'"	.50	11.6	
VI'"	.50	11.4	
VII'"	.50	11.2	
VIII'"	.50	11.2	
IX'"	.50	~ 11.4	
I-H	.50	12.3	
I-F	.50	17.8	
II-F	.50	17.0	
III-F	.50	16.7	
IV-F	.50	15.9	
V-F	.50	16.0	
VI-F	.50	15.6	
VII-F	.50	15.7	
VIII-F	.50	15.7	
I-B	.50	14.7	
II-B	.50	12.9	
III-B	.50	12.5	
IV-B	.50	12.3	
V-B	.50	11.5	
VIII-B	.50	9.7	
IX-B	.50	9.5	$1/(0.1425 - 0.005565\|F_o\| + 0.0001168\|F_o\|^2)$
X-B	.50	9.5	

*The weighting function remains constant from cycle to cycle unless a change is noted.

assumption (7) that the uncertainty in a reflection, σ_F, is proportional to the magnitude of a reflection (at least for the great majority of reflections, excepting only the weak ones), it is clear that the weighting function should be $\sqrt{w} = 1/|F_o|^2$ at the termination of refinement. This function, however, gives very large weight to small reflections and should not be used in early cycles where the signs of many of these weak reflections are probably wrong. Accordingly, in the early stages of the refinement, the inverse of the carbon form factor, $1/f_C$, was used for $\sqrt{w}$. These cycles also used only low order data, to further minimize the effects of incorrect signs. Use of $1/f_C$ rather than 1 for $\sqrt{w}$ is justified chiefly by its relationship to the difference synthesis method of refinement. Lipson and Cochran (8) show that minimization of $\Sigma 1/f_C(|F_o| - |F_c|)^2$ is equivalent to refinement by difference synthesis. As Table 1 shows, this procedure led to an impasse at Cycle IX. Different weighting functions were used for Cycles X and XI, with poor results. A reduction in the amount of data used and a change in $\sqrt{w}$ to $1/|F_o|$ resulted in further, although slow, refinement, in Cycles I' through VIII'. During this stage of refinement, the number of data being used was increased gradually; Cycle VII' included all data for the first time. The R-factor for this cycle was 20%. At this time it was decided that nearly all signs should be correct, and $\sqrt{w}$ was changed to the theoretically proper $1/|F_o|^2$. Five cycles were executed using this weighting function; some atoms were given shifts based on a few sections of a difference function computed using parameters suggested by Cycle I". None of these attempts to improve the structure had apparent beneficial effect, judging from bond lengths of the trial structure and from the R-factor. In Cycle IV" (see table 1),

a weighting function was used which would give small weights both to strong reflections with presumably large errors in magnitude and to weak reflections with possible errors in sign. This cycle did not reduce the R-factor, nor did it improve the worst bond lengths. Because it seemed to consistently reduce the R-value, $1/|F_o|$ was used as a weighting function for several more cycles. The iterative least squares process apparently converged with R about 16% using this function.

To discover whether the many very small reflections were impeding progress, the data list was restricted to reflections with unitary structure factor, $U_o = F_o/94\ f_c \exp[-3.8\ \sin^2\theta/\lambda^2]$, greater than 0.1, on the judgement that the magnitude of U rather than the magnitude of F is important in determining the probability of correct sign determinations. This restriction reduced the data list to about 40% of its previous size; R for the reduced list was 12.7%. Four cycles with $\sqrt{w} = 1/|F_o|$ lowered R for these data to 11.2%, but the R-value then began to climb and many bond distances remained poor (although the sum of weighted squares of residuals continued to drop slowly). Introduction of hydrogen atoms at calculated positions led to an increase in R.

Because of the slow progress of the refinement and the great length of time (about 4.5 hours) for each cycle of least squares computations on the Burroughs 220 computer, it was decided to continue refinement on IBM 7090 computers available at the Jet Propulsion Laboratory and the Western Data Processing Center. Dr. K. Trueblood of the University of California in Los Angeles made available copies of the full matrix (9) and block diagonal least squares programs of Gantzel, Sparks, and Trueblood for this machine. With help from Mr. R. Deverill, these programs were modified

to accept 4500 rather than 2100 data, and were further changed to operate under the California Institute of Technology monitor programs.

The full matrix program was used first, to see whether neglect of inter-atom off-diagonal terms in the normal equation matrix was significantly slowing the refinement. Because of program and time limitations, most of the full matrix cycles refined only portions of the structure, containing on the average 20 atoms. This program minimizes $\Sigma w (|F_o| - |F_c|)^2$, and the weight $\sqrt{w} = 1/|F_o|$ was used for all cycles except the last two. It should be noticed that "refinement" Cycles I'" to IX'", based on a part of the data list, had actually increased the overall value of R to 17.8% from its value of 16.6% at Cycle VIII". Five of the partial-structure, full matrix refinement cycles had reduced the R-factor only slightly, when time considerations suggested a change to the block diagonal program. The full matrix refinement had shown that neglect of off-diagonal terms was not a prime cause of slow refinement.

Addition to the structural model of hydrogen atoms on ring diagonals and 1.0 Å from the appropriate carbon atoms lowered the R-value (based on Cycle VIII-F) from 15.7% to 14.7%. It was considered appropriate to begin refinement of anisotropic (ellipsoidal) temperature factors of the form $\exp-[B_{11}h^2 + B_{22}k^2 + B_{33}\ell^2 + B_{12}hk + B_{13}h\ell + B_{23}k\ell]$ at this stage. Six cycles, refining positional and ellipsoidal temperature parameters reduced R to 9.7%. A graph made by plotting the average error in F_o (as measured by $||F_o| - |F_c||$) versus $|F_o|$ after Cycle VIII-B showed that the function $\sqrt{w} = 1/(0.2604 + 0.0384\ |F_o| + 0.001852\ |F_o|^2)$ more closely represented the pattern of error than $1/|F_o|$. Qualitatively, this function concurs with a personal evaluation of the data measurement,

giving smaller weight to very small reflections than the simpler function. These very weak reflections are felt to have a larger relative error than somewhat larger reflections. Refinement was continued for two more cycles with this weighting function, but the parameters shifted by negligible amounts. As during all refinement on the IBM 7090 computer, unobserved reflections were included in the least squares equations only if the calculated values exceeded the minimum observable values. In the latter cases, these reflections were assigned twice the weight that would be given an observed reflection of the same magnitude. In the last set of structure factors calculations, only 94 of the 1152 unobserved reflections were calculated to be larger than the minimum observable value, and none of these greatly exceeded that value.

The parameters used throughout the discussion of this structure are those obtained from Cycle IX-B, for which R = 9.5%. These parameters, together with their standard deviations obtained by inversion of the least squares matrices, are listed in Tables 2 and 3. The listed hydrogen parameters are those calculated following refinement Cycle V-B, by placing the atoms 1.00 Å along the ring diagonals from the appropriate carbon atoms. The shifts in carbon parameters after Cycle V-B were not felt large enough to warrant recalculation of the hydrogen positions. For all cycles in which the hydrogen atoms were included, each was given the isotropic temperature factor of 5.5 Å. Table 8 gives a list of structure factors calculated using the final parameters, together with the observed values.

Atomic form factors used for the final refinement were those of Freeman (10) for fluorine, McWeeny (11) for hydrogen, and Hoerni and Ibers (12) for carbon. For earlier calculations on the Burroughs 220 computer, the

TABLE 2

Final Positional Parameters

Atom	(x/a)	σ(x/a)	σ(x)Å	(y/b)	σ(y/b)	σ(y)Å	(z/c)	σ(z/c)	σ(z)Å
C(1)	.1604	.00051	.0047	.2873	.00033	.0048	.1886	.00030	.0040
C(2)	.0390	.00049	.0045	.3263	.00031	.0045	.2264	.00032	.0042
C(3)	-.1199	.00052	.0048	.2759	.00034	.0049	.1709	.00033	.0043
C(4)	-.1767	.00049	.0045	.2015	.00035	.0051	.2336	.00031	.0041
C(5)	-.0291	.00051	.0047	.2432	.00033	.0048	.3031	.00031	.0041
C(6)	.0964	.00048	.0044	.2005	.00033	.0048	.2628	.00031	.0041
C(7)	.2581	.00049	.0045	.2622	.00034	.0049	.3178	.00032	.0042
C(8)	.3150	.00049	.0045	.3308	.00034	.0049	.2489	.00031	.0041
C(9)	-.1827	.00057	.0053	.3019	.00036	.0052	.0832	.00034	.0045
C(10)	-.0804	.00062	.0057	.3564	.00041	.0059	.0094	.00039	.0051
C(11)	-.1421	.00074	.0068	.3802	.00043	.0062	-.0759	.00040	.0053
C(12)	-.3028	.00078	.0072	.3481	.00048	.0070	-.0856	.00043	.0057
C(13)	-.4028	.00072	.0066	.2972	.00050	.0072	-.0130	.00048	.0063
C(14)	-.3434	.00059	.0054	.2736	.00040	.0058	.0720	.00038	.0050
C(15)	-.3211	.00052	.0048	.1060	.00034	.0049	.2316	.00033	.0043
C(16)	-.3783	.00070	.0065	.0437	.00044	.0064	.1429	.00039	.0051
C(17)	-.5096	.00082	.0076	-.0480	.00050	.0072	.1408	.00052	.0068
C(18)	-.5895	.00072	.0066	-.0783	.00044	.0064	.2299	.00052	.0068
C(19)	-.5355	.00063	.0058	-.0165	.00043	.0062	.3194	.00045	.0054
C(20)	-.4020	.00057	.0053	.0756	.00037	.0054	.3217	.00036	.0047
C(21)	-.0519	.00050	.0046	.2676	.00034	.0049	.4146	.00031	.0041
C(22)	-.0397	.00057	.0053	.2098	.00041	.0059	.4881	.00034	.0045
C(23)	-.0762	.00062	.0057	.2282	.00050	.0072	.5887	.00036	.0047
C(24)	-.1240	.00064	.0059	.3039	.00048	.0070	.6196	.00037	.0049
C(25)	-.1365	.00069	.0064	.3632	.00045	.0065	.5482	.00045	.0059
C(26)	-.1010	.00059	.0054	.3459	.00039	.0056	.4463	.00039	.0051
C(27)	.0521	.00055	.0051	.0899	.00036	.0052	.2232	.00034	.0045
C(28)	.1286	.00074	.0068	.0637	.00044	.0064	.1417	.00045	.0059
C(29)	.0887	.00105	.0097	-.0378	.00053	.0077	.1045	.00057	.0075
C(30)	-.0277	.00081	.0075	-.1157	.00044	.0064	.1502	.00049	.0065
C(31)	-.1024	.00071	.0066	-.0905	.00042	.0061	.2303	.00050	.0066
C(32)	-.0678	.00062	.0057	.0110	.00039	.0057	.2683	.00042	.0055
C(33)	.3192	.00053	.0049	.2515	.00036	.0052	.4151	.00032	.0042
C(34)	.3062	.00065	.0060	.1571	.00042	.0061	.4379	.00039	.0051
C(35)	.3639	.00078	.0072	.1477	.00051	.0074	.5309	.00047	.0062
C(36)	.4332	.00072	.0066	.2308	.00055	.0080	.6005	.00042	.0055
C(37)	.4413	.00071	.0066	.3247	.00054	.0078	.5816	.00042	.0055
C(38)	.3855	.00064	.0059	.3354	.00043	.0062	.4895	.00038	.0050
C(39)	.4657	.00053	.0049	.4182	.00035	.0051	.2321	.00034	.0045
C(40)	.6024	.00056	.0052	.4345	.00041	.0059	.2844	.00044	.0058
C(41)	.7440	.00060	.0055	.5134	.00044	.0064	.2658	.00047	.0062
C(42)	.7487	.00069	.0064	.5803	.00052	.0072	.1962	.00052	.0069
C(43)	.6149	.00061	.0056	.5628	.00042	.0061	.1422	.00044	.0058

TABLE 2 (continued)

Atom	(x/a)	σ(x/a)	σ(x)Å	(y/b)	σ(y/b)	σ(y)Å	(z/c)	σ(z/c)	σ(z)Å
C(44)	.4731	.00056	.0052	.4828	.00037	.0054	.1599	.00037	.0049
F(45)	.1692	.00031	.0029	.2693	.00021	.0030	.0828	.00018	.0024
F(46)	.0972	.00031	.0029	.4317	.00019	.0028	.2546	.00019	.0025
H(47)	.0357			.3777			.0168		
H(48)	-.0700			.4179			-.1302		
H(49)	-.3444			.3645			-.1478		
H(50)	-.5183			.2754			-.0219		
H(51)	-.4159			.2354			.1256		
H(52)	-.3219			.0642			.0798		
H(53)	-.5470			-.0929			.0755		
H(54)	-.6863			-.1461			.2296		
H(55)	-.5931			-.1372			.3833		
H(56)	-.3632			.1209			.3870		
H(57)	-.0074			.1531			.4660		
H(58)	-.0694			.1852			.6407		
H(59)	-.1506			.3164			.6942		
H(60)	-.1703			.4193			.5683		
H(61)	-.1805			.3892			.3935		
H(62)	.2113			.1198			.1094		
H(63)	.1489			-.0539			.0464		
H(64)	-.0565			-.1906			.1238		
H(65)	-.1869			-.1471			.2624		
H(66)	-.1251			.0290			.3269		
H(67)	.2561			.0969			.3865		
H(68)	.3545			.0791			.5456		
H(69)	.4727			.2228			.6680		
H(70)	.4923			.3841			.6337		
H(71)	.3950			.4036			.4765		
H(72)	.5970			.3873			.3350		
H(73)	.8421			.5252			.3036		
H(74)	.8538			.6400			.1832		
H(75)	.6199			.6103			.0921		
H(76)	.3756			.4713			.1221		

TABLE 3

Final Thermal Parameters

Atom	B_{11}*	B_{22}	B_{33}	B_{12}	B_{13}	B_{23}
C(1)	.0153(7)	.0072(3)	.0050(2)	.0072(7)	-.0000(6)	.0022(4)
C(2)	.0135(6)	.0063(3)	.0064(2)	.0089(7)	.0012(6)	.0021(4)
C(3)	.0152(7)	.0072(3)	.0066(3)	.0084(7)	-.0021(7)	.0022(4)
C(4)	.0133(6)	.0081(3)	.0058(2)	.0108(7)	.0008(6)	.0018(4)
C(5)	.0155(7)	.0068(3)	.0057(2)	.0098(7)	.0010(6)	.0016(4)
C(6)	.0130(6)	.0074(3)	.0059(2)	.0092(7)	-.0005(6)	.0014(4)
C(7)	.0138(7)	.0074(3)	.0064(2)	.0088(7)	.0006(7)	.0031(4)
C(8)	.0131(6)	.0075(3)	.0062(2)	.0089)7)	.0004(6)	.0014(4)
C(9)	.0188(8)	.0078(3)	.0065(3)	.0125(8)	-.0024(8)	.0017(5)
C(10)	.0201(9)	.0090(4)	.0080(3)	.0116(9)	-.0007(9)	.0041(5)
C(11)	.0308(13)	.0092(4)	.0079(4)	.0187(12)	-.0006(10)	.0043(6)
C(12)	.0305(13)	.0111(5)	.0085(4)	.0229(13)	-.0081(11)	.0001(7)
C(13)	.0222(10)	.0115(5)	.0106(4)	.0153(12)	-.0084(11)	.0029(7)
C(14)	.0184(8)	.0087(3)	.0078(3)	.0104(9)	-.0048(8)	.0021(5)
C(15)	.0159(7)	.0070(3)	.0067(3)	.0091(7)	.0005(7)	.0020(4)
C(16)	.0264(11)	.0097(4)	.0066(3)	.0081(11)	-.0011(9)	.0003(6)
C(17)	.0295(13)	.0090(4)	.0109(5)	.0036(12)	-.0085(12)	-.0021(7)
C(18)	.0231(11)	.0077(4)	.0125(5)	.0027(10)	-.0035(12)	.0044(7)
C(19)	.0185(9)	.0091(4)	.0104(4)	.0093(10)	.0038(10)	.0060(6)
C(20)	.0171(8)	.0080(3)	.0072(3)	.0082(8)	.0019(8)	.0024(5)
C(21)	.0135(6)	.0075(3)	.0059(2)	.0068(7)	-.0003(6)	.0017(4)
C(22)	.0180(8)	.0099(4)	.0061(3)	.0093(9)	-.0010(7)	.0042(5)
C(23)	.0178(9)	.0139(5)	.0061(3)	.0100(11)	.0028(8)	.0048(6)
C(24)	.0191(9)	.0124(5)	.0063(3)	.0057(11)	.0024(8)	-.2000(6)
C(25)	.0219(10)	.0095(4)	.0097(4)	.0096(11)	.0063(10)	-.1500(6)
C(26)	.0172(8)	.0076(3)	.0083(3)	.0071(8)	-.0001(8)	-.1000(5)
C(27)	.0166(7)	.0076(3)	.0067(3)	.0101(8)	-.0011(7)	.0016(4)
C(28)	.0276(12)	.0087(4)	.0098(4)	.0145(11)	.0117(11)	.0028(6)
C(29)	.0443(19)	.0101(5)	.0121(6)	.0235(16)	.0128(16)	-.0003(8)
C(30)	.0325(14)	.0078(4)	.0111(5)	.0154(12)	-.0007(13)	-.0003(7)
C(31)	.0231(10)	.0072(3)	.0123(5)	.0094(10)	.0050(11)	.0042(7)
C(32)	.0193(9)	.0077(3)	.0097(4)	.0102(9)	.0067(9)	.0035(6)
C(33)	.0159(7)	.0079(3)	.0061(12)	.0100(8)	.0003(8)	.0021(4)
C(34)	.0230(10)	.0094(4)	.0082(3)	.0167(10)	-.0026(9)	.0037(6)
C(35)	.0275(12)	.0119(5)	.0097(4)	.0192(13)	.0002(11)	.0071(7)
C(36)	.0246(11)	.0150(6)	.0073(3)	.0184(13)	-.0015(10)	.0061(7)
C(37)	.0235(11)	.0137(6)	.0075(3)	.0150(13)	-.0032(10)	-.0002(7)
C(38)	.0214(9)	.0096(4)	.0071(3)	.0119(10)	-.0034(8)	.0012(5)
C(30)	.0151(7)	.0077(3)	.0067(3)	.0076(8)	-.0009(7)	.0025(5)
C(40)	.0144(7)	.0085(4)	.0104(4)	.0064(9)	-.0017(9)	.0044(6)
C(41)	.0154(8)	.0089(4)	.0118(5)	.0039(9)	-.0021(10)	.0061(7)
C(42)	.0191(9)	.0106(5)	.0119(5)	.0080(11)	.0033(11)	.0063(8)
C(43)	.0185(8)	.0089(4)	.0100(4)	.0097(9)	.0027(9)	.0060(6)
C(44)	.0172(8)	.0080(3)	.0077(3)	.0091(8)	-.0005(8)	.0047(5)
F(45)	.0188(4)	.0090(2)	.0054(1)	.0107(5)	.0005(4)	.0018(3)
F(46)	.0189(5)	.0065(2)	.0075(2)	.0089(4)	-.0008(4)	.0015(3)

*The figures in parentheses are standard deviations multiplied by 10^4.

above fluorine and hydrogen form factors were used, and the average of the Hoerni-Ibers (12) and the Berghuis, et al. (13) form factors was used for carbon.

Accuracy

The uncertainties (standard deviations) in individual positional parameters obtained by inversion of the normal equation matrices are listed in Table 2. Mean values are 0.0044 Å for the carbons of the C_8 tricyclic skeleton, 0.0048 Å for the α-phenyl carbons, 0.0056 Å for the ortho phenyl atoms; 0.0093 Å for the meta and para phenyl atoms, and 0.0029 Å for the fluorine atoms. If these groups of atoms are denoted by the subscripts s, α, o, and m respectively, the above values of σ lead to uncertainties of 0.0053 Å for the C_s-F bonds, 0.0062 Å for C_s-C_s bonds, 0.0065 Å for C_s-C_α bonds, 0.0074 Å for C_α-C_o bonds, 0.0087 Å for C_o-C_m bonds, and .0092 for C_m-C_m bonds. The mean uncertainty in the phenyl C-C bonds of 0.0085 Å may be compared with the root mean square (rms) deviation of these presumably nearly equal bonds from their mean of 1.381 Å. This rms value is 0.017 Å. The rms deviation of these 36 carbon atoms from their respective least-squares planes is 0.009 Å, compared with a mean σ of 0.0057 Å. It is known that partial diagonalization of the least squares matrix results in somewhat low standard deviations; comparison of the σ and rms values found for positions and bonds in the phenyl rings suggests that the σ's obtained from the least squares matrices should be increased by approximately 50% to give true estimates of the errors in the structure. Therefore, average values of σ = 0.0066 Å for the carbon atoms of the C_8 skeleton, 0.0072 Å for the α phenyl carbon atoms, 0.0086 Å

for the remaining phenyl atoms, and 0.0044 Å for the fluorine atoms will be adopted as meaningful estimates for the following discussion. These figures imply $\sigma(C_s-C_s)$ = 0.0094 Å, $\sigma(C_s-C_\alpha)$ = 0.0098 Å, $\sigma(C-C)$ = 0.012 Å for the remaining carbon bonds, and $\sigma(C_s-F)$ = 0.0075 Å. Approximate uncertainties in bond angles of 90° and 120° of the central skeleton derived from these positional uncertainties are 0.8° and 0.9° respectively.

Discussion of the Structure

Despite its complexity, this structure determination represents the most accurate data currently available on the structural parameters of a cyclobutane ring and, with one exception, of cyclobutene rings. Furthermore, most previous studies have utilized gas-phase diffraction of electrons and have obtained only average C-C single bond lengths. The bond lengths found in the three four-membered rings (see figure 4) in general confirm the average lengthening of bonds deduced from previous studies, but also prove that assumption that the single bonds of a substituted cyclobutane ring are equal may be far from the truth.

Dunitz and Schomaker (14) have discussed the lengthening of C-C bonds in four-membered rings, and their explanation of the effect in terms of cross-ring repulsion between the abnormally close non-bonded carbon atoms is generally accepted. They estimate the size of the effect as 0.04 Å in single bonds and 0.02 Å in double bonds. In the present study, the $C_{sp^3}-C_{sp^3}$ bonds C(1)-C(6), C(2)-C(5), and C(5)-C(6) with lengths of 1.589, 1.579, and 1.578 Å respectively, average 1.581 Å, or 0.037 Å longer than the "normal" $C_{sp^3}-C_{sp^3}$ single bond of 1.544 Å. The two $C_{sp^2}-C_{sp^2}$ double bonds C(3)-C(4) and C(7)-C(8) are both 1.357 Å

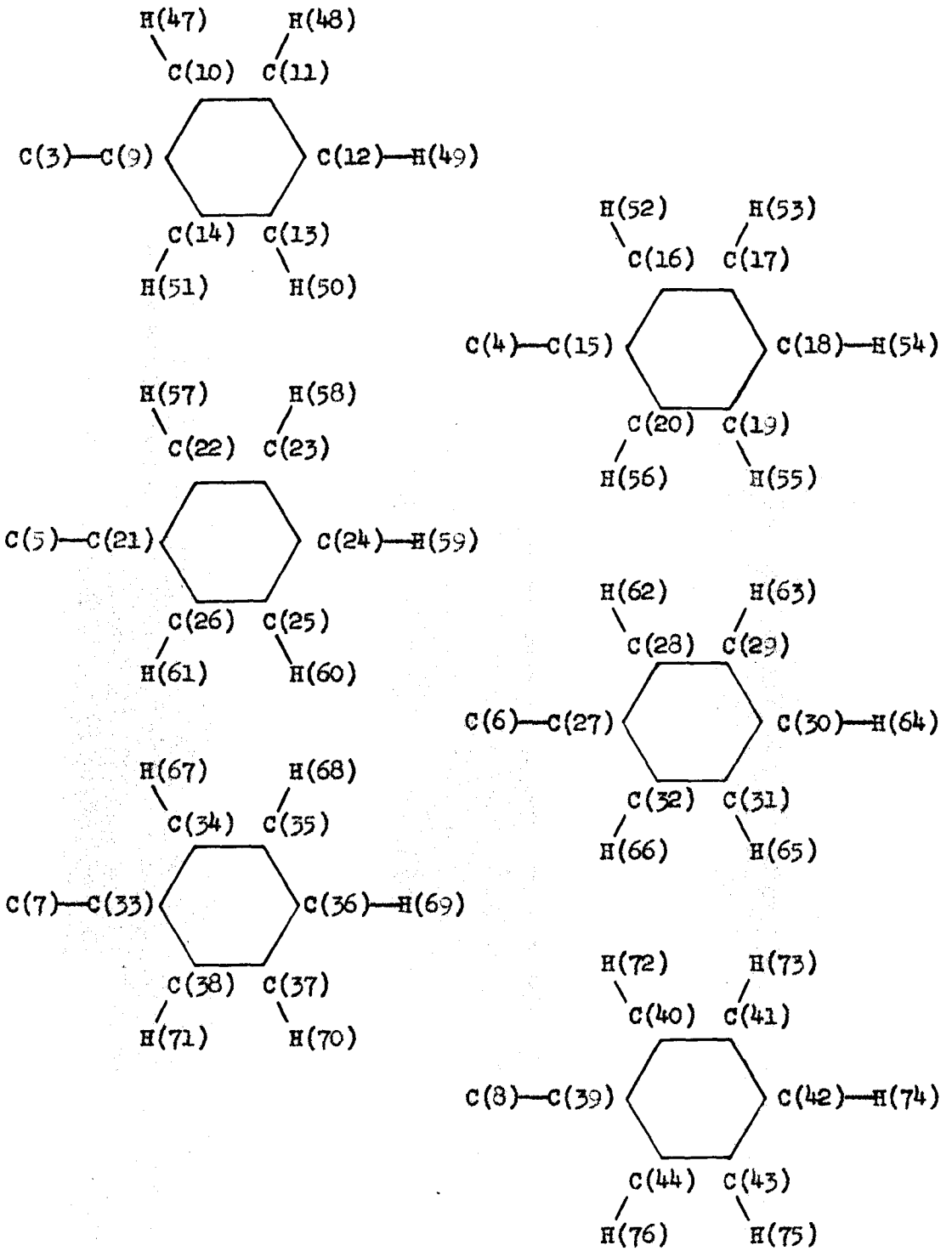

Figure 3. Phenyl Groups Numbering System.

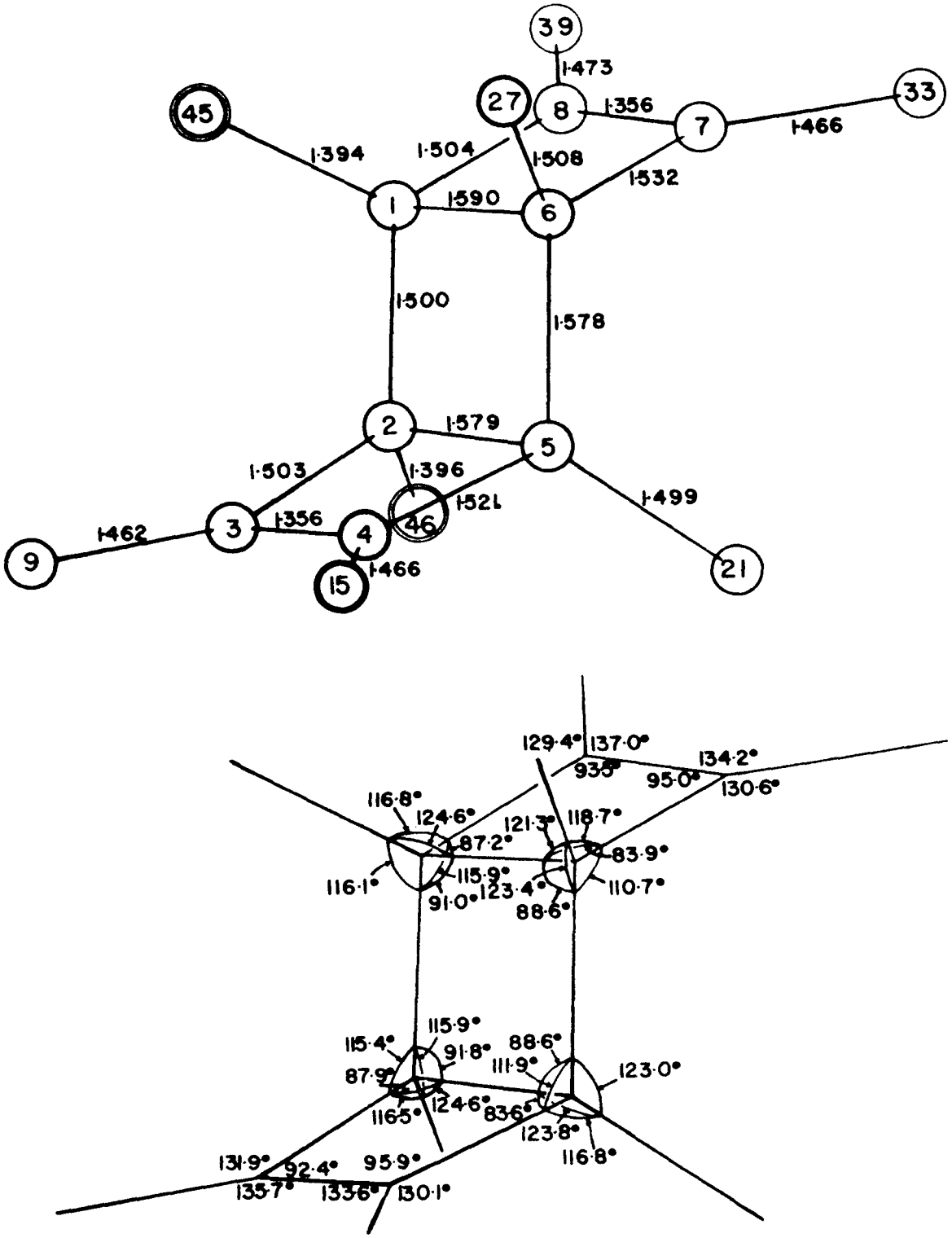

Figure 4. Bond Distances and Angles. Fluorine atoms are encircled.

in length, 0.019 Å longer than the value of 1.338 Å given recently by Dewar and Schmeisling (15) as normal. These observations fit Dunitz's and Schomaker's estimates almost perfectly. However, the remaining bonds show either no lengthening, or even shortening. The four C_{sp^2}-C_{sp^3} single bonds in the cyclobutene rings are 1.521, 1.504, 1.532, and 1.504 Å long respectively. The average of these bonds, 1.515 Å, is almost exactly the "normal" value of 1.517 Å (14). Finally, one of the C_{sp^3}-C_{sp^3} bonds in the cyclobutane ring is 1.500 Å in length, significantly shorter than the other three and even significantly shorter than the normal unconstrained value of 1.544 Å. If Dunitz and Schomaker's explanation of the lengthening observed in some of the bonds is accepted, then some other, opposing effect must be put forward to explain the absence of this lengthening in five of the ten bonds observed here.* Furthermore, the idea of cross-ring repulsion does not explain the fact that all C-C distances between the C_4 rings and the phenyl substituents are shorter than normal. The four C_{sp^2}-C_{sp^2} bonds of this type are 1.466, 1.462, 1.466, and 1.473 Å in length, averaging 1.467 Å in length, or 0.012 Å shorter than the expected value of 1.479 Å (15). The two C_{sp^3}-C_{sp^2} bonds of 1.507 and 1.499 Å average 1.503 Å, 0.014 Å shorter than the expected 1.517 Å.

---

*The cyclobutene ring in phenylcyclobutenedione (16) also shows one distance which is slightly shorter than expected. One of the C_{sp^2}-C_{sp^2} bonds in this compound is 1.463 ± 0.006 Å. The remaining distances are lengthened: C_{sp^2}=C_{sp^2}=1.358 Å, and two other C_{sp^2}-C_{sp^2} distances are 1.507 and 1.543 Å.

In view of the recent revival of respect for the importance of hybridization states in determining bond lengths, consideration should be given to the previous suggestion (17, for example) that strain in the four-membered rings forces ring bonds to have more p-character and thus external bonds to have more s-character than in unconstrained systems. Such changes in hybridization would explain both the observed lengthening of bonds within the C_4-rings and shortening of the external bonds attached to these rings. The shortening of some of the bonds within the C_4 rings can also be explained in terms of changes in hybridization ratio. The only bonds within C_4 rings showing shortening are adjacent to carbon atoms bearing fluorine substituents. In fact, the average of the two cyclobutene C_{sp^2}-C_{sp^3} bonds nearest the fluorine atoms is 1.504 Å, slightly shorter than normal, whereas the average of the corresponding two bonds on the opposite side of the molecule is 1.527 Å, 0.010 Å longer than normal. Although the latter lengthening is not statistically significant and is less than expected, it is interesting that the distortions from mirror symmetry in the cyclobutene rings have the same sense in the two rings. It is well known that the normal C_{sp^3}-F bond distance varies from 1.39 Å when one fluorine atom is bonded to the carbon, to 1.33 Å when there are three or four fluorine atoms on the same carbon. This shortening can be explained in terms of increasing s-character in the C-F bond as the number of fluorine atoms attached to the carbon increases. Bent (18) has estimated the amount of s-character in the C-F bond in CH_3F as 15-20%, compared with 25% in CF_4. The s-character in the remaining bonds in which the carbon participates must increase with a decreasing number of fluorine substituents, and thus one

TABLE 4

Bond Distances Not Given in Figure 4 (Phenyl C-C Bonds)

Atoms	Length	Atoms	Length	Atoms	Length
C(9)-C(10)	1.404 Å	C(21)-C(22)	1.390 Å	C(33)-C(34)	1.391 Å
C(9)-C(14)	1.371	C(21)-C(26)	1.404	C(33)-C(38)	1.394
C(10)-C(11)	1.414	C(22)-C(23)	1.382	C(34)-C(35)	1.394
C(11)-C(12)	1.362	C(23)-C(24)	1.360	C(35)-C(36)	1.351
C(12)-C(13)	1.366	C(24)-C(25)	1.386	C(36)-C(37)	1.384
C(13)-C(14)	1.398	C(25)-C(26)	1.392	C(37)-C(38)	1.382
C(15)-C(16)	1.358	C(27)-C(28)	1.371	C(39)-C(40)	1.373
C(15)-C(20)	1.401	C(28)-C(32)	1.398	C(39)-C(44)	1.393
C(16)-C(17)	1.373	C(28)-C(28)	1.387	C(40)-C(41)	1.371
C(17)-C(18)	1.385	C(29)-C(30)	1.380	C(41)-C(42)	1.399
C(18)-C(19)	1.360	C(30)-C(31)	1.341	C(42)-C(43)	1.357
C(19)-C(20)	1.386	C(31)-C(32)	1.399	C(43)-C(44)	1.376

TABLE 5

Bond Angles in Phenyl Rings

Angle	Value	Angle	Value	Angle	Value
10,9,14	119°	22,21,26	118°	34,33,38	118°
9,10,11	121°	21,22,23	121°	33,34,35	121°
10,11,12	119°	22,27,24	121°	34,35,36	120°
11,12,13	121°	23,24,25	119°	35,36,37	120°
12,13,14	121°	24,25,26	121°	36,37,38	120°
13,14,9	120°	25,26,21	120°	37,38,33	120°
16,15,20	118°	28,27,32	118°	40,39,44	119°
15,16,17	122°	27,28,29	121°	39,40,41	120°
16,17,18	120°	28,29,30	121°	40,41,42	120°
17,18,19	119°	29,30,31	118°	41,42,43	120°
18,19,20	121°	30,31,32	123°	42,43,44	120°
10,9,3	121°	22,21,5	122°	34,33,7	121°
14,9,3	120°	26,21,5	120°	38,33,7	121°
16,15,4	121°	28,27,6	121°	40,39,8	120°
20,15,4	121°	32,27,6	121°	44,39,8	121°

TABLE 6

Closest Intermolecular Approaches*

H-H distances ≤ 3.0 Å

Atoms	Dist.	Atoms	Dist.	Atoms	Dist.
$52\text{-}63^{C}_{J}$	2.31 Å	$64\text{-}52^{C}_{D}$	2.31 Å	$73\text{-}61^{F}_{I}$	2.35 Å
$53\text{-}50^{J}$	2.95	$65\text{-}58^{F}$	2.99	$74\text{-}47^{I}$	2.82
$53\text{-}52^{D}$	2.57	$67\text{-}55^{F}$	2.82	$74\text{-}48^{K}$	2.52
$55\text{-}68^{H}$	2.73	$68\text{-}55^{D}$	2.72	$74\text{-}64^{E}$	2.46
$58\text{-}54^{H}$	2.70	$68\text{-}66^{D}$	2.72	$75\text{-}49^{E}$	2.78
$58\text{-}55^{B}$	2.95	$69\text{-}65^{A}$	2.59	$75\text{-}50^{E}$	2.49
$59\text{-}48^{B}$	2.54	$71\text{-}71^{F}$	2.66	$76\text{-}49^{I}$	2.50
$59\text{-}49^{H}$	2.92	$72\text{-}61^{A}$	2.20	$76\text{-}75$	2.93
$59\text{-}54$	2.60	$73\text{-}59$	2.81		

H-F distances ≤ 3.0 Å

$45\text{-}64^{C}$	2.87	$46\text{-}48^{E}$	2.47	$46\text{-}60^{G}$	2.87

H-C distances ≤ 3.2 Å

$10\text{-}48^{E}_{F}$	3.20	$54\text{-}23^{H}_{H}$	3.19	$67\text{-}19^{F}_{D}$	3.06
$40\text{-}61^{F}$	2.83	$54\text{-}24^{H}$	3.13	$68\text{-}19^{D}$	2.93
$41\text{-}61^{I}$	2.90	$55\text{-}23^{D}$	3.20	$68\text{-}20^{D}$	3.17
$48\text{-}42^{E}$	3.06	$58\text{-}31^{B}$	3.13	$69\text{-}18^{R}$	3.16
$49\text{-}43^{E}$	3.08	$59\text{-}11^{C}$	3.05	$79\text{-}39^{A}$	3.06
$49\text{-}44^{J}$	2.94	$63\text{-}16^{D}$	3.20	$70\text{-}40^{A}$	3.16
$53\text{-}13^{J}$	2.82	$65\text{-}35^{D}$	3.14	$70\text{-}43^{A}$	3.20
$53\text{-}14^{A}$	2.89	$65\text{-}36^{I}$	2.81	$70\text{-}44^{E}$	3.08
$73\text{-}24^{A}$	2.85	$74\text{-}11^{E}$	3.08	$76\text{-}12^{E}$	3.05
$73\text{-}25$	3.11	$75\text{-}13^{E}$	3.10		

C-C distances ≤ 3.6 Å

$11\text{-}10^{E}_{J}$	3.51	$34\text{-}19^{F}$	3.59	$40\text{-}14^{F}$	3.58
$17\text{-}13^{J}$	3.57				

F-C distance ≤ 3.6 Å

$45\text{-}30^{C}$	3.50				

*Absence of superscript indicates an atom in the molecule at (x,y,z) with parameters listed in Table 2. Superscript indicates a symmetry-related atom with the following code: A, [(1-x), (1-y), (1-z)]; B, [x,y,(1+z)]; C, [-x, -y, -z]; D, [-x, -y, (1-z)]; E, [-x, (1-y), -z]; F, [(1+x), y,z]; G, [-x, (1-y), (1-z)]; H, [(-1-x), -y, (1-z)]; I, [(1-x), (1-y), -z]; J, [(-1-x), -y, -z]; K, [(1+x), (1+y), z].

or more of these bonds must be shortened. The surplus of s-character to be divided among the three C-C bonds in the present case should be similar to that estimated by Bent for CH_3F because the C-F bonds are nearly equal (1.395 and 1.391 Å) in the two compounds. That this effect is of sufficient size to account for at least most of the shortening of the C(1)-C(2) bond and probably also of C(2)-C(3) and C(1)-C(8) is seen when it is realized that a change of 8% in s-character between sp^3 and sp^2 hybridization changes the length of a carbon-carbon bond by 0.065 Å. If in the present case, a small amount of the surplus s-character on carbons (1) and (2) enters the C(1)-C(2) and C(2)-C(3) bonds, and the major part enters the C(1)-C(2) bond, the observed deviations from normalcy are at least qualitatively explained. Why the C(1)-C(2) bond is so extremely short is not clear. Additional accurate experimental data on the length of C-C bonds in the configuration F-C-C-F would be very valuable in clarifying this point.

The C-F bonds of 1.394 and 1.396 Å compare well with other recent determinations in similar compounds (1.391 and 1.385 Å in CH_3F (19,20); 1.379 Å in CH_3CH_2F (21); 1.43 ± 0.02 Å in $(CH_3)_3CF$ (22)). The C-C bonds in the latter two compounds are also short: 1.533 Å in CH_3CH_2F and 1.516 ± 0.005 Å in $(CH_3)_3CF$. A slight shortening is also observed in the pair of compounds $H_2C{=}CH_2$ (1.337, 1.339 Å (23)) and FHC=CHF (1.324 ± 0.005 Å (24)).

The angles between least squares planes P1 and P2, and between P1 and P3 (see table 7 for atoms defining each plane), the mean planes of the various C_4 rings, are 113°40' and 113°20' respectively. These should be regarded as only approximate values, however, because the mean deviation

TABLE 7

Least-Squares Planes*

Plane	Atoms used to calculate plane	cos A	cos B	cos C	Distances from plane Atom	D	Atom	D
P1	1,2,5,6	-.45238	-.30305	-.65250	1	-0.005	5	-0.005
					2	0.005	6	0.005
P2	2,3,4,5	.63400	-.72563	-.50075	2	0.016	5	-0.015
					3	-0.018	9	-0.080
					4	0.018	15	0.190
P3	1,6,7,8	.63828	-.72756	-.49582	1	-0.027	8	0.031
					6	0.026	33	-0.194
					7	-0.031	39	0.108
P4	9,10,11,12,13,14	.28785	-.85631	-.40263	9	0.010	13	-0.006
					10	-0.003	14	-0.006
					11	-0.009	3	0.034
					12	0.014		
P5	15,16,17,18,19,20	-.86060	.79860	-.23941	15	-0.006	19	0.003
					16	0.008	20	0.001
					17	-0.004	4	-0.054
					18	-0.001		
P6	21,22,23,24,25,26	-.75591	-.25394	-.13747	21	0.003	25	-0.001
					22	-0.003	26	0.000
					23	0.002	5	0.135
					24	0.001		
P7	27,28,29,30,31,32	-.77715	.40196	-.65109	27	-0.004	31	-0.007
					28	-0.006	32	0.010
					29	0.009	6	-0.017
					30	-0.002		
P8	33,34,35,36,37,38	.88416	-.14416	-.39799	33	0.018	37	-0.012
					34	-0.011	38	-0.007
					35	-0.008	7	0.007
					36	0.019		
P9	39,40,41,42,43,44	.47700	-.66353	-.63526	39	-0.010	43	0.010
					40	-0.002	44	0.006
					41	0.018	8	0.026
					42	-0.022		

*A, B, and C are the angles between the plane normal and the unit cell vectors a, b, and c respectively. D is the distance of the given atom from the plane.

of a given atom from planes P2 and P3 is 0.023 Å, and thus the cyclobutene rings are not really planar. The various C-C-C angles which should approximately equal these interplanar angles are: angle 1,2,3 = 115.4° (P1,P2); angle 8,1,2 = 115.9° (P1,P3); angle 6,5,4 = 111.9° (P1,P2); and angle 7,6,5 = 110.7° (P1,P3). The angles on the "fluorine side" of the molecule are nearly equal and those on the opposite side are also nearly equal, but differ significantly (about 4.3°) from the former pair. This difference probably reflects the hybridization change of carbons (1) and (2). This factor and possibly steric repulsion, between neighboring phenyl groups, to be discussed more fully later, probably are responsible for the non-planar cyclobutene rings. The cyclobutane ring is accurately planar, with a maximum deviation from planarity of 0.005 Å.

Table 7 lists the least squares planes of the six phenyl rings, P4-P9, together with planes P1-P3. (Figures 3 and 4 relate the phenyl rings to the C_8 skeleton.) These planes were computed on the Burroughs 220 computer with a program written by Mr. Noel Jones. The maximum deviation from planarity of the phenyl carbon atoms is 0.022 Å, a statistically insignificant distance. The many close approaches between atoms in this molecule do result in the distortion of other relationships normally observed in phenyl rings. Many of the atoms to which the phenyl groups are attached are significantly out of the planes of these rings. The phenyl carbon atoms attached to the cyclobutene rings are also far out of the mean planes of these latter rings. C(3) is found to be 0.034 Å from P4; C(4) is 0.054 Å from P5; C(5) is 0.135 Å from P6; and C(8) is 0.026 Å from P9. C(7) is accurately in plane P8, and C(6) is only 2σ from P7. The phenyl carbon atoms attached to the two cyclobutene rings are on

opposite sides of the planes of these rings; they are -0.080 and +0.190 Å from P2 and -0.194 and +0.108 Å from P3. These distortions are certainly caused by the close approaches of the phenyl rings. It is interesting to note, in comparison with this out-of-plane distortion, that apparently no in-plane distortion of the C=C-C angles external to the cyclobutene rings is caused by the cis phenyl substituents. The mean C=C-C external angle observed here is 135.1°, almost the same as that found (135.3°) by Wong, Marsh, and Schomaker (16) in phenylcyclobutenedione.

In addition to the distortions from planarity just mentioned, the presence of cis phenyl substituents on the cyclobutene rings causes the phenyl groups to twist out of the plane of the C_4 rings. These twists can be approximately described by the angles between the normals of the phenyl rings and of the mean cyclobutene planes. Angle P2, P4 is 26.9°; angle P2, P5 is 45.7°. Angle P3, P8 is 48.0°, and angle P3, P9 is 12.1°. The twists of the phenyl groups joined to a single cyclobutene ring have the same sense, as is required by steric factors.

Viewed along the molecule's approximate 2-fold axis, the four phenyl rings attached to carbons 4, 5, 6, and 7 are seen to possess a "propeller" configuration, if allowance is made for the fact that the four "blades" are attached at the vertices of a rhombus rather than of a square. Neither examination of a model nor consideration of very short intramolecular distances makes it clear whether this configuration is required in an isolated molecule. There are many intramolecular C···C distances between 3.0 and 3.3 Å which could be lengthened by rotation of phenyl groups. In the cases of rings C(21)-C(26) and C(27)-C(32), some of these very short distances would be made even shorter by rotation in either direction. The

remaining four phenyl rings would be allowed free rotation over fairly large angles in an isolated molecule. Their configuration in the solid state are thus largely determined by intermolecular packing.

A major feature of the "propeller" packing arrangement--the close approach of a hydrogen atom on one phenyl ring to the center of another ring--is observed many times in intermolecular as well as intramolecular packing in HPT. Within a single molecule there are five of these "nestings" of hydrogen "eggs" by phenyl groups. H(57) is 2.85, 2.88, 3.59, and 3.48 Å from carbons 33, 34, 35, and 38; H(56) is 2.77, 2.99, 3.01, and 3.16 Å from carbons 21, 22, 23, and 26. H(66) is 2.87, 3.50, 3.57, and 2.91 Å from carbons 15, 16, 19, and 20; carbons 27, 28, and 32 "nest" hydrogen (67) at distances of 2.86, 3.38, and 3.10 Å; and carbons 33, 37, and 38 act as a "nest" for hydrogen (72) at distances of 2.77, 3.58, and 2.73 Å. These are all <u>ortho</u> hydrogens with respect to the points of attachment of the phenyl rings to the central C_8 skeleton. <u>Meta</u> atoms of four of the phenyl rings show intermolecular nesting in the same fashion. Thus, H(70) is 3.06, 3.16, 3.28, 3.26, 3.20, and 3.08 Å respectively from carbons B-39 to B-44 (see table 6 for explanation of labelling of symmetry-related molecules). H(53) is 3.50, 3.38, 2.82, and 2.89 Å from carbons P-10, 12, 13, and 14; carbons C-37, 38, and 39 "nest" H(65) at distances of 3.14, 2.81, and 3.51 Å respectively, and carbons B-23, B-24, and B-25 do the same for H(73). Thus, "nesting" of this type plays a major role in the packing of the molecules. Figure 5 is a drawing of packing models of HPT, two unit cells high and wide, and one unit cell deep, projected down the <u>a</u>-axis. Examination of this figure will show the importance and manner of "nesting" between the various phenyl rings.

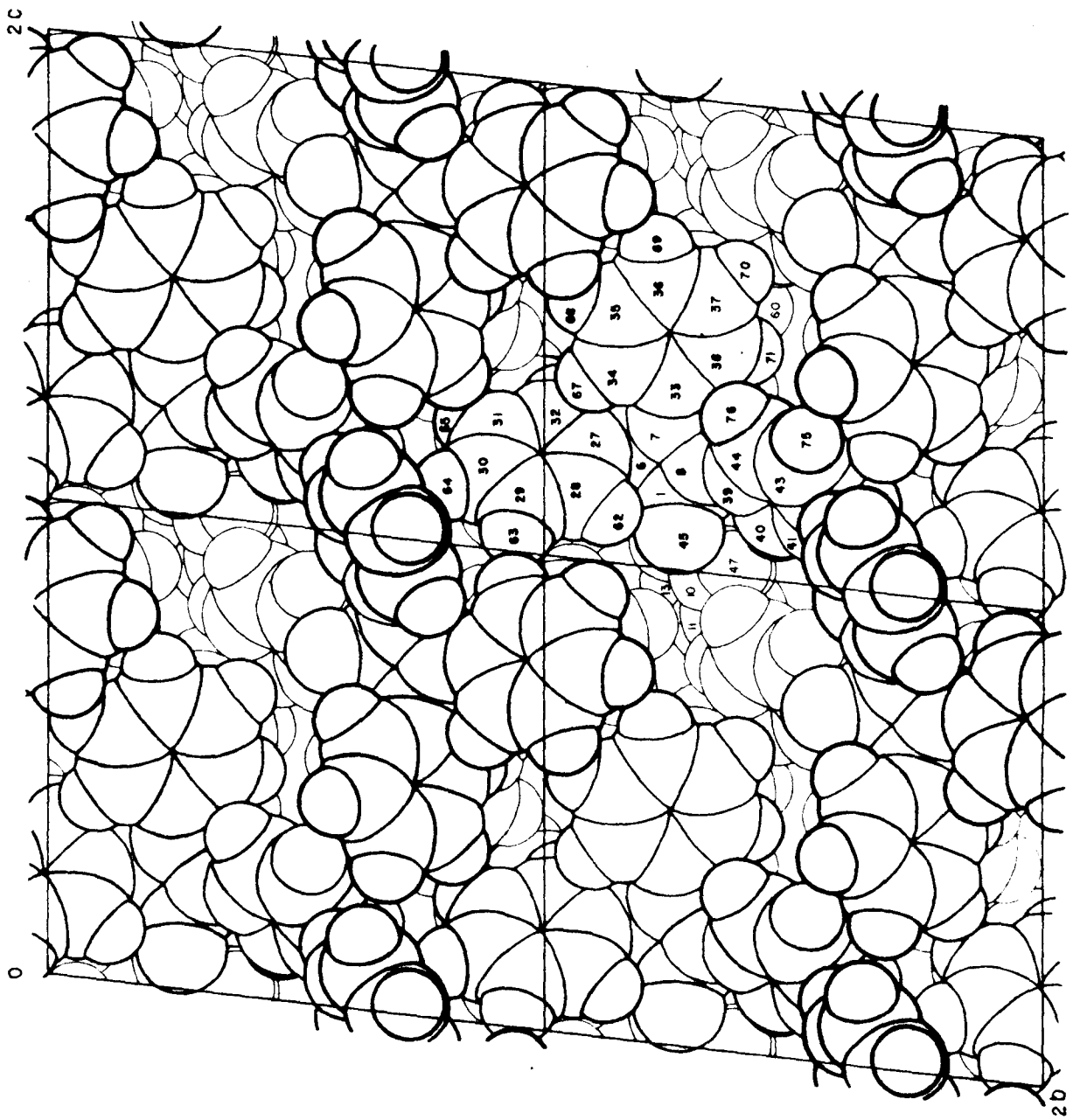

Figure 5. $C_{44}H_{30}F_2$ Packing Drawing.

The visible atoms of one molecule are labelled.

Table 6 lists the closest approaches between molecules. None of these is abnormally short.

Conclusions

This study has proved the structure of the dimer $C_{44}H_{30}F_2$ reported by Kitahara, et al. (1) to be anti-1,2-difluoro-3,4,5,6,7,8-hexaphenyl-tricyclo[4·2·0·$0^{2,5}$]-octa-3,7-diene. The central $C_{14}F_2$ rigid framework displays symmetry 2(=C_2) within experimental error, but the amounts of rotation of the phenyl rings about their bonds of attachment to the tricyclic skeleton do not obey this symmetry. A lengthening of the average C-C bond in the C_4 rings in comparison with the value expected for unconstrained bonds is found, but the amount of this lengthening varies from bond to bond, thus warranting reexamination of Dunitz's and Schomaker's attribution (14) of this lengthening to cross-ring repulsion. The C-C bond in the configuration F-C-C-F is abnormally short, 1.500 ± 0.009 Å, particularly for a bond in a cyclobutane ring. This shortening is attributed to change in hybridization of the carbon atoms by the attached fluorine atoms. The cyclobutane ring in the dimer is accurately planar, but the two cyclobutene rings are not. Intramolecular crowding and the above-mentioned change in carbon hybridization by fluorine are probable causes of the lack of planarity of the cyclobutene rings.

TABLE 8. Observed and Calculated Structure Factors

Each group of three columns lists ℓ, $10F_o$, and $10F_c$, and is headed by the common values of h and k for the group. Negative numbers in the $10F_o$ column are $10F_{min}$ for unobserved reflections. Asterisks identify reflections omitted from the final least squares calculations.

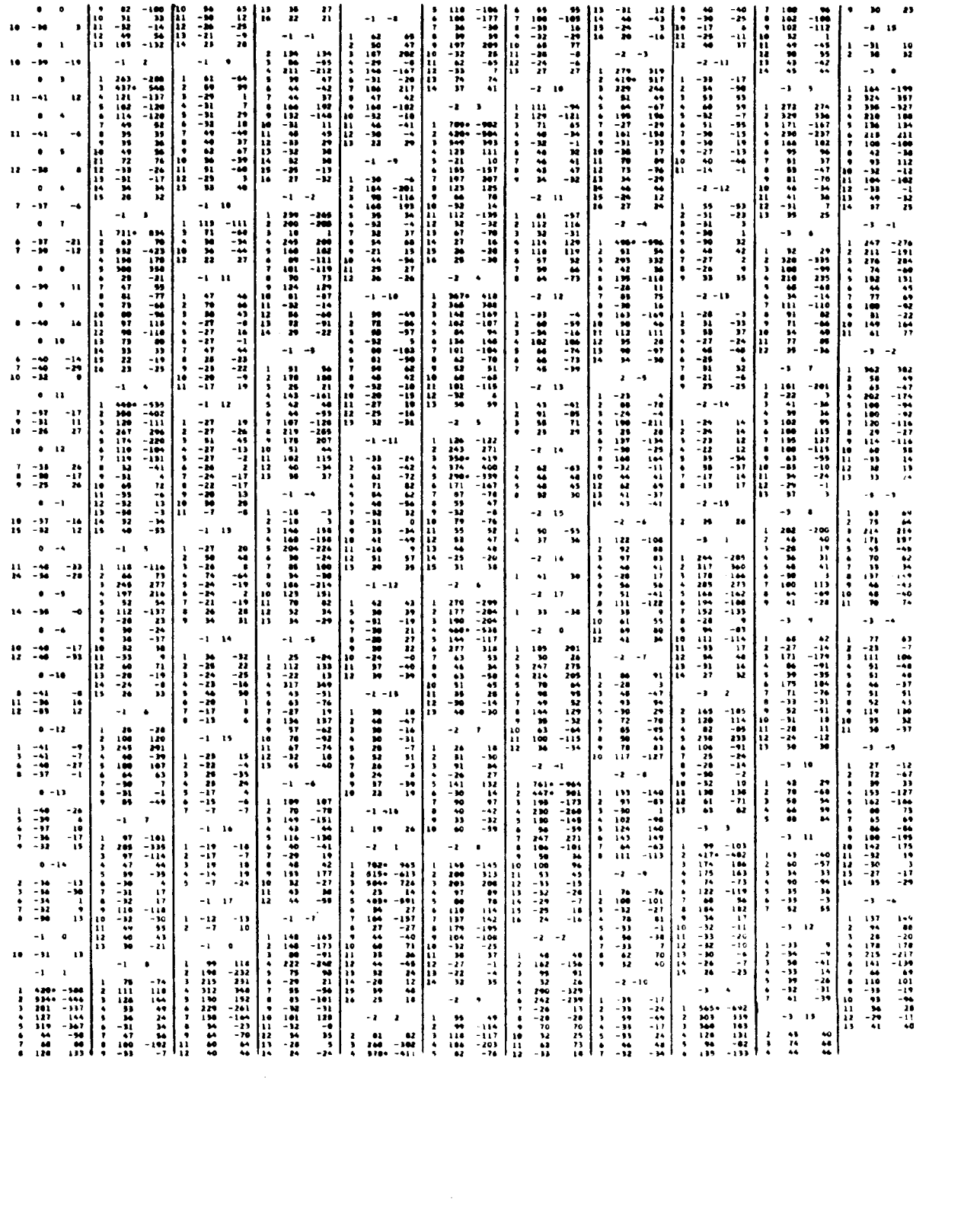

TABLE 8 (continued)

THE CRYSTAL STRUCTURE OF BIS-(2-BROMOPYRIDINE)-DODECAHYDRODECABORANE

INTRODUCTION

Some time after the determination of the molecular structures of the boron hydrides, attention shifted to the structures of derivatives of these compounds, which were then being prepared. The first derivatives of decaborane, $B_{10}H_{14}$, were halides of formulas $B_{10}H_{12}X_2$ and $B_{10}H_{13}X$, with X = I or Br. Schaeffer (25) showed $B_{10}H_{12}I_2$ to be a substitution derivative with the iodine atoms in positions 1 and 4 (standard $B_{10}H_{14}$ numbering system; see (26)). Further work has shown that all of these halogen derivatives are probably formed by substitution of one or more of the "lower" hydrogen atoms in positions 1, 2, 3, and 4. Somewhat later, examples of a second class of compound of the general formula $B_{10}H_{12}R_2$, in which R is an electron donor, appeared. Reddy and Lipscomb (26) soon showed that $B_{10}H_{12}(NCCH_3)_2$ could not be considered a substitution derivative of $B_{10}H_{14}$ because B-B bond lengths and hydrogen atomic positions are different from those in $B_{10}H_{14}$. They conclude that the new series of $B_{10}H_{12}R_2$ compounds should be regarded as substitution derivatives of $B_{10}H_{14}^{-2}$, in which the R-groups replace H^- ions in the 6 and 9 positions.

When Burkardt and Fetter (27,28) obtained a stable crystalline complex between decaborane and pyridine and were able to prove that this complex loses two moles of hydrogen at elevated temperatures, presumably to form a compound of the $B_{10}H_{12}R_2$ type, but is very stable at room temperature, interest was immediately aroused by the possibility of determining the molecular structure of a member of this possibly new class of boron compound. Drs. Fetter and Burkardt supplied a sample of

an equally stable complex prepared in the same manner as the pyridine complex, but containing 2-bromopyridine rather than the unsubstituted material. This compound unfortunately was not subjected to the same series of tests for hydrogen loss as the parent compound; when a satisfactory trial model for the structure had been determined and partly refined, the B-B distances and the locations of the nitrogen atoms resembled very closely the corresponding features in $B_{10}H_{12}(NCCH_3)_2$. A difference Fourier map computed at this stage, although inconclusive, also seemed to show bridge hydrogen atoms in the positions found in the acetonitrile compound. Further chemical investigation by Dr. Fetter (29) showed that the complex $B_{10}H_{14}\cdot 2(C_5H_4NBr)$ which may be formed at low temperatures loses two moles of hydrogen below room temperature to form $B_{10}H_{12}(C_5H_4NBr)_2$, the material which is the subject of this investigation. By the time this disappointing news was available, the crystal structure refinement was virtually complete. It therefore furnishes a confirmation of Reddy and Lipscomb's determination of the altered hydrogen locations in the borohydride portion of the molecule and an indication that the altered structure is common to all members of the $B_{10}H_{12}R_2$ series of compounds prepared in fashions similar to $B_{10}H_{12}(NCCH_3)_2$. About the time the true molecular formula for $B_{10}H_{12}(C_5H_4NBr)_2$ became known, a determination of the crystal structure of $B_{10}H_{12}[S(CH_3)_2]_2$ (30) appeared in print, also showing the borohydride skeleton found in diacetonitrile-dodecahydrodecaborane.

The sudden proliferation of $B_{10}H_{12}R_2$ crystal structure determinations makes this investigation of less importance than was initially expected, but this work does provide comment on one structural point

not touched by either of the two previously published structures. Graybill and Hawthorne (31) have attributed the colors of complexes between decaborane and various substituted pyridines to a mechanism involving extension of the π-electron system of the pyridine ligand into the borohydride skeleton. The location of the pyridine rings in the $B_{10}H_{12}(C_5H_4NBr)_2$ structure (hereafter called DBBY) shows π-overlap of the kind proposed by Graybill and Hawthorne to be of little, if any, importance in determining the molecular configuration about the B-N bonds. Rather, hydrogen-hydrogen and bromine-hydrogen contacts between the borohydride and pyridine parts of the molecule and possibly, in the crystal, intermolecular packing requirements determine the configuration at these points.

EXPERIMENTAL DATA

Unit Cell and Space Group

All of the material used in this investigation was obtained from one of two samples supplied by Drs. Burkardt and Fetter. One of these samples was macrocrystalline and consisted of a few tablet-shaped crystals up to 3 mm in maximum length mixed with a much greater number of multiply twinned needles. The only single crystals found were the tablets, and fragments of these were used for all photographs. The second of the original samples was a bright yellow powder which was recrystallized from acetone-carbon tetrachloride mixtures to give more of the orange-yellow macrocrystals. With less than about 20% by volume of $CC\ell_4$ in the solvent, only the needles (again invariably twinned) were obtained, and in a solvent mixture containing more than about 50% $CC\ell_4$, much of the complex decomposed to give a yellow oil and clear crystals. The untwinned tablets, together with needles, were obtained from solvent mixtures of about 40% $CC\ell_4$ and 60% acetone.

Most of the tablets were approximately the shape of bricks, with {100} present as the largest faces, and {010}, the smallest. Frequently faces {011} and $\{01\bar{1}\}$ were also developed; in a few cases these were as large as {010}.

An ($h0\ell$) Weissenberg film prepared with CuKα radiation and ($0k\ell$) and ($hk0$) precession photographs exposed with MoKα radiation, together with ($h1\ell$) through ($h7\ell$) equi-inclination Weissenberg photographs taken to identify systematic extinctions, were used to obtain a preliminary unit cell. Refined values of $a = 13.710 \pm 0.006$ Å, $c = 30.087 \pm 0.012$ Å,

and $\beta = 90°56' \pm 01'$ were obtained from least squares fitting of the $\sin^2\theta$ values of 19 high-order reflections measured on a precision zero layer [010] Weissenberg film exposed in the Straumanis arrangement. For this determination, the $K\alpha_1$ wavelength of copper was assumed to be 1.54050 Å. A refined value of $b = 9.011 \pm 0.012$ Å was obtained from an (hk0) precession photograph, using the value of a^* for calibration.

The density of the compound was determined by the flotation method using a CCl_4-EtBr-EtI mixture, and was found to be 1.560 ± 0.003 gm/cm^3. The theoretical density, assuming eight molecules of $B_{10}H_{12}(C_5H_4NBr)$ per unit cell, is 1.561 ± 0.002 gm/cm^3.

The monoclinic unit cell and 2/m Laue symmetry, together with the systematic extinctions

$$hk\ell \text{ with } h + k + \ell = 2n + 1$$

$$h0\ell \text{ with either } h = 2n + 1 \text{ or } \ell = 2n + 1$$

define the probable space groups to be Ic or I2/c. The presence in the (h0ℓ) Patterson projection of two single and two double bromine-bromine vectors, as required by the presence of two independent bromine atoms in a cell of I2/c symmetry, rather than six single vectors as expected with four independent bromine atoms obeying only Ic symmetry requirements, indicated I2/c to be the proper choice of space group. This choice has been shown to be correct by the success of the structure determination. The asymmetric unit thus consists of one complete molecule, and no molecular symmetry is required.

Intensity Data

A General Electric XRD-5 diffraction unit, together with an SPG goniostat, served for collection of all of the intensity data used for this structure determination. For this purpose, a large crystal from the original sample of crystalline material was selected and ground to as nearly spherical a shape as possible. The resulting ball was 0.15 mm. in diameter, with a maximum error of less than about 8% in radius. Molybdenum Kα radiation, filtered through zirconium filters, was used for collection of the intensity data. Although it was realized that other methods are more accurate, the stationary crystal-stationary counter method was used because of the almost prohibitive time required by the other techniques.

Furnas (32) discusses the equipment specifications necessary for the use of the stationary crystal-stationary counter method of intensity measurement. Briefly, these are a uniformly sensitive X-ray detector large enough to collect all the radiation diffracted by the crystal (for the wavelengths of interest) and a uniform X-ray source of sufficient area to allow simultaneous satisfaction of the diffraction conditions for all the mosaic blocks in the crystal specimen.

The window of the proportional counter was scanned with a very narrow X-ray beam, and was adjusted so that an area about 1.1° wide which was uniformly responsive to within less than 1% in intensity was centered in the direct beam with the 2θ dial set equal to zero. The distribution of X-ray intensity across the source was measured with a tiny crystal of DBBY and a very narrow counter aperture, and was found

to be constant within 3%. As Figure 6 shows, the angular width of the source and of the counter necessary to satisfy the stationary crystal-stationary counter requirements is given by the sum (in angular measure at the source and counter positions with reference to the crystal as arc vertex) of the crystal diameter, the mosaic spread, the dispersion of the α_1 and α_2 radiation peaks, the separation of α_1 from α_2, and, if settings are calculated, a tolerance for setting error. In the present case, the crystal diameter of 0.15 mm. is equivalent to 0.060° on the circle representing possible counter positions. Experimentally, the sum of the crystal width, mosaic spread, α_1 and α_2 peak dispersion, and α_1-α_2 separation was found to be 0.25° in 2θ by a scan through the (008) reflection with a very narrow slit at the counter and a very small (0.6°) take-off angle at the X-ray source. At this reflection angle (2θ = 10.89°), the α_1-α_2 separation amounts to 0.060° (32, p. 79) and should be subtracted from 0.25° to give a measure of the remaining terms. Of these terms, only the α_1 and α_2 peak dispersions are functions of 2θ, and these are negligible, increasing from 0.005° at 10° (2θ) to 0.024° at 50° (30, p. 80). A take-off angle of 5.6° at the X-ray source, giving an effective source angular width of 0.69°, and an allowed setting tolerance of 0.20°, will thus allow maximum α_1-α_2 separation of (0.69-0.19-0.20-0.02) = 0.28°. According to Furnas (30), Table VII-3, p. 79, the α_1-α_2 separation of MoKα radiation at 2θ = 40° is about 0.25°. Therefore it was concluded that the above experimental arrangement was adequate to allow collection of α_1 and α_2 integrated intensities from the crystal used, for all 2θ values under 40°. The counter area of uniform sensitivity, 1.1°, greatly exceeded the required 0.69° width. For scattering

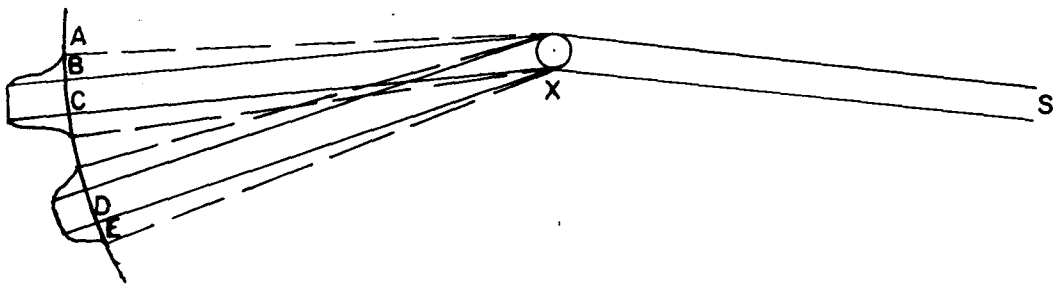

Figure 6. Diffraction Geometry.

AB = 1/2 of mosaic spread + 1/2 α_1 peak dispersion

BC = crystal width

CD = α_1-α_2 separation

DE = 1/2 of mosaic spread + 1/2 α_2 peak dispersion

S = X-ray source

X = crystal

angles of less than 40°, the counter was set at 1/2 $(2\theta_{\alpha_1} + 2\theta_{\alpha_2})$. If this mean exceeded 40°, the counter was set at $2\theta_{\alpha_1}$ and an empirical correction was made for the diffracted intensity lost by lack of a sufficiently wide X-ray source.

To determine the correction factor $S(2\theta)$, for the fraction of intensity lost because of α_1-α_2 separation, the diffracted intensity of a strong reflection at low scattering angle, where the separation could be neglected, was traced as a function of 2θ using the adopted take-off angle of 5.6° and with a very narrow slit at the detector. The integral of the intensity, $I(2\theta) = K \int_{2\theta_o}^{2\theta} I'(2\theta')d(2\theta')$, where $2\theta_o$ represents the minimum value of 2θ at which intensity above background was detected, $2\theta'$ is allowed to range only over the interval at which intensity from the reflection was measurably above background, and I' represents the intensity collected through the narrow slit at the angle $2\theta'$, was determined graphically, scaled to a maximum of 0.5, and plotted against 2θ as a function of the α_1-α_2 separation at 2θ. That is, $S(2\theta) = I(\psi(2\theta))$, where ψ is $(2\theta_{\alpha_2} - 2\theta_{\alpha_1})$. Figure 7 shows the resulting graph. For reflections with scattering angles greater than 40°, the intensity actually measured was multiplied by $(1 + S(2\theta))$ to give the total intensity expected from both the α_1 and α_2 radiation peaks.

The background scattering from the crystal was determined as a function of 2θ for twelve different orientations of the crystal. The resulting functions varied by no more than about 10% from a mean function, for any given value of 2θ. Background corrections were calculated from the mean function and were not measured for each reflection.

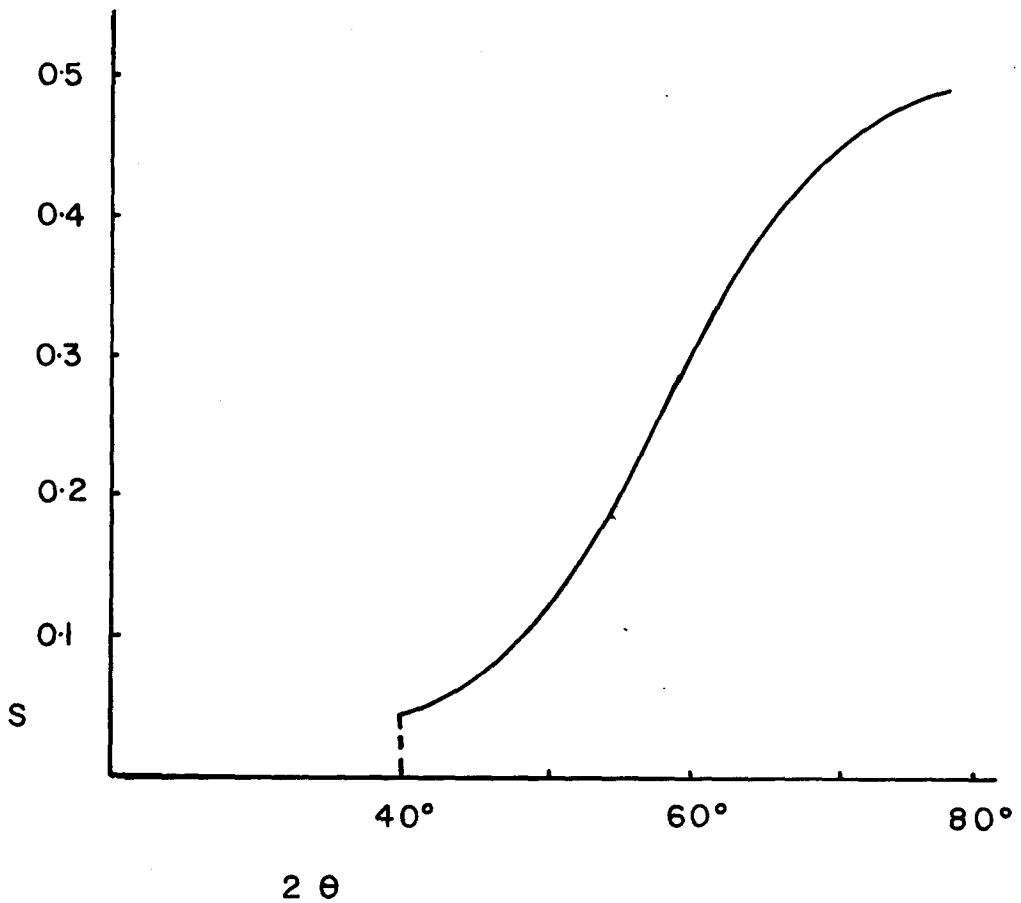

Figure 7. Correction Factor for Partial Loss of α_2 Reflection.

The day-to-day fluctuations in intensity of a single reflection (008), were used to obtain daily scale factors for correlation of data collected at different times. The variation in this reflection did not exceed 2%. Hourly fluctuations were even smaller and were neglected. There was no systematic drift in intensity, but the precaution of allowing the X-ray tube and all counting circuits to warm up for at least 15 minutes before use was observed.

When about two-thirds of the data within the copper diffraction sphere had been collected, the first X-ray tube became faulty, and a second one was used to finish the data collection. The background was remeasured with this tube and found to be slightly higher than with the former tube. The S-correction was assumed to be the same for the two tubes.

With the General Electric diffractometer and the manner in which the crystal was mounted, the most convenient sequence of data collection was to follow rows parallel to c^*. Data collection proceeded systematically in this manner until the crystal was accidentally knocked from the instrument and lost. Because the instrument was to be accessible for only a few more days, it was not deemed feasible to attempt to prepare and mount another crystal. At the time the crystal was lost, 2398 reflections had been measured, covering about 95% of the copper diffraction sphere. The uncollected data are $(5,6,\ell)$, $(5,7,\ell)$, $(6,7,\ell)$, $(7,5,\ell)$, $(7,6,\ell)$, $(8,5,\ell)$, $(9,4,\ell)$, $(9,5,\ell)$, and $(11,4,\ell)$ for all non-zero values of ℓ within the copper diffraction sphere.

A program (SPGLP, see the Appendix) was written in Fortran for the IBM 704 computer for extraction of $|F_o|^2$ and $|F_o|$ values from the experimental data. This program calculates the Lorentz-polarization factor for

each reflection and applies the appropriate background, S-corrections, and daily scale factors. Printed output is h, k, ℓ, sin θ, 1/LP, $|F_o|^2$, and $|F_o|$ for each reflection. Cards suitable for use in the Cantzel-Sparks-Trueblood least squares programs (9) are also produced.

Structure factors obtained from the experimental data and multiplied by the scale factor projected by the last least squares cycle are listed, together with structure factors calculated using atomic parameters derived from the same least squares calculation, in Table 9. Some of the weak or unobserved $|F_o|$ values listed are based on the (hnℓ) Weissenberg films taken with CuKα radiation, because it was discovered near the end of the refinement that such $|F_o|$ values derived from the counter-measured intensities frequently differed by factors of 2 or more from the film data. In the range $|F_o| \leq 2|F_{min}|$, the standard deviations (derived from counter statistics and the estimated accuracy of the background corrections) of the counter data are about five times as large as those of the film data.

Determination of the Trial Structure

Use of the heavy atom technique made interpretation of the diffraction data for this structure fairly simple. The (h0ℓ) data were collected first and were used to compute the corresponding two-dimensional Patterson function. The positions in projection of the two independent bromine atoms were easily obtained by study of the major peaks in this function. The bromine atoms were used to phase the experimental $|F_o|$ values for a Fourier synthesis which, after a few weeks of study, was interpreted in terms of the expected molecular structure.

TABLE 9

Observed and Calculated Structure Factors for $B_{10}H_{12}(C_5H_4NBr)_2$.

Each group of three columns contains ℓ, F_o and F_c, and is headed by the common values of h and k for the group. Negative numbers in the F_o column give minimum observable values for unobserved reflections. Asterisks indicate reflections omitted from the final least squares calculations.

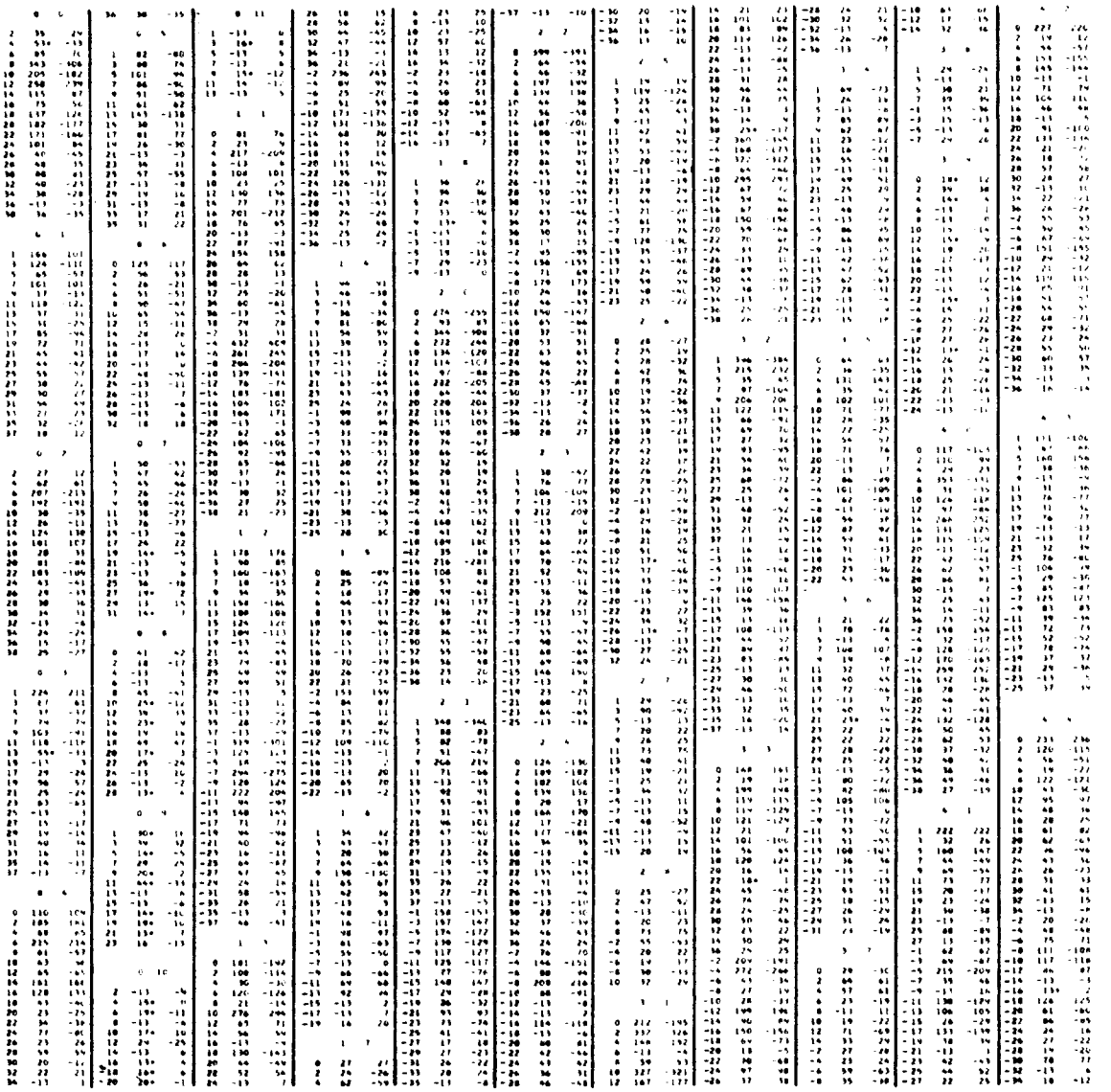

Concurrent with collection of the remainder of the diffraction data, the trial x and z parameters of the atoms were refined with a series of F_o and (F_o-F_c) Fourier maps. The value of R at the termination of this refinement was 18%. Rather than carry this two-dimensional work further, the (hk0) Patterson function was calculated and the y coordinates of the two bromine atoms were found. A wire and plasticene molecular model was used to obtain very crude values of y for the remainder of the atoms in the molecule, by comparison of the model with the (h0ℓ) Fourier function. Attempts to refine these parameters by difference Fourier syntheses were unsuccessful because of the extensive overlapping of atoms in the (0kℓ) projection.

When the three-dimensional data became available, the two projections were correlated by calculation of a few (hkℓ) structure factors and by packing considerations. (Combination of the two projections is indeterminate by a translation of 1/4 in x). The trial structure determined in this way was then independently confirmed by calculation of a three-dimensional Fourier function based on phases fixed by only the bromine atoms. All of the lighter atoms (except hydrogen atoms) were found where the original model had predicted they should be, and no spurious peaks were apparent.

Refinement of the Structural Model

The three-dimensional trial model was refined using the linearized least squares equations of Hughes (7). As in the case of $C_{44}H_{30}F_2$, refinement was rather slow. Errors in the list of data, discovered at various times, and the long use of isotropically oscillating models for

the two heavy bromine atoms are considered the chief causes of the slow convergance of the least squares process. When ellipsoidal temperature factor refinement was finally begun for the bromine atoms, a comparatively startling drop in the discrepancy index was observed.

Least squares Cycles 1" through A-9 were calculated on a Burroughs 220 computer with a block diagonal monoclinic least squares program written by Dr. R. E. Marsh which minimizes $\Sigma w \left| |F_o|^2 - |F_c|^2 \right|^2$. The remainder of the least squares cycles were computed on IBM 7090 computers using the modified Gantzel-Sparks-Trueblood block diagonal least squares program (see discussion, pp. 20-21), which minimizes $\Sigma w \left| |F_o| - |F_c| \right|^2$. The atomic scattering functions used were those of Thomas and Umeda (33) for bromine, Ibers (34) for boron, Hoerni and Ibers (12) for nitrogen, the average of Hoerni and Ibers (12) and Berghuis, et al. (13) for carbon, and McWeeny (11) for hydrogen. An anomalous scattering correction of 0.30 electrons (35) was subtracted from the bromine scattering function.

The progress of the refinement is summarized in Table 10. The weighting function $\sqrt{w} = 1/|F_o|$ which proved most successful in early stages of the refinement of $C_{44}H_{30}F_2$ with the Marsh program was used for Cycles 1" through 7. For the last few of these cycles, it was noticed that calculated values of the structure factors of the strongest reflections were much less than the experimental values. Re-examination of the SPGLP program data showed that an incorrect filter factor had been used. This error affected about 20 of the strong reflections; correction of the data list lowered the R-factor from 25.8% to 22.9%. This is the most serious group of errors found in the data list, although from time to time reflections for which the experimental and calculated structure

TABLE 10

Least Squares Refinement of $B_{10}H_{12}(C_5H_4NBr)_2$

Cycle	$(\sin^2\theta/\lambda^2)_{max}$	R	$\sqrt{w}$ †
1"	0.125	28.5%	$1/\lvert F_o\rvert$ if observed; $1/4\lvert F_o\rvert \cdot \lvert F_{min}\rvert$ if unobserved
2"	0.125	28.5	
3"	0.125	28.1	
3'"*	1.0	37.3	
1	0.20	27.9	
2	0.24	27.9	
3	0.25	27.0	
4	0.25	26.5	
5	0.25	26.0	
6	0.25	25.3	
7	0.25	25.3	
1'*	0.25	22.9	$1/(0.5 - 0.00351\lvert F_o\rvert + 0.000304\ \lvert F_o\rvert^2)$
2'	1.0	30.1	
3'	1.0	28.6	
4'	1.0	28.8	
5'	1.0	27.9	
6'	1.0	27.0	
A-1	0.23	23.4	
A-2	0.23	> 16.9**	
A-3	0.24	18.5	
A-4	0.24	14.7	
A-5	0.24	14.3	
A-6	0.24	13.9	
A-7	1.0	18.1	
A-8	1.0	15.9	
A-9	1.0	14.8	
B-1	1.0	17.5	$1/\lvert F_o\rvert$ if observed; $1/2\lvert F_{min}\rvert$ if unobserved
B-2	1.0	16.2	
B-3	1.0	12.7	
B-4	1.0	12.4	
B-5	1.0	11.5	
B-6	0.4225	10.0	
$B-7_1$	0.4225	9.9	
$B-7_2$	0.4225	9.7	
$B-8_1$	0.4225	9.5	
$B-8_2$	0.4225	9.5	
B-9*	0.4225	9.4	

TABLE 10 (continued)

Cycle	$(\sin^2\theta/\lambda^2)_{max}$	R	$\sqrt{w}$ †
H-1	0.4225	8.5	$1/(4.40 + 0.009352\|F_o\| + 5.825 \times 10^{-5}\|F_o\|^2)$
H-1'*	0.4225	7.0	
H-2	0.4225	6.7	
H-2'*	0.4225	6.4	
H-3	0.4225	6.2	
H-4	0.4225	6.1	
H-5	0.4225	6.0	
H-6	0.4225	5.9	
H-7	0.4225	5.9	

†Weighting functions listed were used for all succeeding cycles until a different function is given.

*The same heavy-atom parameters were used for this cycle as for the preceding cycle.

**This cycle was not finished because of insufficient computer time.

factors were found to differ greatly were examined on the (hnℓ) Weissenberg films, and in nearly every case the original $|F_o|$ value was found to be in error. Most of these errors were apparently due to recording that 10,000 radiation pulses had been counted when the number should have been 1,000, or vice versa. Because of the large difference between these two numbers it was considered safe to presume a simple recording error existed in such cases, and the appropriate changes were made without reducing the weight of these reflections in the least squares calculations.

Following Cycle 7, the weighting function was changed to $\sqrt{w} = 1/(0.5 - 0.00351|F_o| + 0.000304|F_o|^2)$, a function felt more closely to approximate the reciprocals of the σ-values of the structure factors. Six more cycles were calculated using spherical temperature factors for all of the atoms and then a difference Fourier function was calculated, using a program written for the Burroughs 220 computer by Dr. K. Hoogsteen. This map showed some of the hydrogen atoms and was one of the indications (see the Introduction) that the molecular formula is not $B_{10}H_{14}(C_5H_4NBr)$, as was thought at this time. The largest peaks in this map were near the bromine atoms and were such as to show strongly non-spherical thermal vibration of these atoms. In the case of each atom, the greatest amount of vibration was nearly normal to the plane of the attached pyridine ring. Therefore the bromine temperature factors were allowed to refine ellipsoidally for nine cycles. After Cycle A-9 the residual factor, R, was 14.6% for all of the data.

The refinement after Cycle A-9 was executed on IBM 7090 computers. For all of these cycles except the last nine, the weighting function

$\sqrt{w} = 1/|F_o|$ was used. This should approximate the inverses of the standard deviations of the reflections, a constant number of radiation pulses having been recorded for each reflection (for the majority of reflections; for strong reflections ten or 100 times this number were recorded, but in many of these cases additional filters were used, cancelling the gain in statistical accuracy). The large drop in R between Cycles B-2 and B-3 is caused primarily by changes in the data list. Originally the very weak reflections for which the recorded intensity was slightly less than the background intensity because of statistical fluctuations in intensity were included in the data list as zero and were given a weight $\sqrt{w} = 1/|F_{min}|$, with $|F_{min}|$ set at 10, an approximation of the standard deviation of the average background. The remainder of the very weak reflections were entered in the data list at their recorded values, in spite of the known large error in these reflections. As the refinement proceeded it was realized that this procedure was not a good one. Many of these reflections differed from the calculated values by 300% or more. Therefore, σ_B, the standard deviation of the background, was accepted as a minimum observable value and all weaker reflections were included in the least squares and residual (R) calculations only if the calculated values exceeded σ_B. In these cases, $|F_o|$ was set equal to 12, an approximation of σ_B. In Cycle B-6 and all following cycles $(\sin\theta)_{max}$ was fixed at 0.65 Å^{-1}, the CuKα diffraction limit. Only a few zones included reflections recorded at greater scattering angles and most of the reflections outside the copper sphere were weak and therefore subject to large errors.

A second difference function was calculated after Cycle B-9, using a general summation program (GENFS) written for the IBM 7090 computer. This function revealed all of the hydrogen atoms and confirmed the molecular structure as $B_{10}H_{12}(C_5H_4NBr)_2$ rather than the tetradecahydrodecaborane complex originally supposed. Sections through this difference map showing the hydrogen atoms are given in Figure 8. A Fourier series computed using the experimental $|F|$ values and phased by the final set of structure factor calculations is also shown in Figure 8. The largest peak in the difference map has a peak density of 1.7 electrons, about 2 1/2 times as large as the greatest hydrogen peak. This 1.7 electron peak is 1.0 Å from hydrogen 34 and in an open space between molecules. It must be considered spurious. All of the remaining peaks in the function larger than 0.3 electrons represent hydrogen atoms.

Addition of the hydrogen atoms to the structural model lowered the R-factor from 9.4 to 8.5%. For this comparison the same heavy atom parameters were used, and a spherical temperature factor of 5.5 was used for all of the hydrogen atoms. The weighting function was also changed at this time to $1/(4.40 + 0.009352\ |F_o| + 5.825 \times 10^{-5}\ |F_o|^2)$ to fit the root-mean-square distribution of $1/\left|\,|F_o| - |F_c|\,\right|$ as a function of $|F_o|$. This distribution was obtained using the $|F_c|$ values calculated in least squares Cycle B-9.

Further comparison of the weak experimental $|F|$-values with the corresponding calculated magnitudes showed that many serious discrepancies still existed. These weak experimental values were checked on the (hnℓ) Weissenberg films and were altered if the films showed the counter data to be in serious error. Reflections changed at this time were omitted

Figure 8

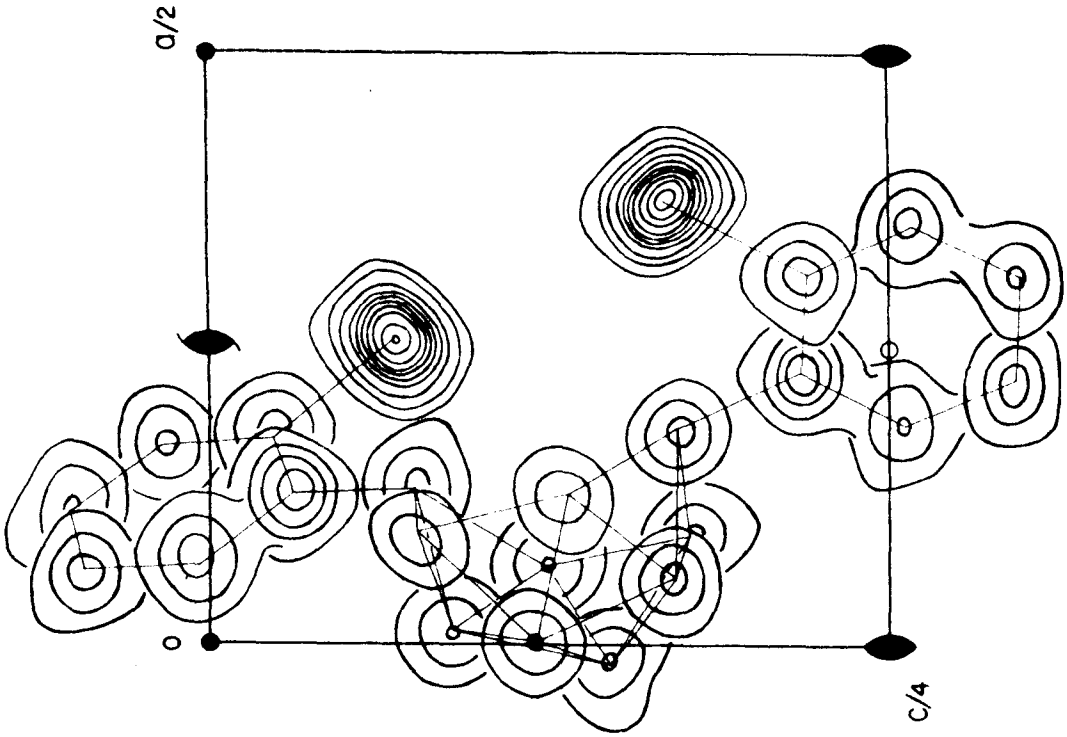

(b) F_{obs} Fourier. Contours at 5 electron intervals for bromine; 2 electron intervals for other atoms, beginning at 2 electrons.

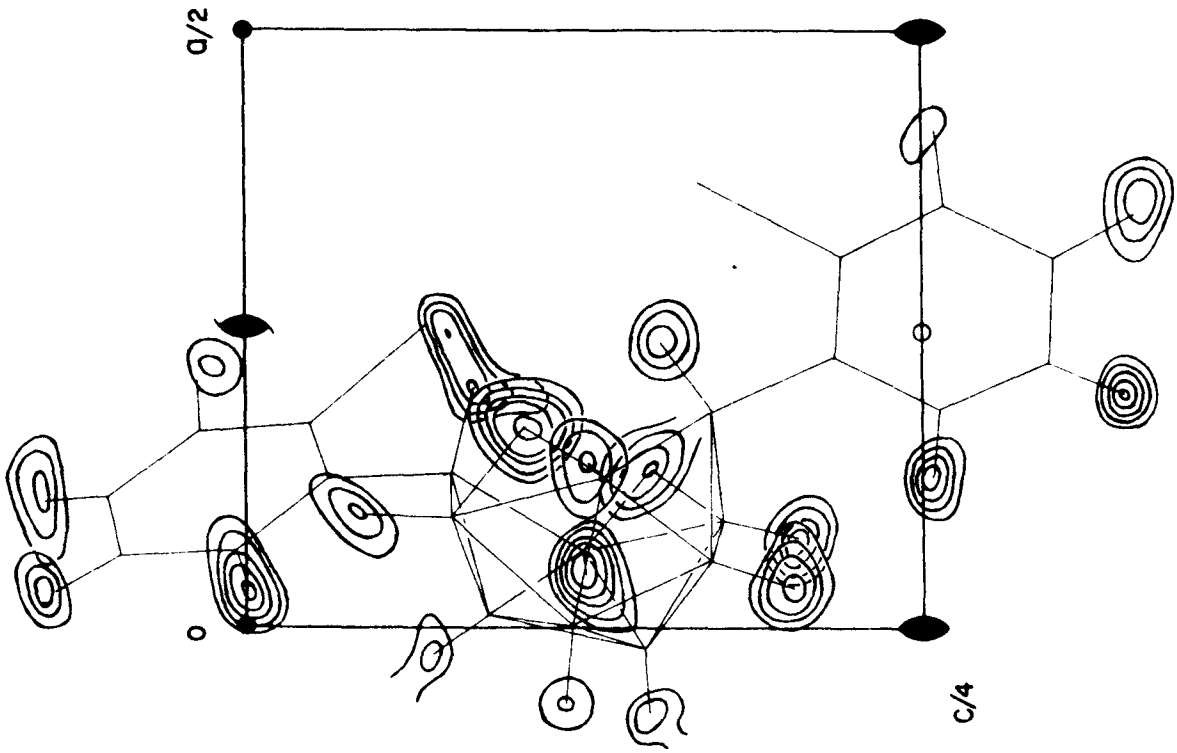

(a) Difference Fourier. Contours at 0.1 electron intervals beginning with 0.3 electrons.

from the final least-squares calculations. These changes in the data list lowered the discrepancy index from 8.5% to 7.0%. Finally, seven more cycles of least squares refinement were executed. The R-value for the final cycle is 5.3%. In the last cycle the sum of weighted residuals dropped by only 0.1%, and the largest positional parameter shift was 0.001 Å. The last six cycles were allowed to refine ellipsoidal thermal parameters for all atoms except hydrogen atoms. Neither the positional nor thermal parameters of the hydrogen atoms were refined.

The atomic parameters and standard deviations obtained by inversion of the final least squares matrices are listed in Tables 11 and 12.

Accuracy of the Structural Parameters

As is the case in the diacetonitrile- and bis-dimethylsulfurdodecahydrodecaboranes the borohydride skeleton shows within experimental error 2mm symmetry which is independent of space group requirements. Assumption that this symmetry is exact and that the boron positional uncertainties are isotropic (an assumption supported by the near-spherical temperature factor ellipsoids) allows a determination of a root-mean-square error in B-B bond lengths for comparison with the σ-value obtained from the least squares normal equations. In DBBY, the rms deviation of the 20 individual B-B bond lengths from the six appropriate means is 0.0175 Å, whereas the value of σ derived from the 9x9 least squares matrices and sum of weighted residuals is 0.014 Å. The values of σ derived from such matrices are known to be small because of neglect of interatom elements of the more appropriate general matrix and because the least squares hypothesis includes no allowance for possible non-Gaussian error distribution, or so-called "systematic errors." The ratio of 1.25 between the above rms and σ values for B-B bonds

TABLE 11

Final Positional Parameters

Atom	(x/a)	σ(x/a)	σ(x)Å	(y/b)	σ(y/b)	σ(y)Å	(z/c)	σ(z/c)	σ(z)Å
Br(1)	.2439	.00009	.0012	.5201	.00015	.0014	.4316	.00003	.0009
Br(2)	.1249	.00007	.0016	-.1299	.00014	.0013	.3334	.00003	.0009
N(3)	.3735	.00046	.0063	.3182	.00074	.0067	.4705	.00020	.0060
N(4)	.2695	.00046	.0063	.0049	.00075	.0068	.2824	.00019	.0057
C(5)	.3266	.00055	.0075	.4483	.00097	.0087	.4770	.00025	.0075
C(6)	.4290	.00063	.0086	.2651	.00100	.0090	.5053	.00024	.0072
C(7)	.4388	.00070	.0096	.3431	.00109	.0098	.5451	.00026	.0078
C(8)	.3911	.00070	.0096	.4755	.00102	.0092	.5503	.00027	.0081
C(9)	.3329	.00069	.0095	.5278	.00106	.0096	.5150	.00028	.0084
C(10)	.1870	.00059	.0081	-.0756	.00095	.0086	.2810	.00026	.0078
C(11)	.3118	.00062	.0085	.0368	.00097	.0087	.2435	.00026	.0078
C(12)	.2740	.00072	.0099	-.0058	.00109	.0098	.2028	.00028	.0084
C(13)	.1884	.00069	.0095	-.0902	.00109	.0098	.2019	.00028	.0084
C(14)	.1453	.00060	.0082	-.1245	.00102	.0092	.2413	.00029	.0087
B(15)	.3764	.00076	.0104	-.0631	.00117	.0105	.3685	.00030	.0090
B(16)	.4412	.00071	.0097	.0360	.00107	.0096	.3289	.00028	.0084
B(17)	.3180	.00072	.0099	.0666	.00116	.0105	.3278	.00028	.0084
B(18)	.4066	.00071	.0097	.2214	.00110	.0099	.3227	.00026	.0078
B(19)	.5132	.00073	.0100	.1799	.00126	.0114	.3520	.00033	.0099
B(20)	.4966	.00074	.0101	.0046	.00119	.0107	.3817	.00030	.0090
B(21)	.4061	.00078	.0107	.0263	.00124	.0112	.4238	.00031	.0093
B(22)	.3697	.00070	.0096	.2294	.00116	.0105	.4252	.00027	.0081
B(23)	.4875	.00073	.0100	.1720	.00111	.0100	.4110	.00032	.0096
B(24)	.4350	.00076	.0104	.3136	.00120	.0108	.3764	.00030	.0090
H(25)	.297			.625			.520		
H(26)	.397			.530			.579		
H(27)	.478			.306			.570		
H(28)	.464			.169			.500		
H(29)	.084			-.186			.240		
H(30)	.158			-.124			.172		
H(31)	.307			.019			.174		
H(32)	.378			.096			.244		
H(33)	.574			.234			.353		
H(34)	.537			.225			.436		
H(35)	.565			-.025			.383		
H(36)	.467			-.008			.298		
H(37)	.452			.425			.376		
H(38)	.293			.225			.415		
H(39)	.400			-.033			.460		
H(40)	.330			-.008			.399		
H(41)	.357			-.200			.375		
H(42)	.260			.125			.347		
H(43)	.430			.300			.297		
H(44)	.367			.275			.350		

TABLE 12

Final Thermal Parameters

Atom	B_{11}*	B_{22}*	B_{33}**	B_{12}*	B_{13}*	B_{23}*
Br(1)	.00789(.8)	.0233(2)	.00107(1)	.0150(2)	-.00224(.5)	-.00276(.9)
Br(2)	.00535(.6)	.0212(2)	.00116(1)	-.0064(2)	.00176(.4)	-.00221(.8)
N(3)	.0036(4)	.0094(9)	.00080(7)	-.0004(11)	-.0004(3)	.0000(4)
N(4)	.0038(4)	.0095(9)	.00078(7)	-.0009(12)	-.0004(3)	.0003(5)
C(5)	.0030(4)	.0119(13)	.00085(9)	.0011(13)	-.0005(3)	.0002(5)
C(6)	.0058(6)	.0107(13)	.00080(8)	-.0002(16)	-.0006(3)	.0008(6)
C(7)	.0069(6)	.0147(15)	.00076(9)	-.0020(18)	-.0008(4)	.0005(6)
C(8)	.0064(6)	.0127(15)	.00086(9)	-.0019(16)	-.0001(4)	-.0011(6)
C(9)	.0059(6)	.0144(16)	.00096(10)	.0001(17)	.0003(4)	-.0011(6)
C(10)	.0040(5)	.0094(12)	.00097(9)	.0018(14)	-.0002(3)	-.0007(6)
C(11)	.0047(5)	.0120(14)	.00086(9)	-.0006(14)	-.0001(4)	-.0002(6)
C(12)	.0068(6)	.0126(14)	.00093(9)	.0000(18)	.0001(4)	-.0006(7)
C(13)	.0060(6)	.0145(15)	.00101(10)	.0008(17)	-.0009(4)	-.0015(7)
C(14)	.0035(5)	.0126(14)	.00122(11)	.0023(15)	-.0009(4)	-.0010(7)
B(15)	.0054(6)	.0099(14)	.00080(10)	-.0021(17)	-.0002(4)	-.0009(6)
B(16)	.0045(6)	.0104(15)	.00070(9)	.0025(15)	-.0003(4)	-.0009(6)
B(17)	.0044(6)	.0116(14)	.00079(9)	.0004(17)	-.0008(4)	-.0008(6)
B(18)	.0048(6)	.0101(14)	.00064(8)	-.0003(16)	.0000(4)	-.0013(6)
B(19)	.0043(6)	.0115(15)	.00113(12)	-.0001(17)	.0000(4)	-.0017(7)
B(20)	.0049(6)	.0099(14)	.00094(10)	.0004(18)	-.0006(4)	-.0011(7)
B(21)	.0055(6)	.0143(18)	.00080(10)	.0003(18)	-.0010(4)	-.0022(7)
B(22)	.0048(6)	.0113(15)	.00067(8)	-.0006(17)	-.0002(4)	-.0012(6)
B(23)	.0045(6)	.0076(13)	.00111(11)	.0000(16)	.0000(4)	-.0008(7)
B(24)	.0051(6)	.0118(15)	.00081(10)	.0000(17)	-.0002(4)	.0000(7)

*The values in parentheses are standard deviations multiplied by 10^4.

**The values in parentheses are standard deviations multiplied by 10^5.

approximately agrees with estimates from other structures of the degree of inadequacy of such least-squares-derived values of σ. All values of σ listed in Tables 11 and 12 should therefore be multiplied by 1.25 to obtain more accurate measures of the indeterminacy of the structural parameters.

The mean revised values of σ are: σ_{Br} = 0.0014 Å; σ_{N} = 0.0079 Å; σ_{C} = 0.0109 Å; and σ_{B} = 0.0122 Å. Uncertainties in hydrogen positions, based on comparison of B-H bond lengths are about 0.07 Å. Extreme variations of individual σ's from these means are about 15%. Uncertainties (σ) in bond lengths corresponding to the above atomic uncertainties are: σ_{Br-C} = 0.010 Å (carbons 5, 6, 10, and 11 have smaller σ's than the remaining six); σ_{C-N} = 0.013 Å; σ_{C-C} = 0.016 Å; σ_{N-R} = 0.014 Å; σ_{B-B} = 0.017 Å; and σ_{B-H} = 0.07 Å. Sigma values for angles derived from the atomic positional uncertainties are: σ_{CCC} = 1.7°; σ_{BrCN} = 1.0°; σ_{BrCC} = 1.1°; and σ_{CNC} = σ_{BNC} = σ_{BBN} = 1.4°.

DISCUSSION

The $B_{10}H_{12}$ radical in this structure is within experimental error identical with the same group in diacetonitrile- and bis-dimethyl-sulfur-dodecahydrodecaborane (26 and 30). All of the determinations of the interatomic distances in this group show it to have 2mm symmetry within experimental error. The mean bond lengths given by each determination, assuming 2mm symmetry, are listed in Table 13. The conventional decaborane numbering system (26) is used in this table. Table 14, where the numbering system adopted for the DBBY structure is used, lists the individual bond lengths found in this compound. The mean terminal H-B bond length of 1.10 Å is identical with the value found in $B_{10}H_{12}(NCCH_3)_2$ and is 0.08 Å shorter than that found in $B_{10}H_{12}[S(CH_3)_2]_2$.

In the two published studies of $B_{10}H_{12}R_2$ molecular parameters, the R-groups show no appreciable structural changes from corresponding uncomplexed molecules. The same is true of the bromopyridine groups in DBBY. The mean C-N distance of 1.353 Å and the mean C-C distance of 1.380 Å agree well with the corresponding values of 1.340 ± 0.005 Å and 1.395 ± 0.005 Å found in pyridine (36). The mean C-Br distance of 1.872 Å agrees with the average of 1.87 Å found in bromobenzene and several oligobromobenzenes (37). The bond angles do seem to show small distortions, apparently as a result of strain imposed by short Br-B and Br-H contacts. The two NCBr angles (see Table 15) average 122.5° and the BNC angles involving carbon atoms nearest the bromine atom average 123.5°. Even with these slightly larger than expected angles, Br(1) is 2.79 Å from H(38) and 3.14 Å from B(22). Br(2) is 2.97 Å from H(42) and 3.19 Å from B(17).

TABLE 13

Comparison of Mean B-B Bond Lengths in the Three $B_{10}H_{12}R_2$ Compounds Studied Crystallographically

Bond	R = $NCCH_3$*	R = $S(CH_3)_2$**	R = C_5H_4NBr	Unweighted Mean
1-2	1.756 ± 0.006 Å	1.76 ± 0.01 Å	1.773 ± 0.009 Å	1.763 Å
1-3	1.837 ± 0.011	1.84 ± 0.02	1.816 ± 0.017	1.831
1-5	1.778 ± 0.006	1.79s ± 0.01	1.778 ± 0.009	1.784
2-5	1.744 ± 0.006	1.77s ± 0.01	1.762 ± 0.009	1.760
2-6	1.746 ± 0.008	1.75 ± 0.01	1.734 ± 0.012	1.743
5-6	1.854 ± 0.006	1.87 ± 0.01	1.878 ± 0.009	1.869
5-10	1.881 ± 0.008	1.91 ± 0.01	1.870 ± 0.012	1.887

*These estimates of error are not explicitly defined. Presumably they are obtained from either 4x4 (isotropic temperature factor) or 9x9 least squares matrices and thus may be about 10-20% too small.

**These estimates of error are obtained from 9x9 least squares matrices and should probably be increased by about 20%.

TABLE 14

Bond Lengths in $B_{10}H_{12}(C_5H_4NBr)_2$

Bond*	Length	Bond	Length
Br(1)-C(5)	1.876 Å	B(20)-B(21)	1.798 Å
Br(2)-C(10)	1.868	B(20)-B(23)	1.754
N(3)-C(5)	1.353	B(21)-B(22)	1.897
N(3)-C(6)	1.370	B(21)-B(23)	1.770
N(3)-B(22)	1.580	B(22)-B(23)	1.755
N(4)-C(10)	1.344	B(22)-B(24)	1.891
N(4)-C(11)	1.345	B(23)-B(24)	1.790
N(4)-B(17)	1.609	C(6)-H(28)	1.00
C(5)-C(9)	1.351	C(7)-H(27)	0.98
C(6)-C(7)	1.392	C(8)-H(26)	1.00
C(7)-C(8)	1.369	C(9)-H(25)	1.02
C(8)-C(9)	1.400	C(11)-H(32)	1.05
C(10)-C(14)	1.387	C(12)-H(31)	1.01
C(11)-C(12)	1.377	C(13)-H(30)	1.03
C(12)-C(13)	1.398	C(14)-H(29)	1.01
C(13)-C(14)	1.370	B(15)-H(40)	1.23
B(15)-B(16)	1.744	B(15)-H(41)	1.28
B(15)-B(17)	1.865	B(16)-H(36)	1.08
B(15)-B(20)	1.795	B(17)-H(42)	1.12
B(15)-B(21)	1.885	B(18)-H(43)	1.10
B(16)-B(17)	1.712	B(18)-H(44)	1.10
B(16)-B(18)	1.746	B(19)-H(33)	0.97
B(16)-B(19)	1.777	B(20)-H(35)	0.97
B(16)-B(20)	1.772	B(21)-H(39)	1.22
B(17)-B(18)	1.858	B(21)-H(40)	1.31
B(18)-B(19)	1.750	B(22)-H(38)	1.09
B(18)-B(24)	1.854	B(23)-H(34)	1.11
B(19)-B(20)	1.811	B(24)-H(37)	1.03
B(19)-B(23)	1.788	B(24)-H(44)	1.26
B(19)-B(24)	1.768		

*See Figure 9 for labelling system.

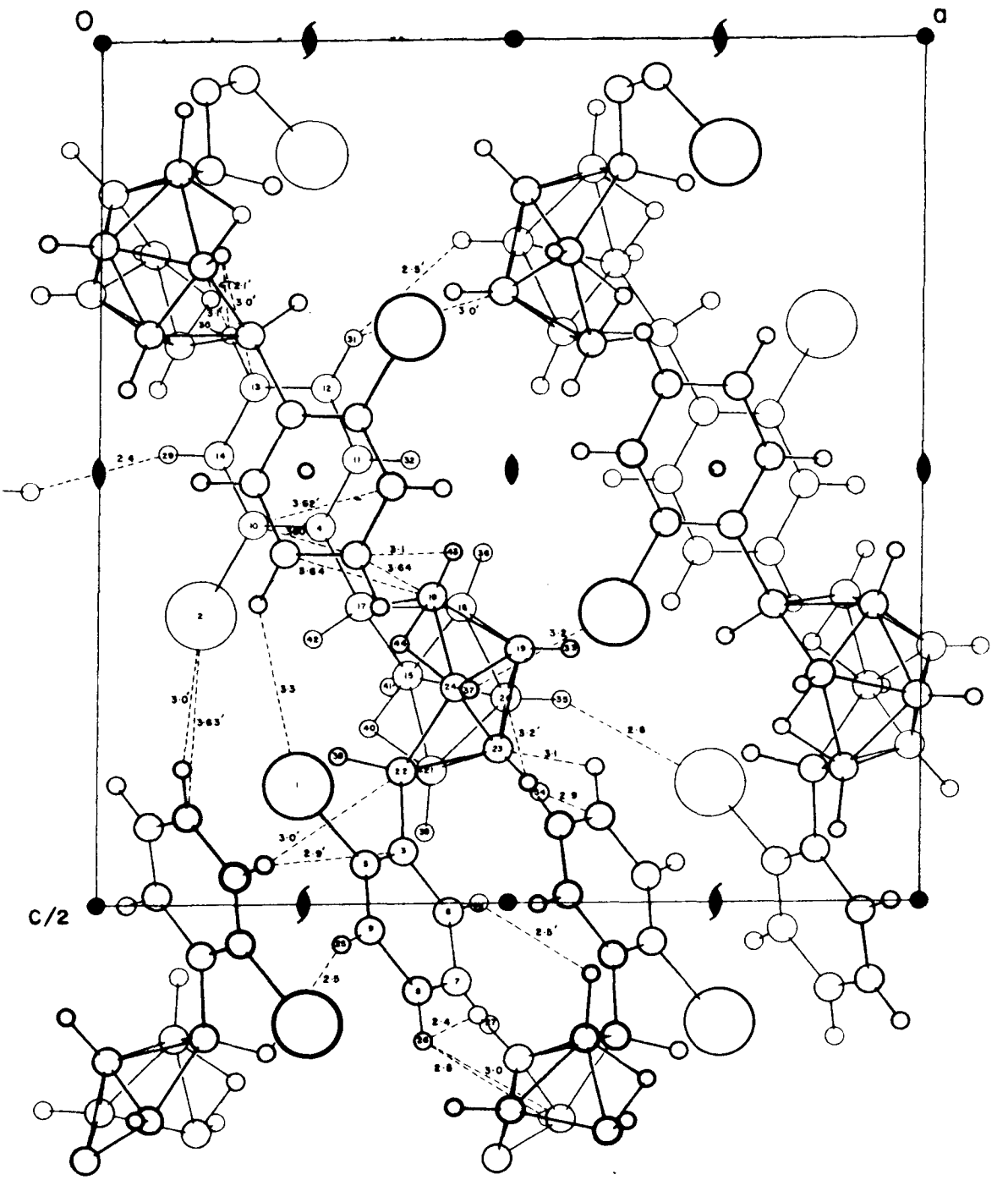

Figure 9. Numbering System and Packing. Primed figures indicate distances between the labelled molecule and molecules below the ones illustrated.

TABLE 15

Some Bond Angles in $B_{10}H_{12}(C_5H_4NBr)_2$

Angle	Value	Angle	Value
Br(1)C(5)N(3)	124°	N(4)C(11)C(12)	124°
Br(2)C(10)N(4)	121°	C(6)C(7)C(8)	120°
Br(1)C(5)C(9)	118°	C(7)C(8)C(9)	118°
Br(2)C(10)C(14)	117°	C(8)C(9)C(5)	119°
C(5)N(3)B(22)	124°	C(11)C(12)C(13)	118°
C(10)N(4)B(17)	123°	C(12)C(13)C(14)	119°
C(6)N(3)B(22)	119°	C(13)C(14)C(10)	120°
C(11)N(4)B(17)	119°	N(3)B(22)B(23)	110°
C(5)N(3)C(6)	117°	N(4)B(17)B(16)	111°
C(10)N(4)C(11)	118°	N(3)B(22)B(21)	120°
N(3)C(5)C(9)	119°	N(3)B(22)B(24)	117°
N(3)C(6)C(7)	122°	N(4)B(17)B(15)	121°
N(4)C(10)C(14)	122°	N(4)B(17)B(18)	117°

These distances are considerably shorter than the van der Waals contact distances of about 3.1 Å and 3.5 Å (extrapolated from Pauling, p. 189 (38)). The mean angles B_2-B_6-R' (conventional numbering system), where R' is the atom in the R-group attached to B_6, are 108° in $B_{10}H_{12}(NCCH_3)_2$ and $B_{10}H_{12}[S(CH_3)_2]_2$, and 110° in DBBY. The larger angle in DBBY may not be statistically significant, but it could reflect repulsion of the pyridine atoms by the "lower" decaborane hydrogen atoms.

The B-N distances found in DBBY (1.609 Å and 1.580 Å) are significantly larger than the value of 1.523 Å found in diacetonitriledodecahydrodecaborane. An increase of about 0.04 Å is expected because of the different hybridization states of the nitrogen atoms in the two compounds, but the observed difference is 0.071 Å, too large to be completely explained in this manner. B-N distances of 1.62 ± 0.15 Å in $(CH_3)_3NBH_3$ (39), 1.58 Å in $(CH_3)_3NBF_3$ (40), 1.64 Å in H_3CCNBF_3 (41), and 1.58 Å in $CH_3H_2NBF_3$ (42) support the longer value found in DBBY.

Packing of the DBBY molecules is apparently dominated by the bromopyridine groups. As Figure 9 shows, every short contact involves one of these groups, and there are no direct contacts between the borohydride groups. Half of the bromopyridine rings pack in pairs across centers of symmetry similar to the one at (1/2, 1/2, 1/2). The distance between these pairs of planes is 3.73 Å, but the ring centers are displaced about 0.75 Å so that the shortest carbon-carbon distances are about 3.80 Å. The remaining pairs of bromopyridine rings, related by centers of symmetry equivalent to that at (1/4, -1/4, 1/4) are only 3.47 Å apart, but the displacement of centers, 1.58 Å, makes the closest contacts 3.50 Å and 3.62 Å. This second class of "pairs" of rings thus consists of rings merely touching each other and not forming distinct overlapping couples like the first group.

The complete pairing of one group of rings and partial pairing of the other may explain the rather odd temperature factors derived for this compound. Only the bromine atoms show strongly anistropic thermal motion. The temperature factor exponents for these atoms can be expressed in ellipsoidal form as $(11.34\ M_1^2 + 3.55\ N_1^2 + 2.51\ P_1^2)$ and $(8.26\ M_2^2 + 4.15\ N_2^2 + 2.65\ P_2^2)$, where the subscripts give the atom numbers and M, N, and P are appropriate functions of h/2a, k/2b, and ℓ/2c. The angle between the major axis of the Br(1) ellipsoid and the normal to the attached pyridine ring is 17.5°, and the corresponding angle in the case of Br(2) is 20.4°. These angles are rather small and thus the major vibrations can be considered normal to the planes of the respective pyridine rings. The rings themselves do not share this strongly anisotropic vibration, probably because of the way in which they are packed. The bromine atoms, however, have no close contacts in direction normal to the rings, and are free to vibrate in these directions, whereas close contact with the boron and hydrogen atoms previously mentioned helps prevent in-plane vibration.

Table 16 lists several least squares planes. Planes P1 and P2 both represent possible planes for the pyridine ring attached to Br(1). Plane 1, calculated giving zero weight to Br(1), has been used for the calculations of interplanar angles involving this ring. Bromine atom 1 is 0.084 Å from this plane, but the small deviations of the remaining atoms from the plane is statistically fortuitous. Plane P2 was calculated giving Br(1) the same weight as the other atoms, and even here, with Br(1) only 0.028 Å from the plane, most other atoms are less than 2σ from the plane. The bromine atom should not be regarded as significantly out of

TABLE 16

Least Squares Planes

Plane	Atoms included in calculating plane	D	Cos A*	Cos B	Cos C	Distances from Plane in Å			
P1	3,5,6,7,8,9	0.243	0.7961	0.4891	-0.3692	Br(1)	-0.084	C(7)	-0.001
						N(3)	-0.008	C(8)	0.007
						C(5)	-0.002	C(9)	-0.005
						C(6)	-0.007	B(22)	0.079
P2	1,3,5,6,7,8,9	0.034	0.7870	0.4951	-0.3809	Br(1)	-0.028	C(7)	-0.019
						N(3)	0.024	C(8)	0.001
						C(5)	0.024	C(9)	0.011
						C(6)	-0.013	B(22)	0.106
P3	2,4,10,11,12,13,14	-2.342	-0.5396	0.8402	-0.0444	Br(2)	-0.010	C(12)	0.001
						N(4)	0.009	C(13)	-0.004
						C(10)	0.012	C(14)	0.003
						C(11)	-0.011	B(17)	0.057
P4	16,17,22,23	-3.464	0.1525	0.8648	-0.4716	B(16)	+0.001	N(3)	0.062
						B(17)	-0.001	C(8)	0.199
						B(22)	0.001	N(4)	0.058
						B(23)	-0.001	C(13)	0.286

*D is the distance of the plane from the origin. A, B, and C are the angles between the plane normal and the unit cell vectors a, b, and c respectively.

coplanarity with the other atoms. The second bromopyridine ring is also coplanar. Plane P4 was calculated primarily for description of the gross molecular structure. Interplanar angles P1, P4 and P3, P4 are 44.4 and 47.7° respectively. These may be regarded as approximate twists about the BN bonds. The twists are such as to give the whole molecule approximate 2-fold symmetry. The twists serve to place pyridine hydrogens 28 and 32 (in positions 6 of the pyridine rings) approximately halfway between pairs of hydrogens attached to the boron skeleton. H(28) is 2.24 Å from H(34) and 2.34 Å from H(39). H(32) is 2.22 and 2.53 Å respectively from H(36) and H(43). The twist also relieves abnormally short contacts between Br(1) and H(38) and between Br(2) and H(42). These latter distances are 2.79 Å and 2.97 Å respectively.

A P P E N D I X

General Information

The programs and subroutines in this appendix have each been checked one or more times using data of the sort likely to be encountered in general use and are free from error, so far as is known. However, they may fail under some peculiar combinations of data, and the user must be prepared to accept the risk of such failure. The subroutines DUBFS and PHOTO were written for the modified version of the Gantzel-Sparks-Trueblood block diagonal program labelled CFLSB and should be carefully checked for compatibility before use with the version CITBD or other versions.

The programs written for the IBM 7090 computer are written in FORTRAN and FAP pseudo-languages, and descriptions of the programs use some technical terms defined within these languages. Such definitions and general restrictions on the use of these languages may be found in references (43) and (44). For definitions of terms used in describing the LP program written for the Burroughs 220 computer, reference should be made to the 220 Reference Manual by K. J. Hebert, available in loose-leaf form from the California Institute of Technology Computing Center.

The subroutines DUBFS and PHOTO are referred to by the main program CFLSB as TESTB. In addition to these two TESTB programs, there may be others. Only one of these subroutines may be used at any given time. The dual naming should be remembered in order to avoid confusion.

ORIENT

Purpose

This program will transform a set of fractional crystallographic coordinates (x,y,z) into orthogonal coordinates (A,B,C) in such a way that any prescribed plane in the original coordinate system becomes the (A,B,0) plane of the transformed system. The program is written for the triclinic case, and has the same input format as the modified Gantzel-Sparks-Trueblood least squares programs (9) so that cards produced by that program can be used as input.

Input

Card 1. Format (4X9A6). This card must contain a title for the crystal.

Card 2. Format (6F10.6,I3). This card gives the unit cell constants and number of atoms in the order a, b, c (all in Å), $\cos\alpha$, $\cos\beta$, $\cos\gamma$, and n. N cannot exceed 200.

Card 3. Format (6F10.6). The direction cosines with respect to the crystallographic coordinate system of the plane to be treated as (A,B,0), and the fractional coordinates (x_o,y_o,z_o) of the point to be treated as the origin of the transformed coordinate system, should be listed on this card, in the order $\cos\rho$, $\cos\sigma$, $\cos\tau$, x_o, y_o, z_o (ρ is the angle between the plane normal P and a; σ, the angle between P and b; and τ, the angle between P and c).

Card 4. The following cards should be $n + n_a$ in number, where n_a is the number of atoms given anisotropic temperature factors. These cards are read using the format (6F10.6, I3), with x, y, and z in the

first three fields. If field 4 is blank the program assumes the atom is anistropic and reads another card. The second card is ignored. Thus each isotropic atom should be represented by a single card containing x, y, z, followed by some non-zero number in field 4. Each anistropic atom must be represented by a pair of cards, field 4 in the first of which is blank.

ORIENT

```
      DIMENSION X(200),Y(200),Z(200),A(200),B(200),C(200),COMPD(9)
    1 FORMAT (6F10.6,13)
    2 FORMAT (68HOTRANSFORMATION OF COORDINATES.  THE CRYSTALLOGRAPHIC
     1PLANE COS A = F8.5,10H, COS B = F8.5,10H, COS C = F8.5/ 34H IS TRE
     2ATED AS THE AB PLANE.  X = F9.6, 6H, Y = F9.6,6H, Z = F9.6,26H IS
     3TREATED AS THE ORIGIN.)
    3 FORMAT (4X9A6)
    4 FORMAT (1H1,9A6)
   10 FORMAT (35HO   N          A          B          C    )
   12 FORMAT (I5,3F10.4)
      READ INPUT TAPE 5,3,(COMPD(I),I=1,9)
      READ INPUT TAPE 5,1,CA,CB,CC,CALF,CBET,CGAM,NAT
      READ INPUT TAPE 5,1,COSA,COSB,COSC,XO,YO,ZO
      DO  5 I=1,NAT
      READ INPUT TAPE 5,1,X(I),Y(I),Z(I),BISO
      IF (BISO) 5,6,5
    6 READ INPUT TAPE 5,1,BISO
    5 CONTINUE
      COSAL = COSF(0.01745329252*CALF)
      COSBE = COSF(0.01745329252*CBET)
      COSGA = COSF(0.01745329252*CGAM)
      SINGA=SQRTF(1.-COSGA*COSGA)
      FUN=(COSBE-COSAL*COSGA)/SINGA
      CONV=CC*SQRTF(1.-FUN*FUN-COSAL*COSAL)
      DO 7 I=1,NAT
      X(I)=X(I)-XO
      Y(I)=Y(I)-YO
      Z(I)=Z(I)-ZO
      A(I) = CA*SINGA*X(I)+CC*FUN*Z(I)
      B(I) = CA*COSGA*X(I)+CB*Y(I)+CC*COSAL*Z(I)
    7 C(I) = CONV*Z(I)
      AX = (1.-COSAL*COSAL)*COSA+(COSAL*COSBE-COSGA)*COSB+(COSAL*COSGA-
     1 COSBE)*COSC
      AY = (COSAL*COSBE-COSGA)*COSA+(1.-COSBE*COSBE)*COSB+(COSBE*COSGA-
     1 COSAL)*COSC
      AZ = (COSAL*COSGA-CCSBE)*COSA+(COSBE*COSGA-COSAL)*COSB+(1.-COSGA*
     1 COSGA)*COSC
      DET=1.+2.*COSAL*COSBE*COSGA-COSAL*COSAL-COSBE*COSBE-COSGA*COSGA
      AX = AX/DET
      AY = AY/DET
      AZ = AZ/DET
      BX = AX*SINGA+AZ*FUN
      BY = AX*COSGA+AY+AZ*COSAL
      BZ = AZ*CONV/CC
      COSE = -SQRTF(BX*BX+BZ*BZ)
      SIND = -BX/COSE
      COSD = BZ/COSE
      AD = SIND*BY
      AE = -COSD*BY
```

```
      WRITE OUTPUT TAPE 6,4, (COMPD(I),I=1,9)
      WRITE OUTPUT TAPE 6,2,COSA,COSB,COSC,XO,YO,ZO
      WRITE OUTPUT TAPE 6,10
      DO 11 I=1,NAT
      BA = COSD*A(I)+SIND*C(I)
      BB = AD*A(I) + COSE*B(I)+AE*C(I)
      BC = BX*A(I)+BY*B(I)+BZ*C(I)
   11 WRITE OUTPUT TAPE 6,12,I,BA,BB,BC
      CALL EXIT
      END(1,1,0,0,0,0,1,1,0,1,0,0,0,0,0)
```

General Fourier Summation Program Package

In order to compute Fourier series of the kind generally encountered in crystallographic work, a series of programs was written, the primary input to which is generated by the CFLSB least squares program. The package requires a TESTB subroutine for CFLSB to generate a magnetic tape containing the independent coefficients in the series, a program to assign the proper triple products of sine and cosine terms to each coefficient and to sort the data, and finally a program to accomplish the actual summation. The summation program, GENFS, is believed to be capable of handling all space groups with explicit accommodation of symmetry. The program which handles symmetry, GCONV, however, can accommodate only triclinic, monoclinic, and orthorhombic symmetries. If other symmetries are required, another version of GCONV must be written. The subroutines COMPR and SORT, which respectively pack the information about each reflection into two words, and sort the resulting words according to the indices for most efficient summation, can be used for any symmetry. Because of the ease of writing in FORTRAN, only one example of a TESTB subroutine is included in this package. This subroutine, DUBFS, generates both F_o and (F_o-F_c) tapes for the general non-centric case.

The time required for summation may be estimated from the example of 5 minutes required to calculate 16 sections of a three-dimensional Fourier of $P\bar{1}$ symmetry, using a 61 x 61 point grid and about 3000 reflections.

Each program is described in detail separately, together with various limitations.

DUBFS

The magnetic tape required by GCONV consists of binary records of five words each, containing h, k, ℓ, A, and B respectively. The final record is recognized by its having a value of h equal to or exceeding 1000. The remainder of the information in the final record is ignored. DUBFS generates separate F_o and (F_o-F_c) tapes on tape units A-5 and B-5 respectively, and insures that h $\geq$ 0. This latter requirement is demanded by the GENFS program. For unobserved reflections (recognized by negative SIGMA values (9)), $(A_{min}-A_c)$ and $(B_{min}-B_c)$ are written on the Δ F tape, and A_{min} and B_{min} on the F_o tape, only if $|F_c|$ exceeds $|F_o|$; otherwise nothing is written on either tape. For reflections with SIGMA equal to 127 (the maximum value, and a signal for omission from the least squares calculations), A_c and B_c are written on the F_o tape and nothing is written on the Δ F tape.

DUBFS

```
      SUBROUTINE TESTB
      DIMENSION SLAM(10,21),FTBL(10,21),RN(48,3),RD(3),S1(48,3),BAC(6),
     1NOT(100),X(100),Y(100),Z(100),B11(100),B22(100),B12(100),G(100),
     2ITBL(100),S2(48,3),S3(48,3),DRV2(1000),DRV1(1000),F(10),JKL(4500)
     3,IDRV(1000),NUM1(72),FN(72),B33(100),B(100,4,5)
     4B13(100),B23(100),NUM2(72),BISO(100),COMPD(9),A(100,9,10),
      EQUIVALENCE (B11,BISO)
      COMMON BISO,X,Y,Z,FOBS,DEL,JR,KR,LR,MP,SIGMA,NFOBS,NSIGMA,
     1FUNOBS,NWOT,NRIT,NTPA,NTPB,NTPC,NTPD,JKL,FOB,SLAM,FTBL,RN,S1,S2,S3
     2,MINI,MAXI,MINJ,MAXJ,LANGL,MANGL,ANGLE,BONDM,U,V,VV,ALPHA,BETA,
     3GAMMA,NSF,COSA,COSB,COSG,EDO,A,B,DRV2,NSERI,COMPD,FRACX,FRACB,
     4FRACA,FRACK,SFOBS,NLS,NAN,NTBL,NEQV,NITER,JITER,NSUPP,NPUNCH,
     5NCENT,MPUNPR,NWT,WA,WB,WP,WQ,WR,S11,S22,S33,S12,S13,S23,RD,NPAR,
     6NISOT,SCALE,A1,A2,B1,B2,FB,SCLUN,SLMX,WTG4,NOT,NUM1,FN,FD,NUM2,
     7G,ITBL,B22,B33,B12,B13,B23,IDRV,DRV1,FCLC,SINC,COSC,SFCALC,SINL,
     8SUMDVQ,SUMFOB,WTG,WSR,R,NTT,DLG,MM,W,T,GB11,GB12,GB22,NHC,SUMFC,F,
     9 NTL
      IF(SINL-SLMX) 10,5,5
   10 IF(M-13)  8,9,8
    8 M=13
      REWIND 14
      REWIND 9
    9  JT=JR
      KT=KR
      LT=LR
      SINT=SINC
      IF(JT) 13,14,14
   13 JT=-JT
      KT=-KT
      LT=-LT
      SINT=-SINT
   14 SIGMA=NSIGMA
      IF(SIGMA-127.*SFOBS) 1,12,5
    1 IF(SIGMA) 3,4,4,
    3 IF(DEL) 4,5,5
    4 ADEL=DEL*COSC
      BDEL=DEL*SINT
      AOBS=FOBS*COSC
      BOBS=FOBS*SINT
      WRITE TAPE 14,JT,KT,LT,ADEL,BDEL
      GO TO 11
   12 AOBS=FCLC*COSC
      BOBS=FCLC*SINT
   11 WRITE TAPE 9,JT,KT,LT,AOBS,BOBS
    5 IF(NTT-NTL) 6,6,7
    6 JT=1000
      WRITE TAPE 14,JT,KT,LT,ADEL,ADEL
      WRITE TAPE  9,JT,KT,LT,ADEL,ADEL
      END FILE 14
      END FILE 9
```

```
      REWIND 14
      REWIND 9
    7 RETURN
      END (1,1,0,0,0,0,1,1,0,1,0,0,0,0,0)
```

GCONV

This program assigns one or more triple products of sine and cosine terms to each reflection and allows for multiplicity of non-general reflections for monoclinic, orthorhombic, and triclinic space groups. It does not specifically check for forbidden combinations of indices, although for some space groups such tests may be implicitly possible. The program as presently written can accept up to 7000 reflections. The indices h, k, ℓ may not exceed 255 in absolute value.

Input

Format (14I3). Input consists of a single card containing in order KI, NAH, NAK, NAL, NBH, NBK, NBL, NCA, NCB, NCC, NCD, NK, and NL, and a single binary tape similar to one generated by DUBFS. KI is the number of the tape unit on which the input tape is mounted. This tape is read and rewound so that the processed data can be written on the same tape unit for input to GENFS. NAH through NBL are coefficients in the parity tests TA and TB, to be described below. NCA through NCD are symmetry code words assigned to the various reflections on the basis of the results of the symmetry tests TA and TB. NK and NL are codes to identify monoclinic and triclinic space groups. Both of these numbers should be negative for triclinic space groups; only NL should be negative for monoclinic space groups; and neither should be negative for orthorhombic space groups.

Triple products assignable to each reflection and code numbers assigned to each, are:

Triple Product	Code number
+ A cos $2\pi hx$ cos $2\pi ky$ cos $2\pi \ell z$	128
- A sin $2\pi hx$ cos $2\pi ky$ sin $2\pi \ell z$	64
- A cos $2\pi hx$ sin $2\pi ky$ sin $2\pi \ell z$	32
- A sin $2\pi hx$ sin $2\pi ky$ cos $2\pi \ell z$	16
+ B sin $2\pi hx$ cos $2\pi ky$ cos $2\pi \ell z$	8
+ B cos $2\pi hx$ cos $2\pi ky$ sin $2\pi \ell z$	4
+ B cos $2\pi hx$ sin $2\pi ky$ cos $2\pi \ell z$	2
- B sin $2\pi hx$ sin $2\pi ky$ sin $2\pi \ell z$	1

NCA, NCB, NCC, and NCD are sums of the code numbers for the appropriate trigonometric terms for various classes of reflections. The identity of these classes will vary with space group and appropriate coefficients for the indices h, k, and ℓ must be selected. General forms for the two parity tests are:

$$\text{Test TA} = \text{NAH}\cdot h + \text{NAK}\cdot k + \text{NAL}\cdot \ell$$
$$\text{Test TB} = \text{NBH}\cdot h + \text{NBK}\cdot k + \text{NBL}\cdot \ell$$

The four possible combinations of even and odd parity of these tests are associated with NCA-NCD as follows:

Symmetry code	Parity test	
	TA	TB
NCA	even	even
NCB	even	odd
NCC	odd	even
NCD	odd	odd

An example may be useful. For space group I 2/c, the expression for the Fourier series is

$$\rho(x,y,z) = \frac{4}{V_c}\Bigg[\sum_{h=0}^{\infty}\sum_{k=0}^{\infty}\sum_{\ell=-\infty}^{\infty}\Big\{A\cos 2\pi hx\cos 2\pi ky\cos 2\pi\ell z - A\sin 2\pi hx$$

$$\underline{\ell \text{ even}}$$

$$\cos 2\pi ky\sin 2\pi\ell z\Big\} + \sum_{h=0}^{\infty}\sum_{k=0}^{\infty}\sum_{\ell=-\infty}^{\infty}\Big\{-A\sin 2\pi hx$$

$$\underline{\ell \text{ odd}}$$

$$\sin 2\pi ky\cos 2\pi\ell z - A\cos 2\pi hx\sin 2\pi ky\sin 2\pi\ell z\Big\}\Bigg]$$

The space group is monoclinic; hence NL = -1 and NK = 0. Only one parity test is required. Thus NAH = NAK = NAL = 0 will give a dummy test TA which is always even. TB should be $0\cdot h + 0\cdot k + 1\cdot\ell$; hence NBH = NBK = 0 and NBL = 1. NCC and NCD are not needed and can be left zero. Reflection assigned symmetry code NCA have ℓ even, so NCA = 128 + 64 = 192. Similarly, NCB = 32 + 16 = 48.

As previously mentioned, subroutines COMPR and SORT are required by GCONV.

GCONV

```
      DIMENSION INDEX(7000),IAMP(7000)
      COMMON J,K,L,NA,NB,IOTA,JOTA,NCA,NCB,NCC,NCD,NTA,NTB,IR,INDEX,IAMP
    1 FORMAT(1413)
    8 READ INPUT TAPE 5,1,KI,NAH,NAK,NAL,NBH,NBK,NBL,NCA,NCB,NCC,NCD,NK,
     1NL
      IF(KI) 3,3,4
    3 CALL EXIT
    4 REWIND KI
      DO 2 I=1,7000
      INDEX(I)=0
    2 IAMP(I)=0
      IR=1
    7 READ TAPE KI,J,K,L,A,B
      IF(J-1000) 5,6,6
    5 IR=IR+1
      NTA=NAH*J+NAK*K+NAL*L
      NTB=NBH*J+NBK*K+NBL*L
      IF(NL) 9,10,10
   10 IF(L) 9,11,9
   11 A=0.5*A
      B=0.5*B
    9 IF(NK) 12,13,13
   13 IF(K) 12,14,12
   14 A=0.5*A
      B=0.5*B
   12 NA=100.*A
      NB=100.*B
      CALL COMPR
      INDEX(IR) =IOTA
      IAMP(IR) =JOTA
      GO TO 7
    6 REWIND KI
      CALL SORT
      WRITE TAPE KI,IR,IR,IR
      WRITE TAPE KI,((INDEX(I),IAMP(I)),I=1,IR)
      END FILE KI
      REWIND KI
      GO TO 8
      END(1,1,0,0,0,0,1,1,0,1,0,0,0,0,0)
```

```
        ENTRY   COMPR
COMPR   LDQ     L
        LLS     9
        CLA     J
        ARS     18
        LGL     9
        SLW     IOTA
        LDQ     K
        LLS     9
        CLA     IOTA
        LGL     17
        SLW     IOTA
        CAL     PARITY
        ANA     NTA
        TZE     AE
        CAL     PARITY
        ANA     NTB
        TZE     BE
        CLA     NCD
        TRA     SEL
BE      CLA     NCO
        TRA     SEL
AE      CAL     PARITY
        ANA     NTB
        TZE     ABE
        CLA     NCB
        TRA     *+2
ABE     CLA     NCA
SEL     ARS     18
        ORS     IOTA
        CAL     NB
        ARS     18
        ORA     NA
        SLW     JOTA
        TRA     1,4
PARITY  OCT     000001000000
J       COMMON  1
K       COMMON  1
L       COMMON  1
NA      COMMON  1
NB      COMMON  1
IOTA    COMMON  1
JOTA    COMMON  1
NCA     COMMON  1
NCB     COMMON  1
NCC     COMMON  1
NCD     COMMON  1
NTA     COMMON  1
NTB     COMMON  1
        END
```

```
        ENTRY   SORT
SORT    SXA     E,4
        CAL     MASK
        ANS     C+1
        ANS     C+9
        CLA     IR
        ORS     C+1
        SUB     ONE
        ORS     C+9
        CLA     COM
        STO     CON
G       AXT     0,4
        AXT     ,2
        AXT     1,1
A       CLA     CON
        ANA     INDEX+1,1
        TZE     B
        TXI     *+1,4,1
        CLA     INDEX+1,1
        STO     INB+1,4
        CLA     IAMP+1,1
        STO     IAB+1,4
        TRA     C
B       TXI     *+1,2,1
        CLA     INDEX+1,1
        STO     INDEX+1,2
        CLA     IAMP+1,1
        STO     IAMP+1,2
C       TXI     *+1,1,1
        TXL     A,1,0
        AXT     0,4
D       TXI     *+1,4,1
        TXI     *+1,2,1
        CLA     INB+1,4
        STO     INDEX+1,2
        CLA     IAB+1,4
        STO     IAMP+1,2
        TXL     D,2,0
        CLA     CON
        ADD     CON
        STO     CON
        CAS     F
        TRA     E
        TRA     E
        TRA     G
E       AXT     0,4
        TRA     1,4
COM     OCT     000000000400
F       OCT     200000000000
ONE     OCT     000001000000
MASK    OCT     700000777777
CON     BSS     1
```

```
DUMMY   COMMON  13
IR      COMMON  1
INDEX   COMMON  7000
IAMP    COMMON  7000
INB     COMMON  7000
IAB     COMMON  7000
        END
```

GENFS

The program which actually performs the summation is flexible enough to calculate a single point or consecutively to perform three dimensional summations on several crystals. Each summation is specified by a single data card that defines a data tape unit, initial point for the summation, increments along each axis, the range along each axis, a scale factor, a title for the summation, and two numbers which control the flexible format output. This program requires two subroutines, FORM and XPAND.

Input

Format (13I3,F8.2,4A6). The numbers to be listed on each data card are NDEL, NXO, NYO, NZO, NDX, NDY, NDZ, MX, MY, MZ, NF, NSPACE, NSHIFT, VOL, and TITLE. The initial point of the summation is (x,y,z) = (NXO/NDEL,NYO/NDEL,NZO/NDEL), and the increments in the three directions are NDX/NDEL, NDY/NDEL, and NDZ/NDEL. All of these numbers, and indeed all numbers on the data card, must be positive or zero. NDX, NDY and NDZ must be positive. NDEL can be any integer between 1 and 500 inclusive; NXO, NYO, NZO, NDX, NDY, and NDZ must be less than NDEL. MX, MY, and MZ are the number of individual x-, y-, and z- values for which the summation is executed. MX and MZ cannot exceed 121, but MY has no limit. NSPACE and NSHIFT allow variations in the output format so the sections can be used for direct contouring. NSPACE lines will be skipped between successive lines of output and each line will begin NSHIFT spaces to the left of the previous line. NF defines the tape unit on which the data tape is mounted. If successive data cards refer to the same unit,

the data are read only once. A value of zero in NF terminates execution; thus a blank card should follow the last card actually specifying a summation. VOL defines a scale factor: if VOL is positive, the scale factor will be 4/VOL. If VOL is negative or zero, unity will be used for scaling. TITLE is a heading of not more than 24 letters, printed at the beginning of each segment of output.

Output

The summation is always printed in the form of sections at constant y. The title, y-value for the section, x and z coordinates for the point in the upper left corner, and x and z increments are printed at the beginning of each segment of output. Each segment consists of MZ lines of output (some of which may be blank for certain combinations of MZ and NSHIFT), each line consisting of summation values at constant z, and with x increasing from left to right. If values of the summation for MX values of x will not fit on a single line, a second segment of output follows the first, beginning on a new page and headed in a fashion similar to the first. This segment, and as many succeeding segments as are necessary, should be fitted to the right of the first.

Only four digits of output (including sign) are allowed for each word; hence scaling is important. If numbers exceed four digits, the least significant four will be printed. The sign will be dropped if a negative number exceeds three digits.

It may be helpful to give the effect of some example of NSHIFT and NSPACE. NSPACE = 2 and NSHIFT = 0 will give an approximately square net of points. An angle of 130° between a and c, with approximately equal increments in the two directions, can be achieved by using NSPACE = NSHIFT = 2.

GENFS

```
  1 FORMAT (13I3,F8.2,4A6)
  4 FORMAT (22HOTOO MANY REFLECTIONS.)
 18 FORMAT (47HOOVERSIZED DATA.  ADVANCE TO NEXT CONTROL CARD.)
 51 FORMAT (6H Y IS I3,1H/I3,18H FOR THIS SECTION./13H (XO,ZO) IS (I3,
   11H/13,1H,I3,1H/I3,26H).  (DELTA X,DELTA Z) IS (I3,1H/I3,1H,I3,1H/I
   23,2H).//)
 70 FORMAT (    0X23F5.1)
 84 FORMAT (/)
104 FORMAT (1H14A6)
    DIMENSION FC(121),FS(121),MXO(121),NREFL(7200),C(500),DC(50),DS(50
   1),R(121,121),TITLE(4)
    COMMON IOTA,JOTA,NJ,NK,NL,IMPLY,NA,NB,MS,R
    NFO=10000
 19 READ INPUT TAPE 5,1,NDEL,NXO,NYO,NZO,NDX,NDY,NDZ,MX,MY,MZ,NF,NSPAC
   1E,NSHIFT,VOL,(TITLE(I),I=1,4)
    NSP=NSPACE +1
    IF(NDEL-500) 16,16,17
 17 WRITE OUTPUT TAPE 6,18
    GO TO 19
 16 IF(MZ-121) 94,94,17
 94 IF(MX-121) 95,95,17
 95 NXO=NXO-(NXO/NDEL)*NDEL
    NYO=NYO-(NYO/NDEL)*NDEL
    NZO=NZO-(NZO/NDEL)*NDEL
 30 IF(MZ) 3,3,2
  2 IF(NF-NFO) 5,103,5
  5 REWIND NF
    READ TAPE NF,NR,NR,NR
    NR=NR+NR
    IF(NR-7200) 102,102,96
 96 WRITE OUTPUT TAPE 6,4
    GO TO 19
102 READ TAPE NF,(NREFL(I),I=1,NR)
  9 REWIND NF
103 NFO=NF
    IF(VOL) 13,13,14
 13 SCALE = .01
    GO TO 15
 14 SCALE=.04/VOL
 15 DEL=NDEL
    IANG=NDEL-(NDEL/4)
    Q=6.2831853/DEL
    DO 20 I=1,NDEL
    AT=I-1
    C(I)=COSF(AT*Q)
    AC=ABSF(C(I))
    IF( AC  -.00001) 107,107,20
107 C(I)=0.
 20 CONTINUE
    NY=NYO-NDY
```

```
 21 NY=NY+NDY
    NC=1-NY
    DO 22 I=1,50
    NC=NC+NY
 25 IF(NC-NDEL) 23,23,24
 24 NC=NC-NDEL
    GO TO 25
 23 DC(I)=C(NC)
    NS=NC+IANG
    IF(NS-NDEL) 26,26,27
 27 NS=NS-NDEL
 26 DS(I)=C(NS)
 22 CONTINUE
    MSA=0
    LJ=0
    IL=0
    NSKIP=0
    DO 28 I=1,MZ
    MXO(I)=1
    DO 28 J=1,MX
 28 R(J,I)=0.
    FCC=0.
    FCS=0.
    FSC=0.
    FSS=0.
    NDT=1
 54 IF (NDT-NR) 53,33,33
 53 IOTA=NREFL(NDT)
    JOTA=NREFL(NDT+1)
    CALL XPAND
    FA=NA
    FB=NB
    IF(NL) 8,97,97
  8 NL=-NL
    SIL=-1.
    GO TO 98
 97 SIL=1.
 98 IF(NK) 99,100,100
 99 KFM=1-NK
    SIK=-1.
    GO TO 101
100 SIK=1.
    KFM=NK+1
101 IF(MJ-LJ) 33,32,33
 32 IF(NL-IL) 33,34,33
 34 CK=DC(KFM)
    SK=DS(KFM )*SIK
    IF(IMPLY-128) 35,36,36
 36 FCC=FCC+FA*CK
    IMPLY=IMPLY-128
 35 IF(IMPLY-64) 37,38,38
```

```
 38 FSS=FSS-FA*CK*SIL
    IMPLY=IMPLY-64
 37 IF(IMPLY-32) 39,40,40
 40 FCS=FCS-FA*SK*SIL
    IMPLY=IMPLY-32
 39 IF(IMPLY-16) 41,42,42
 42 FSC=FSC-FA*SK
    IMPLY=IMPLY-16
 41 IF(NB) 43,44,43
 43 IF(IMPLY-8) 45,46,46
 46 FSC=FSC+FB*CK
    IMPLY=IMPLY-8
 45 IF(IMPLY-4) 47,48,48
 48 FCS=FCS+FB*CK*SIL
    IMPLY=IMPLY-4
 47 IF(IMPLY-2) 49,50,50
 50 FCC=FCC+FB*SK
    IMPLY=IMPLY-2
 49 IF(IMPLY) 44,44,52
 52 FSS=FSS-FB*SK*SIL
 44 NDT=NDT+2
    GO TO 54
 33 ND=NDZ*IL
    NARG=NZO*IL+1-ND
    DO 59 I=1,MZ
    NARG=NARG+ND
 55 IF(NARG-NDEL) 56,56,74
 74 NARG=NARG-NDEL
    GO TO 55
 56 NARP=NARG+IANG
    IF(NARP-NDEL) 57,57,58
 58 NARP=NARP-NDEL
 57 FC(I)=FC(I)+FCC* C(NARG)+FCS* C(NARP)
 59 FS(I)=FS(I)+FSC* C(NARG)+FSS* C(NARP)
106 IL=NL
    FCC=0.
    FCS=0.
    FSC=0.
    FSS=0.
    IF(NF-LJ) 31,67,31
 67 IF(NDT-NR) 34,31,31
 31 NHX=NDX*LJ
    NARG=NXO*LJ+1-NHX
    DO 60 J=1,MX
    NARG=NARG+NHX
 61 IF(NARG-NDEL) 62,62,63
 63 NARG=NARG-NDEL
    GO TO 61
 62 CHX=SCALE*C(NARG)
    NARP=NARG+IANG
    IF(NARP-NDEL) 64,64,65
 65 NARP =NARP-NDEL
```

```
64 SHX=SCALE*C(NARP)
   DO 60 I=1,MZ
60 R(J,I)=R(J,I)+CHX*FC(I)+SHX*FS(I)
   DO 66 I=1,MZ
   FC(I)=0.
66 FS(I)=0.
   LJ=NJ
   IF(NDT-NR) 34,68,68
68 WRITE OUTPUT TAPE 6,104,(TITLE(KT),KT=1,4)
   WRITE OUTPUT TAPE 6,51,NY,NDEL,NXO,NDEL,NZO,NDEL,NDX,NDEL,NDZ,NDEL
   MS=(MZ-1)*NSHIFT+1
88 JZ = 1
72 IF(MS-116) 69,71,71
71 DO 73 I=1,NSP
73 WRITE OUTPUT TAPE 6,84
   NSKIP=NSKIP+1
   JZ = JZ + 1
   MS=MS-NSHIFT
   GO TO 72
69 MSB=MS+((120-MS)/5)*5-115
83 MTXO=(120-MS)/5+MXO(JZ)-1-NSHIFT/5
   IF(MX-MTXO) 87,75,75
87 MTXO=MX
75 CALL FORM
   JOX=MXO(JZ)
   IF( MTXO-JOX) 89,79,79
79 WRITE OUTPUT TAPE 6,70,(R(JX=JZ)=JX=JOK,MTXO)
   MXO(JZ)=MTXO+1
   GO TO 93
89 WRITE OUTPUT TAPE 6,84
93 IF (NSPACE) 77,77,76
76 DO 78 I=1,NSPACE
78 WRITE OUTPUT TAPE 6,84
77 JZ=JZ+1
   MS=MS-NSHIFT
80 IF(MS) 81,81,82
81 MS=MS+5
   GO TO 80
82 IF(JZ-MZ) 83,83,85
85 WRITE OUTPUT TAPE 6,104,(TITLE(KT),KT=1,4)
   MX=(MXO(1)-1)*NDX+NXO
   WRITE OUTPUT TAPE 6,51,NY,NDEL,NX,NDEL,NZO,NDEL,NDX,NDEL,NDZ,NDEL
   IF(MX-MXO(1)) 91,86,86
86 MS=MSB+NSKIP*NSHIFT-5+(NSHIFT/5)*(NSKIP/NSKIP)*5
   IF  (MS)  90,90,92
90 MS = MS+5
92 NSKIP=0
   GO TO 88
91 IF(MY-NYO-(MY-1)*NDY) 21,19,19
 3 CALL EXIT
   END(1,1,0,0,0,0,1,1,0,1,0,0,0,0,0)
```

```
        ENTRY   FORM
FORM    CLA     MS
        LRS     35
        DVP     HUN
        RQL     18
        STQ     HQ
        LRS     35
        DVP     TEN
        RQL     12
        STQ     TQ
        ARS     12
        ORA     TQ
        ORA     HQ
        ORA     X
        SLW     207,4
        TRA     1,4
HQ      BSS     1
TQ      BSS     1
HUN     OCT     000144000000
TEN     OCT     000012000000
X       OCT     607400000067
DUM     COMMON  8
MS      COMMON  1
        END
```

```
        ENTRY   XPAND
XPAND   CLA     IOTA
        LGR     26
        ALS     18
        STO     NJ
        LLS     8
        ALS     18
        STO     NL
        RQL     1
        LLS     8
        ALS     18
        STO     NK
        LGL     9
        ALS     18
        SLW     IMPLY
        LDQ     JOTA
        SLQ     NA
        RQL     18
        SLQ     NB
        TRA     1,4
IOTA    COMMON  1
JOTA    COMMON  1
NJ      COMMON  1
NK      COMMON  1
NL      COMMON  1
IMPLY   COMMON  1
NA      COMMON  1
NB      COMMON  1
        END
```

PHOTO

One of the little-used but useful subroutines written for the block diagonal least squares program as a TESTB subroutine is PHOTO, a program which prepared the lists of data in Table 9 of this thesis. This subroutine is included here as an example that even programs to be used only infrequently are worth writing if a pseudo-language is used, and in appreciation to the authors of FORTRAN.

PHOTO

```
      SUBROUTINE TESTB
      DIMENSION DA(400),DB(3),DC(17537),DD(34),DE(3018),DF(5),DG(19)
      COMMON DA,FOBS,DEL,JR,KR,LR,DB,NSIGMA,DC,SFOBS,DD,SLMX,DE,FCLC,
     1SINC,COSC,SFCALC,SINL,DF,NTT,DG,NTL
   14 FORMAT (1H1)
   16 FORMAT (/7X214//)
   17 FORMAT (4X13,15,16)
   18 FORMAT (4X13,15,1H*I5)
      IF (SINL-SLMX) 10,5,5
   10 IF(M-13) 8,9,8
    8 M=13
      WRITE OUTPUT TAPE 6,15
      IHO=1000
      IKO=1000
    9 SIGMA=NSIGMA
      IH=JR
      JFOBS=FOBS
      JFCAL=SFCALC
      IF(COSC) 2,11,11
    2 JCOSC=-1
      GO TO 13
   11 JCOSC=1
   13 ZFOBS=JFOBS
      ZFCAL=JFCAL
      IF(    FOBS-ZFOBS-0.5) 22,23,23
   23 JFOBS=JFOBS+1
   22 IF(SFCALC-ZFCAL-0.5) 24,25,25
   25 JFCAL=JFCAL+1
   24 JFCAL=JFCAL*JCOSC
      IF(IH-IHO) 20,21,20
   20 IHO=IH
   30 IKO=KR
      WRITE OUTPUT TAPE 6,16,IH,KR
      GO TO 31
   21 IF(KR-IKO) 30,31,30
   31 IF(SIGMA-127.*SFOBS) 1,12,12
    1 IF(SIGMA) 3,4,4
    3 JFOBS=-JFOBS
    4 WRITE OUTPUT TAPE 6,17,LR,JFOBS,JFCAL
      GO TO 5
   12 WRITE OUTPUT TAPE 6,18,LR,JFOBS,JFCAL
    5 IF(NTT-NTL) 6,6,7
    6 WRITE OUTPUT TAPE 6,15
    7 RETURN
      END(1,0,0,0,0,0,1,0,0,1,0,0,0,0,0)
```

SPGLP

Originally written for use on the IBM 704 computer at the Naval Ordnance Test Station at China Lake, California and in such a form as to produce data for input to the structure factors programs in use at that facility, the program was later modified to produce decimal cards usable as input for the modified Gantzel-Sparks-Trueblood programs. This program is rather specialized, in that it assumes the data were collected in exactly the manner used for DEBY. Lorentz-polarization factors suitable to the General Electric SPG goniostat are calculated, together with an analytical background correction, an S-correction for scattering angles greater than 40°, daily scale factors, and a maximum of four different filter factors. The background and S-correction values are obtained by second order interpolation from curves entered as data.

Input

Card 1. Format (72H). The first 72 characters on this card will be used as a title.

Card 2. Format (3F6.2,2F7.5,2I7,4F6.3). The unit cell parameters a, b, c, cos β; the value of λ_{α_1}; two numbers JN and NDATA, which are not used in the present version of the program; and four filter factors F_1-F_4, are read in the order a, b, c, cos β, λ_{α_1}, JN, NDATA, F_1, F_2, F_3, F_4.

Cards 3-5. Format (10F7.4). Alternate values of the abscissa and ordinate of points defining the S-curve are punched on these cards, in order of increasing size of the abscissa. Fifteen pairs of numbers may be used, and the abscissa must be in units of $\sin\theta/\lambda$.

Cards 6-13. Format (5(F7.5,F7.2)). These eight cards may contain abscissa and ordinate pairs of up to 40 points defining a background curve, in terms of counts per second versus $\sin\theta/\lambda$. As with the S-curve, the abscissa and ordinate values are entered alternately, in order of increasing size of the abscissa.

Cards 14 ff. Format (3F4.0,I4,2F9.2). The remaining cards are either "daily scale factor" cards or "reflection" cards. Each card is assumed to contain six numbers, many of which may be zero on "daily scale factor" cards. These numbers are h, k, ℓ, F_1, C, and T, where on "reflection" cards h, k, and ℓ are identified as the Miller indices, F_1 is 1, 2, 3, or 4 and identifies the filter factor to be used for the reflection, C is the number of radiation pulses recorded for the reflection, and T is the time required to record the C pulses. If on any card, T is negative, that card is recognized as a "daily scale factor" card, and the magnitude of T is used as a daily scale factor for all following cards, until a new scale factor card is encountered. A value of T = 0 indicates the end of the data list.

Output

The program prints h, k, ℓ, $\sin\theta/\lambda$, I, I_{mod}, $(LP)^{-1}$, $|F_o|^2$, and $|F_o|$, and in addition punches a data card for the CFLSB least squares program, for each reflection. Here, I is the recorded intensity after subtraction of a background correction, and I_{mod} is I multiplied by the S-correction. If I is negative, I_{mod} is $|I \cdot S(2\theta)|$, and the value of 1 is entered for $|F_o|$ on the CFLSB data card, together with a negative SIGMA value.

SPGLP

```
   DIMENSION IF(500),AC(500),AT(500),          AFILT(500)
   DIMENSION AH(500),AK(500),AL(500),SINTHL(500),DLPINV(500),
  2OINTR(500),OINTM(500),OFSQ(500),OFOBS1(500),OFOBS2(500),
  3   ABSS(15),ORDS(15),ABSB(40),ORDB(40)
61 FORMAT (72H
  2                  )
38 FORMAT (3F4.0,I4,2F9.2)
39 FORMAT (3I5  ,F9.5,2F10.2,F9.5,2F10.2)
40 FORMAT (3F6.2,2F7.5,2I7,4F6.3)
41 FORMAT(10F7.4)
42 FORMAT (5(F7.5,F7.2))
53 FORMAT (2I3,I4,I5,54XI3)
60 FORMAT (73HO  H    K    L    SINTH/L     I RAW   I MOD      2/LP
  2   /F0/2    10/F0///)
   SINSQF  (X,Y,Z) = X**2*A+Y*Y*B+Z*Z*C-X*Z*D
   INT1F(X1,Y1,X2,Y2) = (Y2-Y1)/(X2-X1)
   INT2F(X1,Y1,X2,Y2,X3,Y3)=(INT1F(X2,Y2,X3,Y3)-INT1F(X1,Y1,X2,Y2))/
  2(X3-X1)
   INPF(X1,Y1,X2,Y2,X3,Y3,X)=Y2+(X-X2)*(INT1F(X2,Y2,X3,Y3))+(X-X2)*
  2(X-X1)*(INT2F(X2,Y2,X1,Y1,X3,Y3))
   READ INPUT TAPE 5,61
   READ INPUT TAPE 5,40, CA,CB,CC,CCOSB,CLMB,JN,NDATA,(AFILT(I),
  2I = 1,4)
   READ INPUT TAPE 5,41,(ABSS(I),ORDS(I),I=1,15)
   READ INPUT TAPE 5,42,(ABSB(I),ORDB(I), I=1,40)
   DO 54 I = 1,500
   AH(I) = 0.
   AK(I) = 0.
   AL(I) = 0.
   OINTR(I) = 0.
   OINTM (I) = 0.
   DLPINV(I) = 0.
   OFSQ(I) = 0.
   OFOBS1(I) = 0.
   OFOBS2(I) = 0.
54 SINTHL(I) = 0.
   A=1./(4.*CA**2*(1.-CCOSB**2))
   B=1./(4.*CB**2)
    C = 1./(4.*CC**2*(1.-CCOSB**2)
   D = CCOSB/(2.*CA*CC*(1.-CCOSB**2))
   WRITE OUTPUT TAPE 6,61
   WRITE OUTPUT TAPE 6,60
52 I=0
46 I=I+1
   IF (I-500) 51,51,52
51 READ INPUT TAPE 5,38,AH(I),AK(I),AL(I),IF(I),AC(I),AT(I)
   IF (AT(I)) 14,15,49
49 SINSQT = SINSQF(AH(I),AK(I),AL(I))
   SINTHL(I) = SQRTF(SINSQT)
```

```
   IF(SINTHL(I)-1.409) 26,26,23
23 SINTHL(I) = 0.
   GO TO 46
26 IF (SINTHL(I)-.8087) 24,24,46
17 SCORR    = 1.
   GO TO 27
20 SCORR = ORDS(ITH)
   GO TO 27
24 IF(SINTHL(I)-.34202) 17,17,18
18 SINTHL(I) = .99699*SINTHL(I)
   ITH = 0
21 ITH = ITH + 1
   IF SINTHL  (I)-ABSS(ITH))19,20,21
19 SCORR   = INPF(ABSS(ITH-1),ORDS(ITH-1),ABSS(ITH),ORDS(ITH),
  2ABSS(ITH+1),ORDS(ITH+1),SINTHL(I))
27 ITH = 0
31 ITH = ITH + 1
   IF (SINTHL(I)-ABSB(ITH))29,30,31
30 BCORR = ORDB(ITH)
   GO TO 44
29 BCORR = INPF(ABSB(ITH-1),ORDB(ITH-1),ABSB(ITH),ORDB(ITH),
  2ABSB(ITH+1),ORDB(ITH+1),SINTHL(I))
44 ITH = IF(I)-1
   OINTR(I) = (AC(I)*BK*AFILT(ITH))/AT(I)-BCORR
   S NSQ = CLMB**2*SINSQT
   DLPINV(I) = SQRTF(S NSQ*(1.-SNSQ))/(1.+(1.-SNSQ-SNSQ)**2)
   DLPINV(I) = 8.*DLPINV(I)
   IF (OINTR(I) 45,45,33
33 OINTM (I) = SCORR*OINTR(I)
   OFSQ (I) = OINTM(I)*DLPINV(I)
   OFOBS1(I) = 10.*SQRTF(OFSQ(I))
   OFOBS2(I) = OFOBS1(I)
   NSIG = 1
   GO TO 50
45 OINTM(I)=-SCORR*OINTR(I)
   OFSQ(I) = OINTM(I)* DLPINV(I)
   OFOBS2(I)=-10.*SQRTF(OFSQ(I))
   OFOBS1(I)=1.
   NSIG=-1
50 J=AH(I)
   K=AK(I)
   L=AL(I)
   WRITE OUTPUT TAPE  6,39,  J    , K    , L    , SINTHL(I),OINTR(I),
  2OINTM(I),DLPINV(I),OFSQ(I),OFOBS2(I)
   NF=10,*OFOBS1(I)
   WRITE OUTPUT TAPE 7,53,K,L,NSIG,NF,J
   GO TO 46
14 BK = -AT(I)
   GO TO 46
15 CALL EXIT
   END(1,1,0,0,0,0,1,1,0,1,0,0,0,0,0)
```

LP

To correct data collected on equi-inclination Weissenberg films for the Lorentz-polarization factors, this program was constructed. The output consists of sin μ_e, the sine of the equi-inclination angle, for each net of reciprocal space normal to the rotation axis, and of h, k, ℓ, $\sin^2\theta$, $(LP)^{-1}$, I_o, $|F_o|^2$, and $|F_o|$ for each reflection.

Error Indications

If the machine halts with 0325 in the P register, the product $R_{11}h^2$ exceeds unity. If this occurs, either h (located in the address which appears in the B register) or R_{11} (located in cell 0398) is in error. The error should be corrected and the START switch pressed to continue. If the machine halts with 0327 in the P register, the $\sin^2\theta$ value of some reflection exceeds unity. The address of the incorrect reflection appears in the B register. To ignore this reflection, control switch 1 should be placed in the OFF position and the START switch depressed. If control switch 1 is in the ON position, the program will try again to process the incorrect reflection; thus if an error is found, the correct data word can be entered in the address which appears in the B register, control switch 1 placed ON, and START depressed. The program will in this case process the corrected data word and continue normally.

Data

A data tape should be prepared containing the unit cell constants, a code word to indicate the proper order of printing of the indices, and the data for each reflection, in the following order:

a control word,	6 0000 30 0076
$\lambda \times 10^{-6}$	
$m \times 10^{-6}$	
$n \times 10^{-6}$	
$p \times 10^{-6}$	
$\cos \alpha_m \times 10^{-6}$	
$\cos \alpha_n \times 10^{-6}$	
$\cos \alpha_p \times 10^{-6}$	
$r_1 r_2 r_3$	0 0000 00 $0r_1r_2r_3$
m' code word,	0 8888 88 88m'm'
reflection word,	$\pm$n'n'$\pm$p'p'IIIII
reflection word,	$\pm$n'n'$\pm$p'p'IIIII
etc.	
end of tape code,	0 9999 99 9999
control word,	6 0000 30 0221

m, n and p are the lengths of the unit cell edges, chosen so that m is the rotation axis of the crystal. The corresponding angles are α_m, α_n, and α_p; i.e., if m, n, and p are b, a, and c respectively, then $\alpha_m = \beta$, $\alpha_n = \alpha$, and $\alpha_p = \gamma$. The numbers $r_1 r_2$ and r_3 are some permutation of the digits 1, 2, and 3, indicating the printing order of m', n', and p', the indices associated with m, n, and p respectively. In the example just given where n corresponds with a, n' will correspond with h, and should be printed first. Similarly m' should be printed second, and p' third. The proper word $r_1 r_2 r_3$ would be 213.

Following the above words must be a list of m' code words and words for individual reflections. Each value of m' detected by the program will be used for all following reflections until a new m' word is found. The code word 0 9999 99 9999 and a branch command end the tape.

Operation

The following steps should be obeyed in using this program.

1. Read program into the computer with the PZT switch down. Place Leading Zeroes switch up, and set output switches in the desired positions. All output uses the SPO command.

2. Mount the data tape, place a read command in the C register, place the computer in the execute phase, and depress the START switch. The program will automatically be executed.

LP

```
0013   0 0000 10 CAD 0202
0014   0 0410 40 STA 0302
0015
0016   0 0000 10 CAD 0202
0017   0 0410 40 STA 0302
0018   0 0000 30 BUN 0335
0019   0 4041 09 SPO 0384
0020   0 0100 09 SPO 0031
0021   0 0000 10 CAD 0241
0022   0 2310 40 STA 0388
0023   0 0000 10 CAD 0422
0024   0 0000 14 MUL 0422
0025   0 0408 27 DFL 0302
0026   0 0000 30 BUN 0201
0027   0 0000 14 MUL 0422
0028   0 0408 26 IFL 0302
0029   0 0000 30 BUN 0201
0030   2 0000 00     0000
0031   2 1600 00     4800
0032   2 0000 52     0000
0033   2 0053 00     0062
0034   2 4955 82     0063
0035   2 0000 00     0049
0036   2 0000 00     0000
0037   2 8121 53     5700
0038   2 0000 00     0046
0039   2 8200 00     0000
0040   2 8180 80     4616
0041   0 0002 48 SRS 0008
0042   0 0000 12 ADD 0326
0043   1 0001 12 ADA 0412
0044   0 0000 30 BUN 0309
0045   0 0000 40 STA 0073
0046   0 0000 41 LDR 0074
0047   0 0000 36 BFA 0071
0048   0 8800 36 BFA 0053
0049   0 6600 36 BFA 0055
0050   0 4400 36 BFA 0057
0051   0 2200 36 BFA 0059
0052   0 0000 30 BUN 0061
0053   0 0000 49 SLA 0002
0054   0 0001 48 SRT 0001
0055   0 0000 49 SLA 0002
0056   0 0001 48 SRT 0001
0057   0 0000 49 SLA 0002
0058   0 0001 48 SRT 0001
0059   0 0000 49 SLA 0002
0060   0 0001 48 SRT 0001
0061   0 0001 40 STR 0075
0062   0 0000 19 ADL 0075
```

```
0063   0 0000 10 CAD 0073
0064   0 0000 15 DIV 0075
0065   0 6610 18 CFA 0075
0066   0 0000 12 ADD 0075
0067   0 0000 14 MUL 0072
0068   0 0000 16 RND 0000
0069   0 0000 40 STA 0075
0070   0 0001 35 BCU 0063
0071   0 0000 30 BUN 0071
0072   0 5000 00 HLT 0000
0073   0 0000 00 HLT 0073
0074   0 2500 00 HLT 0000
0075   0 0000 00 HLT 0075
0076   0 0081 03 PRD 0430
0077   0 0000 10 CAD 0437
0078   0 0110 40 STA 0107
0079   0 0000 48 SRA 0001
0080   0 0110 40 STA 0113
0081   0 0000 48 SRA 0001
0082   0 0110 40 STA 0116
0083   0 0000 42 LDB 0087
0084   1 0000 11 CSU 0434
0085   1 0000 14 MUL 0434
0086   0 0001 49 SLT 0006
0087   0 0000 16 RND 0002
0088   1 0000 19 ADL 0380
0089   0 0000 19 ADL 0378
0090   0 0001 21 DBB 0084
0091   0 0000 42 LDB 0087
0092   0 0000 10 CAD 0379
0093   1 0000 14 MUL 0434
0094   0 0001 49 SLT 0006
0095   0 0000 16 RND 0001
0096   0 0001 21 DBB 0093
0097   0 0000 12 ADD 0378
0098   0 0000 14 MUL 0379
0099   0 0001 49 SLT 0006
0100   0 0000 16 RND 0417
0101   0 0000 40 STA 0378
0102   0 0000 10 CAD 0430
0103   0 0000 14 MUL 0430
0104   0.0001 49 SLT 0001
0105   0 0000 15 DIV 0378
0106   0 0001 48 SRT 0001
0107   0 0000 16 RND 0003
0108   0 0000 40 STA 0378
0109   0 0000 42 LDB 0087
0110   1 0000 10 CAD 0431
0111   1 0000 14 MUL 0431
0112   0 0001 49 SLT 0006
```

```
0113   0 0000 16 RND 0002
0114   0 0000 14 MUL 0379
0115   0 0001 49 SLT 0006
0116   0 0000 16 RND 0001
0117   0 0000 40 STA 0397
0118   0 0000 10 CAD 0378
0119   1 0000 14 MUL 0380
0120   0 0001 49 SLT 0003
0121   0 0000 15 DIV 0397
0122   0 0001 48 SRT 0001
0123   0 0000 16 RND 0000
0124   1 0000 40 STA 0398
0125   0 0001 21 DBB 0110
0126   0 0000 10 CAD 0431
0127   0 0000 14 MUL 0432
0128   0 0001 49 SLT 0006
0129   0 0000 16 RND 0000
0130   0 0000 40 STA 0401
0131   0 0000 10 CAD 0434
0132   0 0000 14 MUL 0435
0133   0 0001 49 SLT 0006
0134   0 0000 16 RND 0000
0135   0 0000 13 SUB 0436
0136   0 0001 48 SRT 0002
0137   0 0000 15 DIV 0401
0138   0 0001 48 SRT 0002
0139   0 0000 16 RND 0000
0140   0 0000 40 STA 0402
0141   0 0000 10 CAD 0431
0142   0 0000 14 MUL 0433
0143   0 0001 49 SLT 0006
0144   0 0000 16 RND 0000
0145   0 0000 40 STA 0401
0146   0 0000 10 CAD 0434
0147   0 0000 14 MUL 0436
0148   0 0001 49 SLT 0006
0149   0 0000 16 RND 0000
0150   0 0000 13 SUB 0435
0151   0 0001 48 SRT 0002
0152   0 0000 15 DIV 0401
0153   0 0001 48 SRT 0002
0154   0 0000 16 RND 0000
0155   0 0000 40 STA 0403
0156   0 0000 10 CAD 0432
0157   0 0000 14 MUL 0433
0158   0 0001 49 SLT 0006
0159   0 0000 16 RND 0000
0160   0 0000 40 STA 0401
0161   0 0000 10 CAD 0435
0162   0 0000 14 MUL 0436
```

```
0163   0 0001 49 SLT 0006
0164   0 0000 16 RND 0000
0165   0 0000 13 SUB 0434
0166   0 0001 48 SRT 0002
0167   0 0000 15 DIV 0401
0168   0 0001 48 SRT 0002
0169   0 0000 16 RND 0000
0170   0 0000 40 STA 0401
0171   0 0000 42 LDB 0053
0172   1 0000 10 CAD 0401
0173   0 0000 14 MUL 0378
0174   0 0001 49 SLT 0006
0175   0 0000 16 RND 0000
0176   1 0000 40 STA 0401
0177   0 0001 21 DBB 0172
0178   0 0000 10 CAD 0431
0179   0 0000 12 ADD 0431
0180   0 0000 40 STA 0404
0181   0 0000 10 CAD 0430
0182   0 0000 15 DIV 0404
0183   0 0001 48 SRT 0005
0184   0 0000 16 RND 0000
0185   0 0000 40 STA 0404
0186   0 0001 03 PRD 0438
0187   0 0000 30 BUN 0221
0188   1 0001 10 CAA 0000
0189   0 0000 17 EXT 0171
0190   0 0000 40 STA 0408
0191   0 0000 42 LDB 0116
0192   1 0000 40 STA 0411
0193   0 0000 42 LDB 0383
0194   0 0000 14 MUL 0404
0195   0 0001 49 SLT 0009
0196   0 0000 16 RND 0000
0197   0 0000 40 STA 0386
0198   0 0000 40 STA 0422
0199   0 5108 26 IFL 0386
0200   0 0000 30 BUN 0019
0201   0 0001 49 SLT 0006
0202   0 0000 16 RND 1340
0203   0 0000 40 STA 0386
0204   0 0000 10 CAD 0408
0205   0 0000 14 MUL 0408
0206   0 0001 49 SLT 0010
0207   0 0000 14 MUL 0398
0208   0 0001 49 SLT 0008
0209   0 0000 16 RND 9999
0210   0 0000 40 STA 0405
0211   0 0010 18 CFA 0323
0212   0 0000 34 BCH 0324
```

```
0213   0 0000 42 LDB 0095
0214   0 0000 10 CAD 0408
0215   1 0000 14 MUL 0402
0216   0 0001 49 SLT 0009
0217   0 0000 16 RND 0000
0218   1 0000 40 STA 0406
0219   0 0001 21 DBB 0214
0220   0 0401 26 IFL 0383
0221   0 0000 42 LDB 0383
0222   1 0000 10 CAD 0000
0223   0 8888 36 BFA 0366
0224   0 2310 18 CFA 0388
0225   0 0000 35 BCE 0249
0226   0 0099 36 BFA 0343
0227   0 0000 17 EXT 0324
0228   0 0000 40 STA 0388
0229   0 0001 48 SRT 0008
0230   0 0000 42 LDB 0113
0231   1 0000 40 STA 0411
0232   0 0000 42 LDB 0383
0233   0 0000 14 MUL 0401
0234   0 0001 49 SLT 0009
0235   0 0000 16 RND 0000
0236   0 0000 12 ADD 0407
0237   0 0000 40 STA 0409
0238   0 0000 10 CAD 0388
0239   0 0000 14 MUL 0399
0240   0 0001 49 SLT 0001
0241   0 8900 16 RND 0438
0242   0 0000 12 ADD 0406
0243   0 0000 14 MUL 0388
0244   0 0001 49 SLT 0001
0245   0 0000 16 RND 0000
0246   0 0000 12 ADD 0405
0247   0 0000 40 STA 0410
0248   1 0000 10 CAD 0000
0249   0 0002 49 SLS 0003
0250   0 0000 17 EXT 0324
0251   0 0000 40 STA 0411
0252   0 0001 48 SRT 0008
0253   0 0000 42 LDB 0107
0254   1 0000 40 STA 0411
0255   0 0000 42 LDB 0383
0256   0 0000 14 MUL 0400
0257   0 0001 49 SLT 0009
0258   0 0000 16 RND 0000
0259   0 0000 12 ADD 0409
0260   0 0000 14 MUL 0411
0261   0 0001 49 SLT 0001
0262   0 0000 16 RND 0000
```

```
0263   0 0000 12 ADD 0410
0264   0 0000 40 STA 0415
0265   0 0010 18 CFA 0323
0266   0 0000 34 BCH 0326
0267   1 0000 10 CAD 0000
0268   0 0000 17 EXT 0331
0269   0 0000 40 STA 0416
0270   0 0000 10 CAD 0390
0271   0 0001 13 SUA 0415
0272   0 0000 40 STA 0420
0273   0 0001 13 SUA 0415
0274   0 0000 40 STA 0421
0275   0 0000 14 MUL 0421
0276   0 0001 49 SLT 0006
0277   0 0000 16 RND 0800
0278   0 0000 12 ADD 0390
0279   0 0000 40 STA 0421
0280   0 0001 10 CAA 0415
0281   0 0000 13 SUB 0386
0282   0 0000 14 MUL 0420
0283   0 0001 49 SLT 0006
0284   0 0000 16 RND 0540
0285   0 0000 44 STP 0071
0286   0 0000 30 BUN 0045
0287   0 0001 48 SRT 0003
0288   0 0000 16 RND 0004
0289   0 0000 14 MUL 0379
0290   0 0001 49 SLT 0002
0291   0 0000 15 DIV 0421
0292   0 0001 48 SRT 0002
0293   0 0000 16 RND 0540
0294   0 0000 40 STA 0417
0295   0 0000 14 MUL 0416
0296   0 0001 49 SLT 0007
0297   0 0000 16 RND 0540
0298   0 0000 40 STA 0418
0299   0 0000 44 STP 0071
0300   0 0000 30 BUN 0045
0301   0 0001 48 SRT 0003
0302   0 0000 16 RND 1340
0303   0 0000 40 STA 0419
0304   0 0000 42 LDB 0290
0305   1 0000 10 CAD 0412
0306   0 8110 18 CFA 0277
0307   0 0001 34 BCL 0041
0308   1 0001 01 NOP 0412
0309   1 0000 40 STA 0412
0310   0 0001 21 DBB 0305
0311   0 0000 42 LDB 0288
0312   1 5108 26 IFL 0415
```

```
0313   0 0001 21 DBB 0312
0314   0 0000 42 LDB 0297
0315   0 0080 29 RTF 0412
0316   0 0412 40 STB 0297
0317   0 0000 10 CAD 0297
0318   0 0410 18 CFA 0302
0319   0 0001 34 BCL 0220
0320   0 6229 26 IFL 0346
0321   0 0000 30 BUN 0016
0322   0 0000 30 BUN 0335
0323   0 0000 00 HLT 9999
0324   1 1100 00 HLT 0000
0325   0 0000 30 BUN 0188
0326   0 0000 00 HLT 0800
0327   0 1000 38 BCS 0222
0328   1 0000 10 CAD 0000
0329   0 0000 42 LDB 0288
0330   1 0000 46 CLL 0415
0331   0 0001 21 DBB 0330
0332   0 0000 17 EXT 0391
0333   0 0000 40 STA 0416
0334   0 0000 30 BUN 0304
0335   0 0000 42 LDB 0293
0336   0 0010 09 SPO 0389
0337   1 0030 09 SPO 0000
0338   1 4011 09 SPO 0003
0339   1 0010 09 SPO 0004
0340   1 4011 09 SPO 0005
0341   1 0020 09 SPO 0006
0342   0 0408 26 IFL 0293
0343   0 0000 10 CAD 0293
0344   0 0410 18 CFA 0297
0345   0 0001 34 BCL 0335
0346   0 0000 01 NOP 0359
0347   0 0000 10 CAD 0390
0348   0 0000 40 STA 0378
0349   0 0000 40 STA 0380
0350   0 0000 40 STA 0381
0351   0 0000 40 STA 0382
0352   0 0000 10 CAD 0241
0353   0 0410 40 STA 0383
0354   0 2310 40 STA 0388
0355   0 0000 10 CAD 0284
0356   0 0410 40 STA 0293
0357   0 0410 40 STA 0297
0358   0 0000 30 BUN 0013
0359   0 6229 27 DFL 0236
0360   0 0000 10 CAD 0241
0361   0 0410 40 STA 0383
0362   0 0000 10 CAD 0284
```

```
0363   0 0410 40 STA 0297
0364   0 0410 40 STA 0293
0365   0 0000 30 BUN 0186
0366   0 6229 26 IFL 0346
0367   0 0410 26 IFL 0346
0368   0 0000 30 BUN 0343
0369   0 6229 27 DFL 0346
0370   0 0410 27 DFL 0346
0371   0 0000 42 LDB 0383
0372   0 0000 30 BUN 0188
0373
0374
0375
0376
0377
0378   0 0000 01      0000
0379   0 0000 02      0000
0380   0 0000 01      0000
0381   0 0000 01      0000
0382   0 0000 01      0000
0383   0 0000 00      0438
0384   2 1616 62      4955
0385   2 0054 64      0033
0386
0387   2 0202 02      0216
0388   0 8300 00      0000
0389   2 0000 00      0016
0390   0 0000 01      0000
0391   0 0000 01      1111
```

R E F E R E N C E S

REFERENCES

1. Y. Kitahara, M. C. Caserio, F. Scardiglia and J. D. Roberts, JACS (1960), 82, 3106-3111.

2. E. R. Howells, D. C. Phillips and D. Rogers, Acta Cryst. (1950). 3, 210-214.

3. A. J. C. Wilson, Nature (1942), 150, 151-152.

4. A. L. Patterson, Phys. Rev. (1939), 56, 972-977. For a more general discussion, see A. L. Patterson, Computing Methods and the Phase Problem in X-ray Crystal Analysis (1952), pp. 29-35, published X-ray Crystal Analysis Laboratory, Pennsylvania State College, State College, Pennsylvania.

5. M. J. Buerger, Proc. Nat. Acad. Sci. (1950), 36, 738-742.

6. K. Nagarajan and M. C. Caserio, private communication.

7. E. W. Hughes, JACS (1941), 63, 1737-1752.

8. H. Lipson and W. Cochran, The Determination of Crystal Structures, London, G. Bell and Sons, Ltd. (1957), pp. 298-301.

9. P. K. Gantzel, R. A. Sparks and K. N. Trueblood, ACA Computer Program Listing, Ed. 2, American Crystallographic Association (1961). Program number 317 (UCLALS1). A block-diagonal program is also available.

10. A. J. Freeman, Acta Cryst. (1959), 12, 261-271.

11. R. McWeeny, Acta Cryst. (1951), 4, 513-519.

12. J. A. Hoerni and J. A. Ibers, Acta Cryst. (1954), 7, 744-746.

13. J. Berghuis, B. Haanappel, M. Potters, B. Loopstra, C. MacGillavry, and A. Veenendaal, Acta Cryst. (1955), 8, 478-483.

14. J. D. Dunitz and V. Schomaker, J. Chem. Phys. (1952), 20, 1703-1707.

15. M. J. S. Dewar and H. N. Schmeisling, Tetrahedron (1960), 11, 96-120.

16. C. Wong, R. E. Marsh, and V. Schomaker, to be published.

17. J. D. Dunitz, Acta Cryst. (1949), 2, 1-13.

18. H. A. Bent, J. Chem. Phys. (1960), 32, 1582-1583.

19. L. O. Brockway, Acta Cryst. (1954), 7, 682.

20. O.R. Gilliam, H. D. Edwards and W. Gordy, Phys. Rev. (1949), 75, 1014-1016.

21. B. Bak, S. Detoni, L. Hansen-Nygaard, J. Nielsen and J. Rastrup-Anderson, Spectrochim. Acta (1960), 16, 376-383.

22. D. R. Lide, Jr., and D. E. Mann, J. Chem. Phys. (1958), 29, 914-920.

23. H. C. Allen and E. K. Plyler, JACS (1958), 80, 2673-2676. Also J. M. Dowling and B. P. Stoicheff, quoted by C. C. Costain and B. P. Stoicheff, J. Chem. Phys. (1959), 30, 777-782.

24. V. W. Laurie, J. Chem. Phys. (1961), 34, 291-294.

25. R. Schaeffer, JACS (1957), 79, 2726-2728.

26. J. Reddy and W. N. Lipscomb, J. Chem. Phys. (1959), 31, 610-616.

27. L. Burkardt and N. Fetter, Chem. & Ind. (1956), 1191.

28. L. Burkardt and N. Fetter, private communication.

29. N. Fetter, private communication.

30. D. E. Sands and A. Zalkin, Acta Cryst. (1962), 15, 410-417.

31. B. M. Graybill and M. F. Hawthorne, JACS (1961), 83, 2673-2676.

32. T. C. Furnas, Jr. Single Crystal Orienter Instruction Manual, Direction 12130A, X-ray Department, General Electric Company, Milwaukee, Wisconsin, 1957.

33. L. H. Thomas and K. Umeda, J. Chem. Phys. (1957), 26, 293-303.

34. J. A. Ibers, Acta Cryst. (1957), 10, 86.

35. C. H. Dauben and D. H. Templeton, Acta Cryst. (1955), 8, 841-842.

36. B. Bak, L. Hansen, J. Rastrup-Anderson, J. Chem. Phys. (1954), 22, 2013-2017.

37. Interatomic Distance. Chemical Society Special Publication 11, London, 1953.

38. L. Pauling, Nature of the Chemical Bond, Ed. 2. Cornell Univ. Press, Ithaca, N. Y., 1948.

39. S. H. Bauer, JACS (1937), 59, 1804-1812.

40. S. Geller and J. L. Hoard, Acta Cryst. (1951), 4, 399-405.

41. J. L. Hoard, T. Bowen, A. Buzzell, and O. N. Salmon, Acta Cryst. (1950), 3, 130-137.

42. S. Geller and J. L. Hoard, Acta Cryst. (1950), 3, 121-129.

43. Reference Manual, 709/7090 FORTRAN Programming System, International Business Machines Corporation, 1961.

44. FORTRAN ASSEMBLY PROGRAM (FAP) for the IBM 709/7090, International Business Machines Corporation, 1960.

P R O P O S I T I O N S

PROPOSITION I

It is argued that a new coordination state for titanium has been observed, although unrecognized, in recent research. The proposed pentavalent titanium is present in a complex observed so far only in solution, but it is proposed by analogy with a roughly similar complex isolated in crystalline form and of sufficient stability for its crystal structure to have been determined by X-ray diffraction techniques that the postulated complex is real and can be crystallized. It is proposed that crystallization be attempted and if successful that the structure of the crystals be determined as the best way of determining the nature of titanium coordination. In the event crystallization proves impossible, evidence for the existence of the complex in solution can be obtained by several alternate techniques suggested.

In the course of work on ethylene polymerization catalysts, Breslow and Newburg (hereafter BN)(1) have discovered that solutions of bis(cyclopentadienyl) titanium dichloride in toluene or n-heptane react with diethyl aluminum chloride to give almost immediately a red color, which then slowly changes to green and finally to blue. Reaction with triethylaluminum in a slight excess gives the blue color almost immediately. BN suggest that the reaction sequence is (1) formation of a complex; (2) alkylation of the titanium; (3) reduction from Ti^{IV} to Ti^{III}. They propose (I) as the red complex (R = Cl or Et), and present evidence to show that (II) may be the intermediate in alkylation. To explain the difference in reduction rate with $AlEt_3$ or $AlEt_2Cl$ as alkylating agent, BN suggest that the stability of the titanium-carbon bond may depend upon

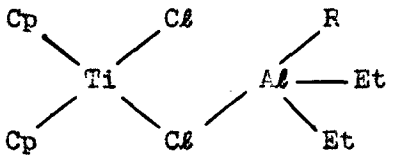

(I)

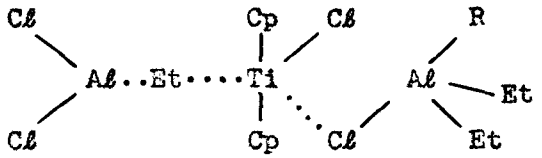

(II)

the compound with which the titanium is complexed, or that reduction involves a bialkylated form of titanium so that the greater alkylating power of $A\ell Et_3$ is important.

It is proposed that (III) is a more likely structure for the complex with $A\ell C\ell Et_2$ and that (I) with R = Et is probably the complex with $A\ell Et_3$. The difference between (I) and (III) would then satisfactorily explain the faster reduction by $A\ell C\ell_3$. An examination of (III) shows that the

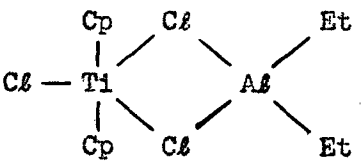

(III)

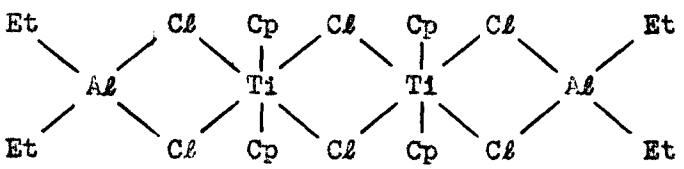

(IV)

C_5H_5 groups must be pushed far to one side by an approaching ethyl group in the alkylation step, as shown in (VI), whereas there is an opening already available in (I). Furthermore the intermediate (I) can be written

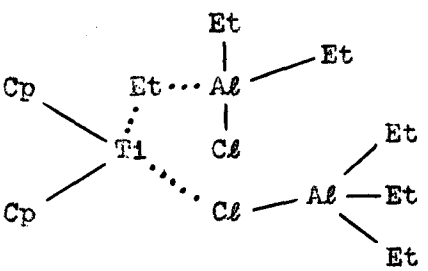

(V)

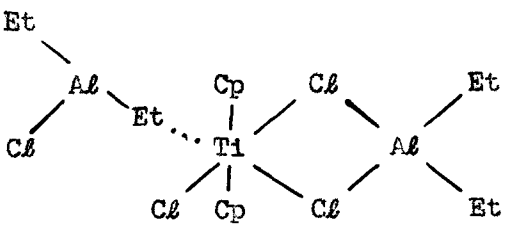

(VI)

in the somewhat more stable form (V), whereas no corresponding structure exists for intermediate (III). With this proposed mechanism, BN's postulate of varying Ti–C strength can be discarded. Proof of the existence of (III) would not, however, invalidate their second suggestion. With the new mechanism, either complex formation or alkylation can control the overall rate of formation of the final blue complex. The details of mechanism are not our purpose here. It is simply noted that the existence of (III) would provide another interpretation of the available data, equally valid with that proposed by BN and much more interesting from the structural viewpoint.

The next question of interest is whether the red complex observed there can be crystallized, and whether crystallization would change the molecular structure. In support of the first point, it is noted that Natta, et al., who apparently did not observe the initial red complex, have isolated the final blue complex in crystalline form and have succeeded in performing a structure determination using the X-ray diffraction technique (2). This material was found to have structure (VII). Indeed, it is by analogy with (VII) and because of the common occurrence

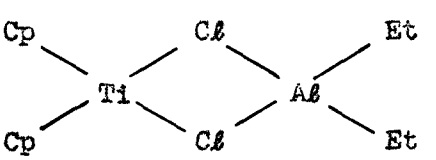

(VII)

of doubly-bridged metal complexes that (III) is favored over (I). As to whether (III) should not be written in the form of a dimer (IV) so that titanium might reside in its fairly common octahedral configuration, it

is observed that the great bulk of the C_5H_5 group renders this possibility very unlikely. Thus structure (III), if it exists, is not likely to dimerize during the process of crystallization. The same may be said of structure (V), inasmuch as tetrahedral coordination is a very commonly observed property of titanium. Thus, it is felt that the complex $(C_5H_5)_2C\ell TiC\ell_2A\ell Et_2$ can be crystallized and that a determination of the structure by X-ray diffraction would unambiguously define the complex which has been observed in solution.

In the event that the proposed crystals could not be obtained, several alternative methods of confirming the existence of the proposed complex are available. These methods all require prior assumptions about the substance under examination. For the sake of example, therefore, we shall assume in the following discussion that a complex exists and that it assumes either form (I) or form (III). The proposed techniques would confirm one of these structures or force consideration of others.

Three methods of obtaining information for the confirmation of one of the proposed structures in solution are considered: (1) X-ray diffraction by the liquid; (2) infrared absorption; and (3) nuclear magnetic resonance absorption (NMR). Because of expected poor resolution in the liquid the X-ray diffraction patterns alone could not distinguish between the structures, but some evidence could be obtained in support of one or the other. The infrared absorption spectra of Cp_2M and Cp_2MX_2 compounds, where M is some transition metal and X is a halide, have not been analyzed except for identification of the CH stretching frequency, but a comparison of several available spectra of the two above classes shows several strong resonance peaks which are invariant in position for many different M and X

atoms. The intensities of these lines may be useful in deciding whether or not the two C_5H_5 groups in the proposed complex are parallel. Finally the NMR spectrum of the postulated complex will be of doubtful usefulness. Only experiment will decide on the value of this method, since it is expected that hydrogen environments on the two complexes are insufficiently dissimilar for a selection of structures to be made on the basis of proton resonance, and since the spectra of chlorine and titanium, which should certainly differ enough to allow identification, might be rendered unobservable by quadrupole relaxation. The three methods in conjunction could probably offer evidence strong enough for selection of one of the two possible structures, however. These will now be examined separately in more detail.

X-ray diffraction. The vector plots expected for structures (I) and (III) are given in Figures 1a and 1b respectively. These show distinct differences between 2.5 and 4 Å. The region around 3.5 Å is most promising as a point of distinction. The twenty peaks Cℓ-Cp of the two structures form a band in each case about 0.8 Å in width, and centered at about 2.8 and 3.3 Å for structures (III) and (I), respectively. The large number of these vectors makes it unlikely that resolution of individual peaks is possible whether or not the cyclopentadienyl groups are rotating, but the conglomerate peak center should serve to distinguish between the two structures.

Infrared spectra. Figures 2 and 3 show respectively the spectra of Cp_2Fe (3) and Cp_2TiBr_2 (4). It will be seen that the strong bands at about 3.3, 7.0, 10.0 and 12.3 μ are virtually unchanged in positions and relative intensities. The same is true of these bands in Cp_2Ni, Cp_2Ru,

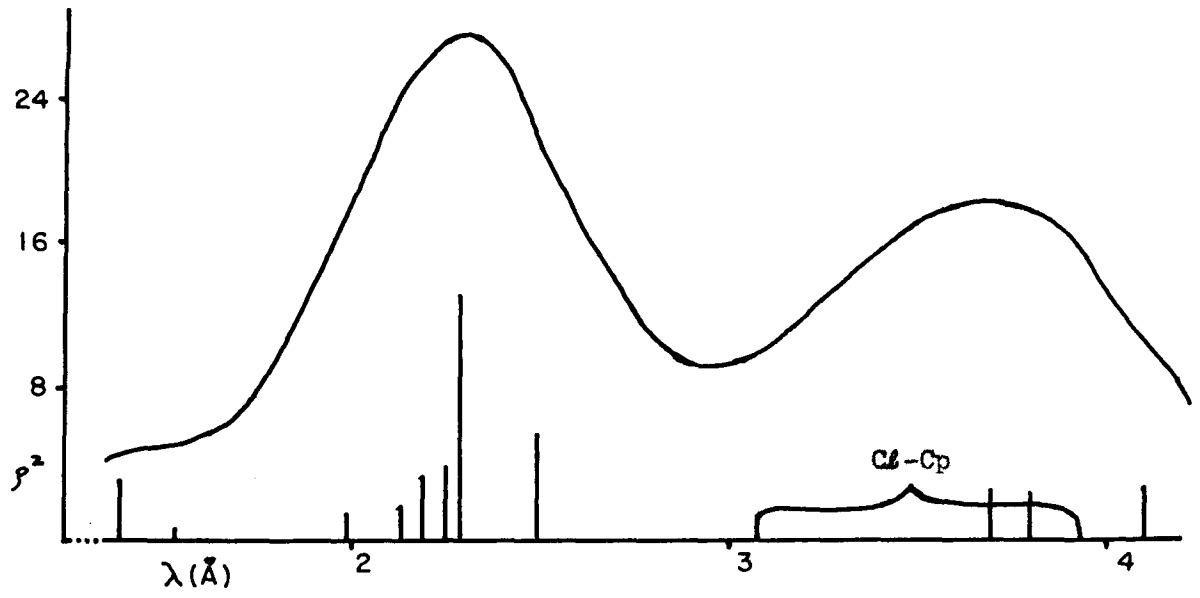

Figure 1a. Hypothetical ρ^2 Distribution for Structure I.

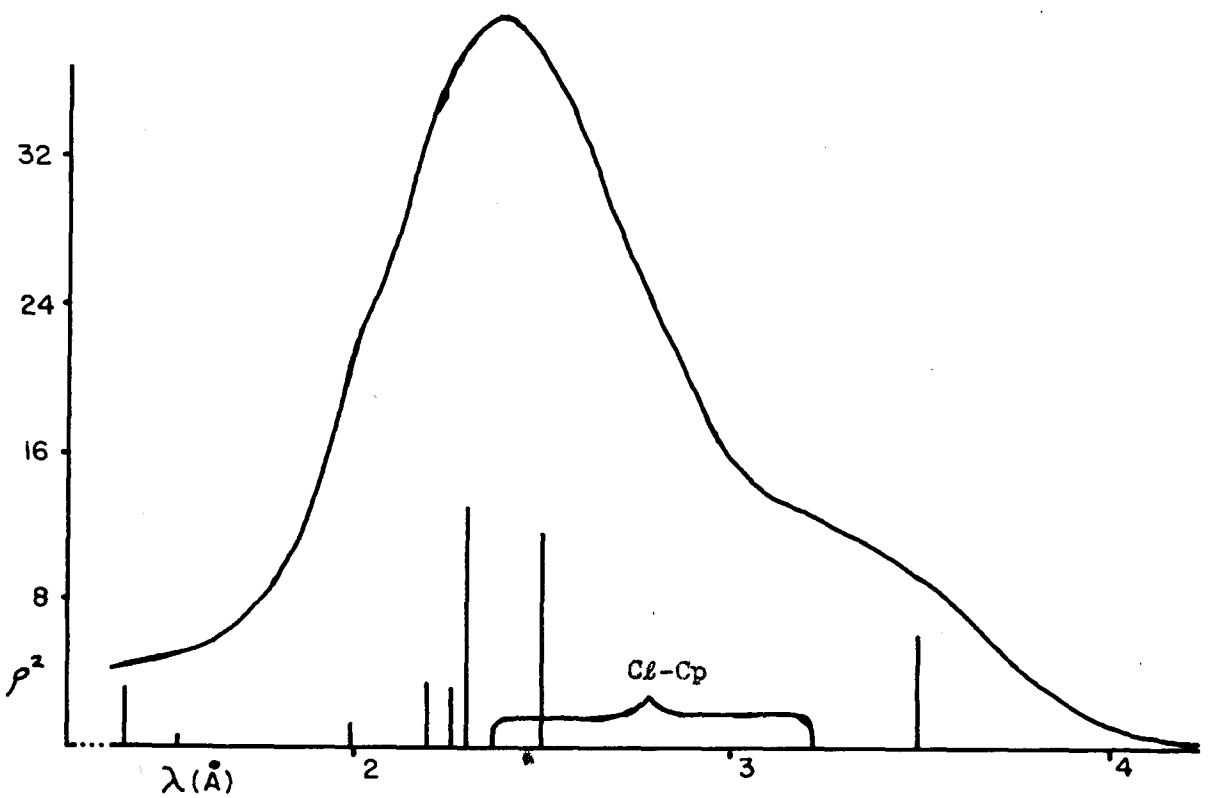

Figure 1b. Hypothetical ρ^2 Distribution for Structure III.

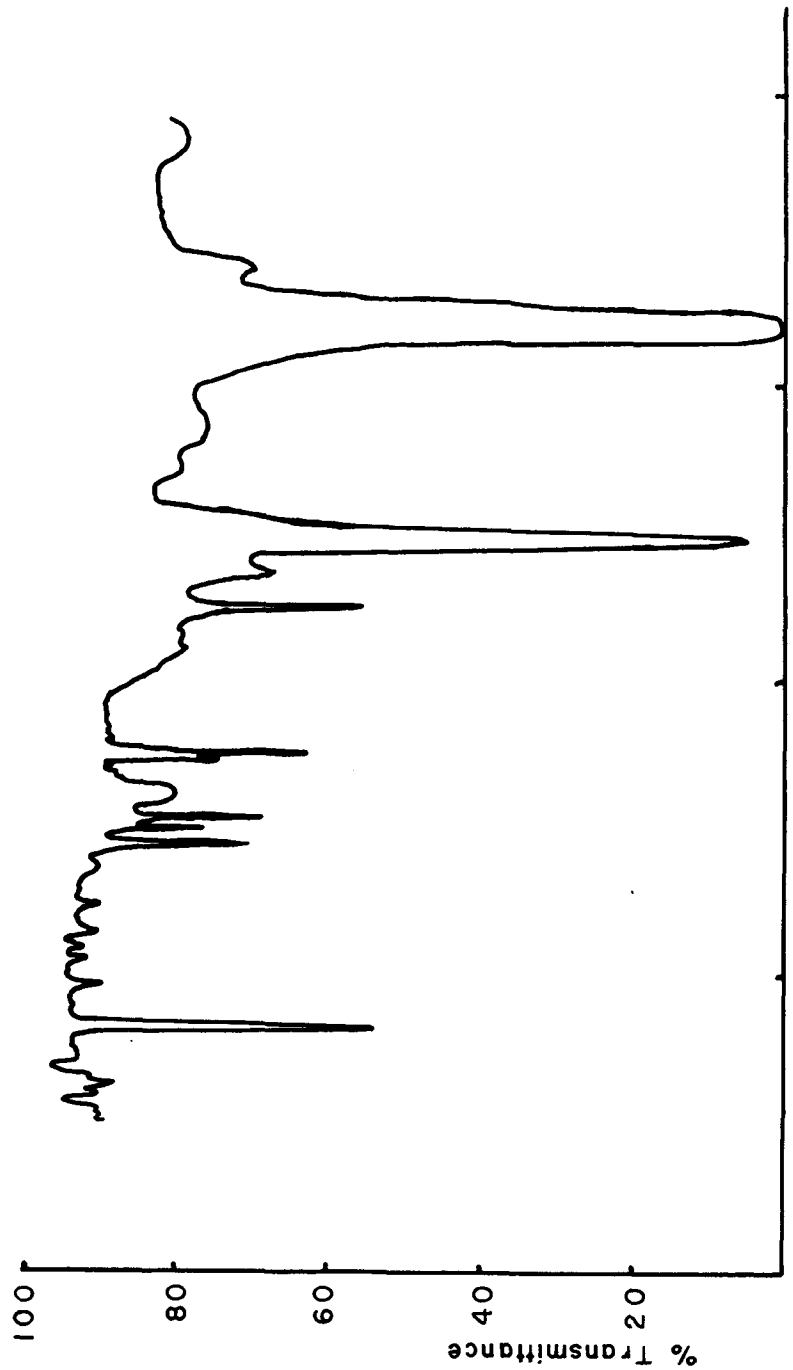

Figure 2. Infrared Absorption Spectrum of $Fe(Cp)_2$.

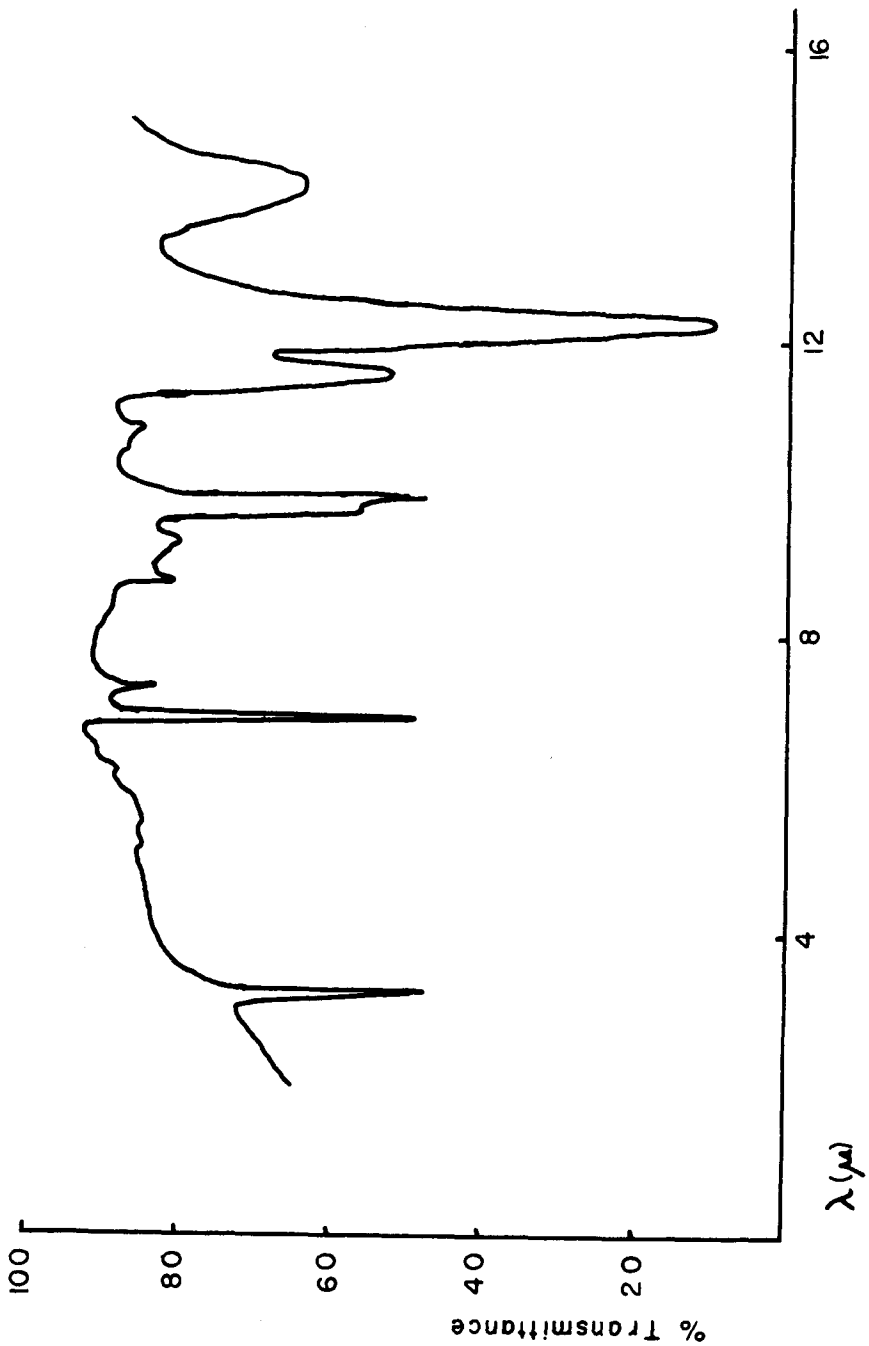

Figure 3. Infrared Absorption Spectrum of Cp_2TlBr_2.

Cp_2ZrBr_2, and Cp_2VCl_2. However, the 9.0 μ band in Cp_2Fe is greatly weakened in Cp_2TiBr_2, although unchanged in position. This change in intensity seems to be common to all of the above halides in comparison with the reduced metal dicyclopentadienyls. Because of the invariance in position of these lines, we may safely assume that they are all associated with energy levels characteristic solely of the C_5H_5 rings, whatever their detailed origin. Furthermore, since the only consistent difference between the rings of the two series of compounds is their relative position (parallel in Cp_2M and tilted in Cp_2MX_2), we may assume that the inhibition of the 9.0 μ absorption is in some way associated with this tilt. This assumption has been made on the basis of a comparison of all relevant published spectra, but cannot be used as a working hypothesis without being tested by the repetition of the spectra under carefully controlled circumstances. It should be further checked with the many pairs of compounds, Cp_2M and Cp_2MX_2, which are now known. In addition, Natta's complex should prove a valuable comparison.

Nuclear magnetic resonance. As has previously been indicated, proton resonance will probably be of little use. The only conceivable difference between structures (I) and (III) would have to come from ring-ring interaction. This is unlikely to be detectable.

NMR spectra of either titanium or chlorine resonance should serve conclusively to distinguish between the two structures, but the possibility of observation of these spectra is questionable. The difficulty in both cases is the same: broadening of the magnetic resonance lines by short quadrupole relaxation times. Some work on chlorine NMR spectra has been successful because of a special symmetry in the environment of

the nuclei which destroys the electric field gradient at the nucleus and forbids quadrupole relaxation. No special symmetry exists in the chlorine environment here, but the nuclei are partly shielded from transient electrical fields due to solvent molecules by the bulky C_5H_5 groups. This may render the spectra observable.

Probably more hope can be held for observation of the titanium NMR spectrum because of the high symmetry of the titanium position, particularly in structure (III). This hope may be naive because no NMR spectrum has been reported for titanium and because the size of the quadrupole moment is not known. This lack of information, however, is probably due more to the relative youth of the NMR technique than to any inherent impossibility of observing the titanium spectrum. Dicyclopentadienyl titanium, the Cp_2Ti halides, and Natta's complex should serve to help in interpreting the titanium spectrum if it can indeed be observed.

In summary, then, several methods have been outlined which could prove the existence, either in the solid state or in solution, of a postulated complex containing pentavalent titanium.* Even if this coordination state is not observed, the alternative complex is one containing two metal atoms bridged by a single halogen atom. The novelty of either structure demands investigation to prove which is correct.

---

*Since this proposition was originally offered additional support for the existence of pentavalent titanium has appeared. Bryce-Smith and Perkins (5) have obtained a yellow solid from a mixture of $TiCl_4$, tertiary-butyl chloride, and cycloheptatriene in n-hexane for which they propose the structure $(C_7H_7)^+(TiCl_5)^-$. However this material is not well-characterized and even if the empirical formula is correct there is no evidence that titanium is not octahedrally surrounded by chlorine atoms in a dimeric $[Ti_2Cl_{10}]^=$ ion. The existence of pentavalent titanium thus remains a very interesting point.

REFERENCES

PROPOSITION I

1. D. B. Breslow and N. R. Newburg, J.A.C.S. (1959), 81, 81.

2. G. Natta, P. Corradini, and I. Bassi, J.A.C.S. (1958), 80, 755.

3. G. Wilkinson, P. L. Pauson, and F. A. Cotton, J.A.C.S. (1954), 76, 1971.

4. G. Wilkinson and J. M. Birmingham, J.A.C.S. (1954), 76, 4283.

5. D. Bryce-Smith and N. A. Perkins, J. Chem. Soc. (1961), 2320-2325.

PROPOSITION II

One popular method of improving present rather desirable varieties of crop plants is by transference of a single chromosome or perhaps only part of a chromosome, bearing genes for a desired trait, to the variety from some more or less distantly related species by crossing the two species, selving or repeatedly crossing the hybrid until an individual appears containing the desired trait, and then repeatedly back crossing selected progeny of this individual to the original crop variety until a new crop variety is obtained, bearing the desired new trait and identical or similar in all other characteristics to the original variety. The most difficult single step in this procedure, particularly when very distantly related species are used, is frequently the obtaining of the original or F_1 hybrid. Apart from cases where the species involved are too dissimilar for fertilization to occur, or where the product of a successful fertilization is a so-called "zygotic lethal" unable to maintain the life processes, many cases are encountered wherein fertilization takes place and the resulting embryo grows to a greater or lesser extent, frequently reaching maturity, but in which the endosperm necessary to sustain the embryo as a germinating seed fails to develop. In these cases a seed may develop, either normal or shrivelled in external appearance but usually light in weight, or the embryo may begin to disintegrate at an early stage and the ovule fail to form a seed. Salvaging of the embryos in the cases where the embryos mature but the endosperm fails to develop properly is possible and very widely practiced, as a result of initial work by Hannig (1), Tukey (2,3), and others. Hannig was the first to obtain seedlings from species

embryos removed from the plant before ripening of the seed and Tukey first suggested the value of the technique in breeding programs. Tukey's first use of the technique was in obtaining both selved and crossed seedlings from early-bearing cherries which form normal embryos but fail to produce ripe seeds. Embryo culture, as the technique is called, involves removal of the mature (or sometimes slightly immature) embryo from the plant, sterile separation of the embryo from any endosperm present, and culture of the embryo for several days or more at about 30°C in sterile capped vials containing a nutrient mixture composed of a carbohydrate (usually sucrose), agar, and various salts, in water. Either immediately or after some initial period the culture is exposed to weak light. When roots and leaves appear the seedlings are transferred to soil and treated like any other valuable seedlings. Time and again, vigorous hybrids develop from such embryos, showing no sign of the difficulties in their birth.

It is proposed that success in raising seedlings by the methods of embryo culture can be extended to the embryos which do not fully mature and possibly even to some of the "zygotic lethals" by inclusion in the nutrient medium of additional factors necessary to embryonic growth. Success of embryo culture is based on the fact that after some period the embryo (now a seedling) becomes self sufficient. Thus there appears no a priori reason why even very immature embryos cannot be successfully raised, provided they are given certain additional growth factors or enzymes normally supplied by the nurturing tissue of the mother plant. In the cases of zygotic lethals, it might be necessary to provide the plant throughout its life with some chemicals or "plant vitamins," but even these plants could produce auto-viable offspring which might be valuable.

It is surprising that even in the breeding of well studied and agriculturally valuable crops where embryo culture is a standard practice, the above-proposed extension of the method is not suggested. An example in the recent literature where this technique would be useful is the sweet-clover cross Melilotus messenensis x M. officinalis, where it is reported (4) that fertilization apparently takes place but the embryos do not develop to such a size that embryo culture could be expected to succeed. This same article reports the successful crossing of two sweetclover species by employment of the embryo culture method of Tukey. Martin (5) in reporting on many crosses of green-sprouting broccoli says that many failures of seed-set occur after partial development of the ovules and hints that zygotic lethality may be a cause. Whether ordinary embryo culture has been tried in this case is not clear.

The idea of extending embryo culture to immature embryos is not new, but does not seem to be appreciated either as an aid to obtaining seed from normally pseudo-sterile species or in breeding programs. Some years ago, initial work in this field was done by van Overbeek, Conklin, Blakeslee, Siu , and Haagen-Smit (6-8), who carefully explored the problem of raising immature embryos of Datura stramonium (Jimson weed) and were able to extend the technique from large embryos in the most mature, or torpedo stage, to smaller torpedo embryos, then to those in the less mature, heart-shaped stage, and finally in one example, to a little-differentiated proembryo. To successfully raise the younger embryos the authors used in addition to sucrose and mineral salts a mixture of chemicals known to promote growth and either coconut milk (endosperm of the coconut) or a coconut-milk extract. The extract had a much higher specific

activity (on a dry-weight basis) and did not contain a root-inhibitor present in the native coconut milk. The use of coconut milk in culture of corn embryos was shown to be either unnecessary or unhelpful, depending on the maturity of the embryo (9), indicating that the growth factor found in this natural endosperm cannot alone be used to raise immature embryos of all kinds of plants.

It is suggested that the van Overbeek, et al. technique be used as a starting point in attempts to culture any immature embryos of interest. If this technique fails, the first change suggested is to replace the coconut-milk extract with a homogenate of the endosperm of the species of interest. The technique for any species should first be perfected on species embryos in order not to waste hybrid material. The procedure below, essentially that of van Overbeek, et al., is suggested as a starting point.

The coconut milk is sterilely extracted, concentrated about five times under vacuum and at temperatures under 50°C, and enough ethanol is added to the concentrate to make an 80% ethanolic solution. A precipitate is obtained, which is successively shaken with butanol, diethyl ether, and 80% ethanol. The resulting material is then added to the basic medium described below at a concentration of about 2.5 mg. of extract per ml. of medium. Van Overbeek, et al. do not mention storage of this extract, but it would probably remain effective for periods of several weeks under refrigeration. The basic medium consists of a water solution of 1% sucrose, 0.8% agar, Tukey's mineral mixture, and chemicals at the following concentrations: 3.0 mM glycine, 0.2 mM adenine, 0.15 mM thiamin, 20.0 mM ascorbic acid, 0.2 mM pyridoxin, 25.0 mM succinic acid, 1.0 mM

nicotinic acid, and 0.5mM pantothenic acid. Tukey's mixture consists of 45.4% KCl, 11.36% each of $CaSO_4$, $MgSO_4$, $Ca_3(PO_4)_2$, and $FePO_4$, and 9.09% KNO_3, and is used at the concentration of 1.5 gms per liter of medium.

The optimum culture temperature for Datura embryos was found to be 32°C (8), growth rate being reduced by a factor of three, five degrees on either side of this temperature. Commonly used temperatures are 25-30°C.

With the use of the above medium as a start, culture techniques for immature embryos of many species could probably be developed. Judging from the widespread distribution of such growth agents as β-indoleacetic acid, similar cultural techniques should apply to large numbers of species.

REFERENCES

PROPOSITION II

1. E. Hannig, Bot. Zeitg. (1904), 62,

2. H. B. Tukey, J. Hered. (1933), 24, 7-12.

3. H. B. Tukey, Proc. Am. Soc. for Hort. Sci. (1934), 32, 313-322.

4. G. T. Webster, Agron. J. (1955), 47, 138-142.

5. F. W. Martin, Euphytica (1962), 11, 81-86.

6. J. van Overbeek, M. E. Conklin, and A. F. Blakeslee, Am. J. Bot. (1942), 29, 472-477.

7. J. van Overbeek, Cold Harbor Springs Symposia on Quant. Biol. (1942), 10, 126-134.

8. J. van Overbeek, R. Siu, and A. J. Haagen-Smit, Am. J. Bot. (1944), 31, 219-224.

9. A. J. Haagen-Smit, R. Siu, and G. Wilson, Science (1945), 101, 234.

PROPOSITION III

It is proposed that a change in weighting scheme from that normally used in the refinement of crystal structures is demanded when the majority of experimental data have standard deviations smaller than about 5% of $|F_o|$ and the structure contains heavy atoms whose scattering factors are not well known. Consideration of the error present in these scattering factors is then required. This consideration is also capable of yielding lower standard deviations for light atoms when more than one heavy atom of identical type are in the structure. The case probably most profitable, that where there are two identical heavy atoms in the asymmetric unit, is considered as an example. Throughout the following discussion, the validity of the general least squares procedure is assumed.

Considering refinement only of positional parameters x_{ij}, where x_{1j}, x_{2j}, and x_{3j} are the three positional parameters of atom j, the usual least squares procedure is to use as observational equations

$$\sum_{i,j} w_k \frac{\partial F_{ck}}{\partial x_{ij}} \Delta x_{ij} = w_k(F_{ok}-F_{ck}) ,$$

or the corresponding expression involving $|F_o|^2$ instead of $|F_o|$. In this expression, $|F_{ok}|$ is the observed value of the $k^{\underline{th}}$ structure factor, $|F_{ck}|$ is the corresponding calculated value based on a set of approximate atomic coordinates, and w_k is a weight assigned to the $k^{\underline{th}}$ observational equation. The summation is taken over all independent positional parameters. Least squares theory shows that if the coefficients $(\partial F_{ck}/\partial x_{ij})$ are accurately known, the most probable values of the Δx_{ij} which the given data are capable of yielding are obtained by equating w_k to $1/\sigma^2_{F_{ok}}$ and solving the

equations in the usual way. With past methods of data collection, errors in the observed structure factors have greatly exceeded errors in the atomic form factors, and the latter sources of error have been neglected. This approximation is still valid when the structure contains only light atoms whose form factors are well known, even if the best of modern methods are used for data collection. But for many of the heavy atoms commonly used in the "heavy atom technique" of solving structures, improvements in the calculation of form factors have not kept pace with the development of experimental technique. For structures containing such atoms, some change in the refinement technique is needed. The general form in which the equations should be recast is

$$\sum_{i,\ell} w_k \frac{\partial F_{ck}}{\partial x_{i\ell}} \Delta x_{i\ell} = w_k(F_{ok}-F_{ck}) \text{ , where the}$$

summation is over light atoms only, and where the "observed" quantity $(F_{ok}-F_{ck})$ can be written $([F_{ok}-F_{hk}]-F_{\ell k})$ to emphasize the fact that errors in the heavy atom contribution to the structure factor, F_{hk}, should be considered in assigning weights. Here, $F_{\ell k}$ is the contribution of the light atoms to F_{ck}.

To consider the size of errors in F_{hk} likely to be encountered, let us consider a specific example. Assume a centrosymmetric structure containing two bromine atoms in the asymmetric unit, and imagine that the experimental data are collected with molybdenum Kα characteristic radiation, in such a way that $\sigma_{F_o} = (0.5 + 0.03|F_o|)$. Probably the best atomic form factor currently available for bromine is that of Thomas and Umeda (1). Comparison of this form factor with the best previously available (2) reveals a difference of about 1.3 electrons, a difference nearly independent

of scattering angle. This difference probably is a lower limit of uncertainty for the older curve. An estimate of the uncertainty in the Thomas-Umeda form factor for bromine can be made by comparison of their Cu^+ form factor with one still more accurate, the Cu^+ form factor derived by Berghuis, et al. (3) from a self-consistent-field electron distribution. The differences between these two Cu^+ curves are as much as 0.3 electrons, and indicate a lower limit on the uncertainty of the Thomas-Umeda Cu^+ curve. Because all of Thomas' and Umeda's form factors were calculated in similar ways with data of presumably similar accuracy, we can also adopt 0.3 electrons, independent of scattering angle, as a limiting accuracy for the bromine form factor. A further correction must be made for the anomalous dispersion of MoKα radiation by bromine: Dauben and Templeton (4) give this correction as -0.3 electrons. Including this correction, the uncertainty of the bromine form factor, $\sigma_{f_{Br}}$, can be set equal to 1.0 electrons. If this value is assumed independent of scattering angle, the error in F_{Br}, the contribution of a bromine atom to the structure factor, is $(1.0|F_{Br}|/f_{Br}) = 1.0\ g_{Br}$, where g_{Br} is the "geometrical" part of the structure factor.

With the assumptions made thus far, it is clear that the proper weight for the $k^{\underline{th}}$ observational equation is

$$1/\sigma_k^2 = 1/\left[(0.5 + 0.03\ |F_{ok}|^2)^2 + \left(\frac{1.0\ F_{Hk}}{f_{Br}}\right)^2 (g_{Hk})^2 + f_{Br}^2 \sum_i \left(\frac{\partial g_{Hk}}{\partial x_i}\right)^2 \sigma_{x_i}^2\right]$$

where F_{Hk} is the contribution to F_{ck} of the heavy atoms, g_{Hk} is the geometrical part of F_c contributed by the heavy atoms, and x_i are the positional parameters of these atoms. It is equally obvious that the weights are biased in favor of reflections dominated by the light atoms. The third

term in the above sum is large for reflections highly sensitive to bromine locations, and the second term is large whenever the total contributions of the bromine atoms to F_c is large. Thus only data which are both insensitive to the locations of bromine atoms and to which the total bromine contribution is small are given highest weights. For this reason, the case of two independent but identical heavy atoms is the most favorable because only in this case can the most favorable case, $g_{H_1} \approx -g_{H_2} \approx \pm 1$, occur with reasonable frequency.

This method affords a generalization of the case where the heavy atoms are in special positions and do not contribute to reflections of certain symmetry classes, and in which case it has frequently been the practice to refine the remaining (usually light) atoms on these data alone.

REFERENCES

PROPOSITION III

1. L. H. Thomas and K. Umeda, J. Chem. Phys. (1957), 26, 293-303.

2. Internationale Tabellen zur Bestimmung von Kristallstrukturen, V. 2 (1935), p. 572.

3. J. Berghuis, B. Haanappel, M. Potters, B. Loopstra, C. Macgillavry, and A. Veenendaal, Acta Cryst. (1955), 8, 478-483.

4. C. H. Dauben and D. H. Templeton, Acta Cryst. (1955), 8, 841-842.

PROPOSITION IV

It has been generally assumed that aromatic carboxylic acids are planar in the absence of crowding from large ortho substituents. It is proposed that involvement of the carboxyl group in hydrogen bonds at large angles to the aromatic plane can cause twists about the $C_{carboxyl}$-$C_{aromatic}$ bond of perhaps 10° or more. To demonstrate cases where such twists are observed and a case where attention should have been paid to this effect but was not, attention is directed to three recent crystal structure determinations, those of copper salicylate tetrahydrate (1), zinc salicylate dihydrate (2), and ammonium hydrogen salicylate hydrate (3).

In copper salicylate tetrahydrate, there is one salicylate radical per asymmetric unit. The only atoms in this radical which are significantly out of the mean plane of the group are the two carboxyl oxygens, at distances of 0.13 Å and 0.17 Å. These distances correspond to a twist of the carboxyl group of about 7.6° about the C_C-C_{Ar} bond, but in this compound one of the oxygens seems to be covalently bonded to a copper atom which is far from the aromatic plane and thus the hydrogen bond in which the second oxygen is involved is only partly responsible for this twist. In the related compound, zinc salicylate dihydrate, the zinc-oxygen bond is probably ionic and thus less likely to cause distortion of the acid radical. Indeed, in this structure the oxygen atom nearest the zinc is nearly coplanar with the aromatic ring although the zinc atom is not. Only the second oxygen atom, which participates in a hydrogen bond directed out of the aromatic plane, is significantly (0.17 Å) out of this plane.

To show that small deviations from planarity can be energetically favorable if they materially reduce hydrogen bond lengths, we can examine the following facts: Lippincott and Schroeder (4) have proposed a potential function for hydrogen bonds of various types which gives a good description of many of the properties of these bonds and which in particular gives a good fit to experimental energy-versus-length data for OH···O bonds. Using their published curve to obtain energy values for a given bonding distance, and calculating the increase in hydrogen bond lengths required by postulated planar carboxyl groups, we find the changes in the copper salicylate structure to be from 2.67 to 2.74 Å in length or 2 kcal/mole in energy, and in the zinc salicylate structure to be from 2.54 to 2.69 Å in length, or about 4 kcal/mole in energy. Pauling (5) estimates 4 kcal/mole as the extra resonance energy found in benzoic acid over that expected for isolated C_6H_5 and COOH groups. If this is assumed to be the total energy lost when the carboxyl group is rotated 90° from its most stable configuration, any reasonable relationship between rotation angle and loss of resonance energy will show a net gain caused by the twists observed in the two metal salicylate structures above in comparison with planar carboxyl groups. In particular, the popular cosine relationship predicts a loss of 0.04 kcal/mole in resonance energy compared with a gain of 2 to 4 kcal/mole in hydrogen bonding energy in the two cases. The wonder, then, is that the rotation is not greater, giving minimum hydrogen-bond lengths, regardless of angle of twist. However the intramolecular hydrogen bonds must also be considered, and these are stretched by any twist. These bonds and possibly other packing factors must be responsible for the small degrees of twisting observed.

As an example of the need for directing attention to the effect considered here, the structure of ammonium hydrogen salicylate hydrate (3) is considered. This structure was determined with two dimensional data (3 zones) on the assumption that the salicylate radicals are completely planar. The published structure gives the ammonium ion five nearest neighbors, but shows that all carboxyl oxygen atoms are involved in hydrogen bonds, mostly at large angles from the planes of the two independent salicylate radicals. If the carboxyl groups are rotated 10-15 degrees, these hydrogen bonds are mostly reduced in length (one of the longer ones is considered to be destroyed) and the number of ammonium nearest neighbors becomes four, all of which seem to be involved in hydrogen bonding. It is dangerous to propose changes in a structure which have not been checked by calculation of structure factors, but these changes represent a very reasonable possibility which was not considered by the original authors. Their R-value of 22% for the less favorable zones, compared with 17% for the zone most nearly parallel with the salicylate radicals, shows that some improvement is possible. Some detailed changes are suggested below, with the realization that the changes are only approximations. Because of the high resolution of the (h0ℓ) zone and the fact that the planes of both salicylate radicals are nearly parallel with this zone, only changes in the y-parameters of the carboxyl oxygen atoms are suggested. The proposed changes correspond approximately to rotations of 15° of both independent carboxyl groups, and they shorten the four hydrogen bond lengths from 2.84, 2.83, 2.88, and 2.72 Å to 2.73, 2.74, 2.76, and 2.57 Å respectively. An O-N distance is lengthened from 2.84 to 3.09 Å, resulting in removal of one of the nearest neighbors of the ammonium ion. The remaining

four neighbors are at reasonable hydrogen-bonding angles. The old and postulated new coordinates of the four atoms involved in changes are:

atom	x/a	old y/b	new y/b	z/c
O_1	0.2237	-0.757	-0.681	-0.1949
O_2	0.2491	0.292	0.220	-0.0951
O_4	-0.0587	-0.650	-0.575	-0.1878
O_5	-0.0208	0.500	0.429	-0.0892

REFERENCES

PROPOSITION IV

1. F. Hanic and J. Michalov, Acta Cryst. (1960), 13, 299-302.
2. H. P. Klug, L. E. Alexander, and G. G. Sumner, Acta Cryst. (1958), 11, 41-46.
3. J. C. Speakman and T. C. Downie, J. Chem. Soc. (1954), 787-793.
4. E. R. Lippincott and R. Schroeder, J. Phys. Chem. (1957), 61, 921-928.
5. L. Pauling, Nature of the Chemical Bond, Ed. 2 (1948), p. 139. Cornell Univ. Press, Ithaca, N.Y.

PROPOSITION V

C. Hackett (1) has recently reported an unexpected response of several kinds of plants under hydroponic culture to the presence in the culture liquid of small amounts of aluminum (about 5 parts per million). Previously only toxic effects of aluminum had been recognized, but Hackett found that in sprouting seeds and very young seedlings of the five species investigated that small amounts of aluminum cause a stimulating effect, particularly on the growth of roots. Increase in the aluminum concentration to 25 ppm in most cases reduced the rate of root growth to or below the rate observed in the absence of aluminum (except for possible trace amounts). In the youngest plants shoot growth was unaffected, but in older plants the growth of shoots was slightly reduced by the presence of aluminum in the nutrient medium. No effect on root growth of older plants was observed.

It is proposed that these effects of aluminum on plant growth are the result of complexing of the natural growth hormone or auxin, β-indoleacetic acid, by aluminum. This hormone is known to stimulate normal growth of both stems and roots greatly when present in amounts not exceeding some optimum concentrations, but to suppress growth when present in excess amounts. Quite generally the optimum concentration is far lower in roots than in other plant tissues, and the amounts of auxin present in roots generally exceeds the optimum amount. Thus removal of excess auxin from availability to the growing root tissues by some method such as formation of a stable complex with aluminum would be expected to produce a stimulative effect on root growth. Conversely, if aluminum served to

remove available auxin from stem or leaf tissue, a reduction in growth rate should normally be observed. Some slight reduction in the growth of shoots, but probably no significant amount, is observed by Hackett. The absence of this effect can be attributed to the fact that aluminum seems to be imperfectly transported in plants.* This probably indicates that little aluminum penetrates to the vascular system in transportable form. Auxin is normally transported from cell to cell quite independently of the vascular system, and of course acts in the growing cell layers outside of this system. Thus if aluminum is supposed to penetrate only into the surface layers of the growing roots but not to the vascular system, and to form within or between the growing cells a stable β-indoleacetic acid complex, destroying the effect of much of this material on the growing cells, the stimulation of root growth, the lack of effect upon stem growth, and the uneven distribution in the plant are explained. The last of these effects is only incidental to this proposal. It may be that aluminum is transported freely about the plant but is stored to a greater extent in the roots. Free transport of aluminum would not in the present case affect the growth of stems because any aluminum transported to the upper plant parts would presumably have been complexed with β-indoleacetic acid in the roots and could not later remove free auxin from other tissues. The retarding effect of higher Al^{+3} concentrations is also

---

*Hutchinson (2, p. 32) reports "A number of authors have concluded that there is a gradient in aluminum content, the amount falling off from the root to the leaf. This is certainly true in a number of species of plants growing on very acid soil, the most extreme cases being the solfatara plants described by von Faber, in which accumulation occurs in the root, but not necessarily in the aerial parts."

explained by this proposal. If too much auxin is removed by complex formation, root growth will suffer from lack of stimulation.

Explanation of the lack of effect of aluminum on the growth of roots in older plants is also possible in view of the indication (3) that seeds contain fairly large quantities of auxin. Sprouting seeds and very young seedlings must retain some of this excess, whereas in a more mature plant necessarily producing its own supply of auxin a lower concentration, not greatly exceeding the optimum, might be expected. In such a case any removal of active β-indoleacetic acid by complexing with aluminum might have no effect or a suppressing effect.

Evidence for the proof of this proposal is obtainable in several ways. The proposed complex between aluminum and β-indoleacetic acid should be investigated for stability in the pH range of 3-7 (Hackett's nutrient solution was kept near pH 3.8, but the pH within the plants is presumably nearer 7). The effect on the growth of roots of ions similar to aluminum in complexing properties should be investigated. (The only ions besides Al^{+3} in Hackett's medium likely to form complexes were 0.01 ppm Cu^{++}, 0.5 ppm Fe^{+3}, and possibly Mg^{++}, at 3 ppm.) Some of these metals should have effects similar to Al^{+3}. The effect of Al^{+3} applied to stem tips should be observed, and should be found to be nonexistent in small concentrations and retarding in higher amounts. Finally the effect of small amounts of Al^{+3} on cultures of root tissues completely deprived of auxin should be investigated. If the above proposal is correct, no effect (or possibly a deleterious effect) should be found. A retarding effect should result upon the addition of aluminum to similar cultures containing extremely small amounts of auxin.

REFERENCES

PROPOSITION V

1. C. Hackett, Nature (1962), 195, 471-472.

2. G. E. Hutchinson, Soil Science (1945), 60, 29-40.

3. L. A. Audus, Plant Growth Substances (1953), pp. 136-139. Leonard Hill, Ltd., London, England.